PL-TR--91-3086

PL-TR--
91-3086

ESTABLISHMENT OF MPD PERFORMANCE

Captain Salvador Castillo

December 1991

Final Report

PHILLIPS LABORATORY
Propulsion Directorate
AIR FORCE SYSTEMS COMMAND
EDWARDS AIR FORCE BASE CA 93523-5000

NOTICE

When U.S. Government drawings, specifications, or other data are used for any purpose other than a definitely related Government procurement operation, the fact that the Government may have formulated, furnished, or in any way supplied the said drawings, specifications, or other data, is not to be regarded by implication or otherwise, or in any way licensing the holder or any other person or corporation, or conveying any rights or permission to manufacture, use or sell any patented invention that may be related thereto.

FOREWORD

This final report was submitted on completion of this phase of JON: 573005RN by the OLAC PL/RKAS Branch, at the Phillips Laboratory (AFSC), Edwards AFB CA 93523-5000. OLAC PL Project Manager was Salvador Castillo, Capt, USAF.

This report has been reviewed and is approved for release and distribution in accordance with the distribution statement on the cover and on the SF Form 298.

Salvador Castillo

SALVADOR CASTILLO, CAPT, USAF
Project Manager

Bernard R. Bornhorst

BERNARD R. BORNHORST
Chief, Space Engineering Branch

FOR THE COMMANDER

PETER A. VAN SPLINTER
Director,
Applications Engineering Division

RANNEY G. ADAMS
Public Affairs Director

REPORT DOCUMENTATION PAGE

Form Approved
OMB No. 0704-0188

1. AGENCY USE ONLY (Leave blank)	2. REPORT DATE	3. REPORT TYPE AND DATES COVERED
	December 1991	Final September 82 to August 91

4. TITLE AND SUBTITLE
ESTABLISHMENT OF MPD PERFORMANCE

5. FUNDING NUMBERS
PE- 62302F
PR- 5730
TA- 05RN
WU- 351970

6. AUTHOR(S)
SALVADOR CASTILLO, Capt, USAF

7. PERFORMING ORGANIZATION NAME(S) AND ADDRESS(ES)
Phillips Laboratory (AFSC), Propulsion Directorate
PL/RKAS
Edwards AFB, CA 93523-5000

8. PERFORMING ORGANIZATION REPORT NUMBER
PL-TR-91-3086

9. SPONSORING/MONITORING AGENCY NAME(S) AND ADDRESS(ES)

10. SPONSORING/MONITORING AGENCY REPORT NUMBER

11. SUPPLEMENTARY NOTES
COSATI CODES: 21/03; 20/08; 20/09

12a. DISTRIBUTION/AVAILABILITY STATEMENT
Approved for public release; distribution is unlimited.

12b. DISTRIBUTION CODE

13. ABSTRACT *(Maximum 200 words)*

The Phillips Laboratory's Electric Propulsion Laboratory has conducted a preliminary experiment in the measurement of magnetoplasmadynamic (MPD) performance for a matrix of various electrode lengths. This data was taken in a single shot pulsed mode which was quasi-steady state with regard to electrical properties. As part of the project, a total impulse stand was built which allowed the calculation of thrust, specific impulse, and thruster efficiency. Limitations in experimental equipment prevented the gathering of accurate data. The data has given general trends in MPD performance and has given a better understanding of MPD test facility requirements. The project will be absorbed into a larger, general plasma thruster development project. The knowledge gained from this project will be used to upgrade the pulsed MPD facility to gather accurate MPD thruster performance data.

14. SUBJECT TERMS
electric propulsion; magnetoplasmadynamic; MPD; rocket test facility; thrust measurement; plasma thruster

15. NUMBER OF PAGES
132

16. PRICE CODE

17. SECURITY CLASSIFICATION OF REPORT	18. SECURITY CLASSIFICATION OF THIS PAGE	19. SECURITY CLASSIFICATION OF ABSTRACT	20. LIMITATION OF ABSTRACT
UNCLASSIFIED	UNCLASSIFIED	UNCLASSIFIED	SAR

TABLE OF CONTENTS

TABLE OF CONTENTS.....i
LIST OF FIGURES.....ii
LIST OF TABLES.....iii
INTRODUCTION.....1
Background.....1
Project Goals.....1
FACILITY COMPONENTS.....2
MEASUREMENT MODEL.....4
PHYSICAL COMPONENTS.....8
Total Impulse Stand.....8
Video Recorder System.....9
Calibration Components.....9
CALIBRATION PROCEDURE.....10
Impulse Stand Calibration.....10
Setup Procedures.....10
Calibration Procedure.....11
Calibration Data Reduction and Analysis.....11
PULSED MPD TESTING.....12
Thruster Operations.....12
Cold Gas Tests.....13
MPD Thrust Determination.....15
Thrust Calculations.....15
Sample Calculation of Thrust.....16
SOURCES OF ERRORS.....17
Thruster/ Ball Support Errors.....17
Dial Indication Errors.....17
Video Tape Errors.....17
Other Stand Errors.....18
Mass Flow Errors.....19
Voltage and Current Measurement Errors.....20
SUMMARY OF RESULTS.....21
LESSONS LEARNED.....22
FUTURE EXPERIMENTS.....23
ERROR ANALYSIS.....23
CONCLUSION.....24
REFERENCES.....25
APPENDIX A.....26
APPENDIX B.....27
APPENDIX C.....28
APPENDIX D.....29
APPENDIX E.....30
APPENDIX F.....58

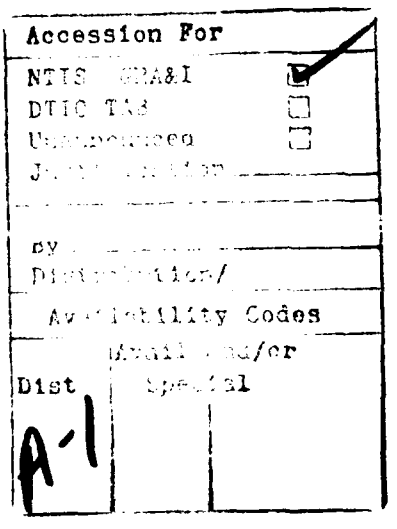

LIST OF FIGURES

1. Facility Layout....2
2. Pulsed MPD Thruster Test Configuration....2
3. Schematic-Pulse Forming Network....3
4. Pulse Forming Network....3
5. MPD Thruster....4
6a. Ball Impacting Stand....5
6b. MPD Pendulum....5
7. Impulse Stand....8
8. Calibration Components....9
9. Impulse Calibration Curve....12
10. Thruster Firing Sequence....13
11. Graphical Integration....14

LIST OF TABLES

1. Ball Parameters.....10
2. Mass Flow Cal Constants and Conversion Factors.....14
3. Example Thruster Data.....16
4. Measurement Uncertainties.....19

INTRODUCTION

This paper discusses the Phillips Laboratory's Electric Propulsion Laboratory (PLEPL) pulsed magnetoplasmadynamic (MPD) thruster performance experiment. Goals in measurement, model selection, calibration procedure and sources of error are described. Also included is a short discussion of statistical error analysis of the data collected.

Background

Certain performance characteristics are desired for comparison and evaluation when demonstrating new technology rockets. Thrust and specific impulse are among these characteristics. Similarly, electric power use efficiency is used to evaluate electric thrusters.

An MPD thruster uses electromagnetic fields to accelerate an ionized gas (plasma). Present experimental MPDs have specific impulses of 2000 - 4000 seconds and efficiencies in the 25 - 30 percent range (Refs. 1,2). High thrust density and structural simplicity make MPD thrusters attractive for a variety of future space missions, such as spacecraft maneuvering and orbit transfer (Ref. 3).

There currently exists little performance baseline data on long electrode length, multi-megawatt pulsed MPD thrusters (Refs. 4,5). The PLEPL is presently testing a 5 cm diameter anode (half scale) variable geometry MPD thruster. PLEPL's goal is to map pulsed MPD thruster performance as a function of electrode geometry. The end goal is to provide data, curves, and trends for different anode and cathode length configurations. Semi-empirical theoretical models may then be derived from the data.

For pulsed MPD thrusters, a high level of electrical noise limits the use of traditional thrust measurement techniques (Ref. 6). Thrust from pulsed MPD effect lasts a few milliseconds and is on the order of tens of pounds. Direct thrust measurement is difficult because of the high currents and voltages associated with electric propulsion.

The PLEPL built a total impulse stand to measure impulse (rather than thrust). Pulsed MPD thrust is found by dividing the impulse by the firing time. The stand consists of a dial indicator attached to the thruster with the measurement end placed against a rigid support.

Project Goals

The goal of this project is to map MPD thruster performance as a function of electrode geometry. Theoretical models and experiments have revealed a dependence of thrust on the ratio of anode diameter to cathode diameter (Ref. 7). There has also been work on scaling of thruster performance (Ref. 8). Finally, some

geometry performance mapping has been conducted by Ref. 9. This project intends to extend the mappings to variation in cathode and anode length. Thus, the cathode and anode length influence on MPD performance may be determined, resulting in a better understanding of MPD physics and a knowledge of the best performing geometry.

FACILITY COMPONENTS

The pulsed multi-megawatt MPD facility, also known as Chamber #2, consists of an 8 foot diameter by 12 foot long stainless steel cylinder. The chamber has one door and six view ports along the sides (Figs. 1,2).

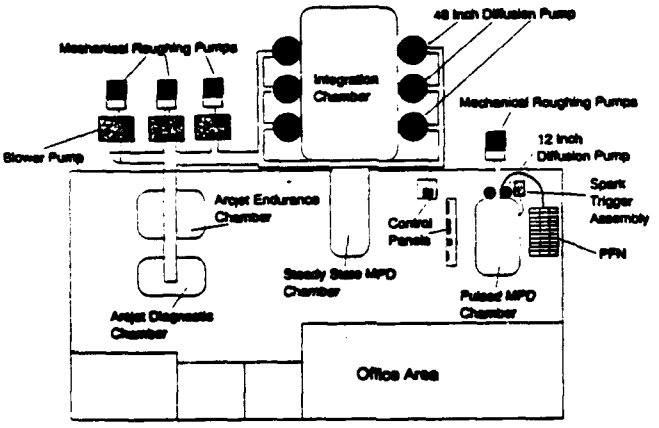

Figure 1
Facility Layout

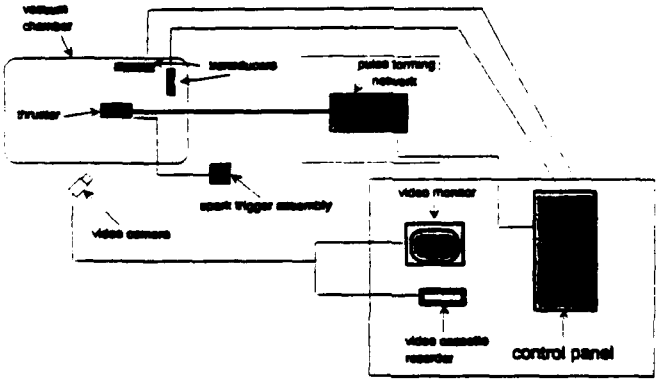

Figure 2
Pulsed MPD Thruster Test Configuration

A Stokes mechanical pump (Model 412H-10), a Roots blower (Model 615 RGS), and two Varian 12 inch diffusion pumps (Model 0185) bring chamber pressure down to 5E-5 Torr with no propellant flow (Fig.1). The pumps also allow a return to this pressure within 5 minutes after a 0.1 second gas pulse and a 6 grams per second mass flow. Heavier gases such as Xenon may take as much as 10 minutes to recover to the minimum pressure.

The propellant system consists of a 326 cubic foot argon T-bottle and regulator, with 28 cubic foot bottles of Hydrogen, Helium, Neon, Xenon, and Krypton also plumbed into the system. A thermocouple attached to the propellant line outside of the chamber gives a measure of the propellant temperature. The propellant lines feed into a 231 cubic inch plenum located inside the chamber. At the plenum, the mass flow is calculated by measuring the pressure drop per gas pulse.

A Del Electronics Corp power supply (Model HPS-1-8000-3) supplies up to 8 kWe of power to a pulse forming network (PFN). The PFN is a ten section LC network with a nominal 0.01 ohm output impedance. Each section consists of three 2000 microfarad Maxwell capacitors (Model 33800) connected in parallel and a 5 turn, 0.53 microhenry inductor. Together they release a one millisecond current pulse at up to 40 kAmps and 400 volts to the thruster, assuming a perfectly matched load (Figs. 3,4).

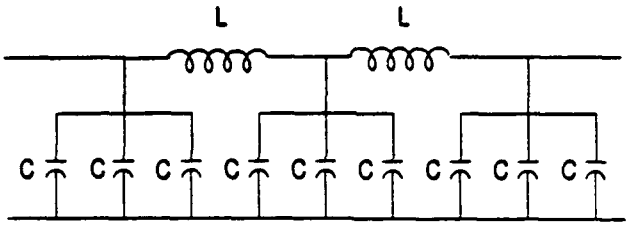

Figure 3
Schematic-Pulse Forming Network

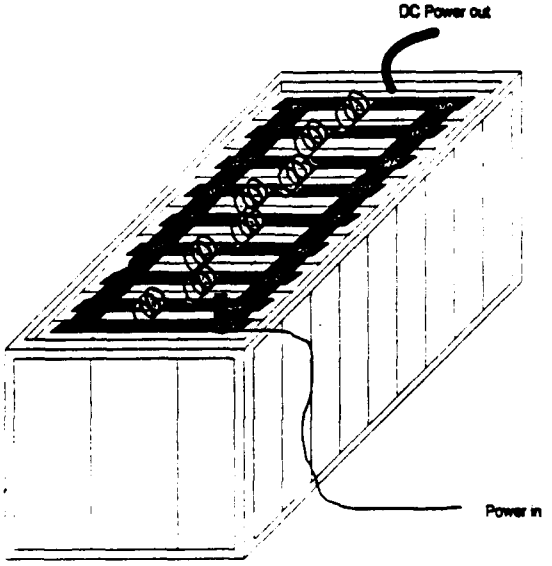

Figure 4
Pulse Forming Network

Facility data is collected with a variety of devices. Chamber pressure is measured with a Varian 843 vacuum ionization gauge. Pearson Electronics current pulse transformers (Model 301X) measure the current flowing through the thruster. Voltage across the thruster is measured by probes attached to the PFN. Both voltage and current data are collected on a Tektronix DAS 601 digital oscilloscope.

MEASUREMENT MODEL

The thruster's motion is modeled for experimental simplicity and repeatability. The thruster is a copper cylinder (about 116 pounds) suspended on two nylon ropes (Fig. 5). Operating a steady-state MPD thruster and knowing the exact thruster weight and displacement can yield a very accurate thrust measurement. However, the PLEPL thruster operates in a pulsed mode with a total firing time of 1.5-2.5 milliseconds. This negates any attempt to use a static force vector model. The alternative is to model the thruster as a pendulum. An instantaneous momentum change is a good approximation (Eq. 1), since the firing pulse time is much less than the period of the thruster swing.

Impulse = mass * change in velocity Equation 1

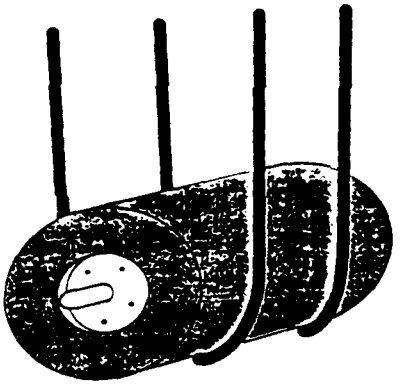

Figure 5
MPD Thruster

The calibration model selected is an inelastic collision of a pendulum colliding with another pendulum. (Fig. 6)(Ref. 10)

Let m = mass of ball

M = mass of thruster

V_b = velocity of ball

V_t = velocity of thruster

K = coefficient of restitution (value between 0 and 1)

subscript 1 indicates values before collision and subscript 2 values after collision.

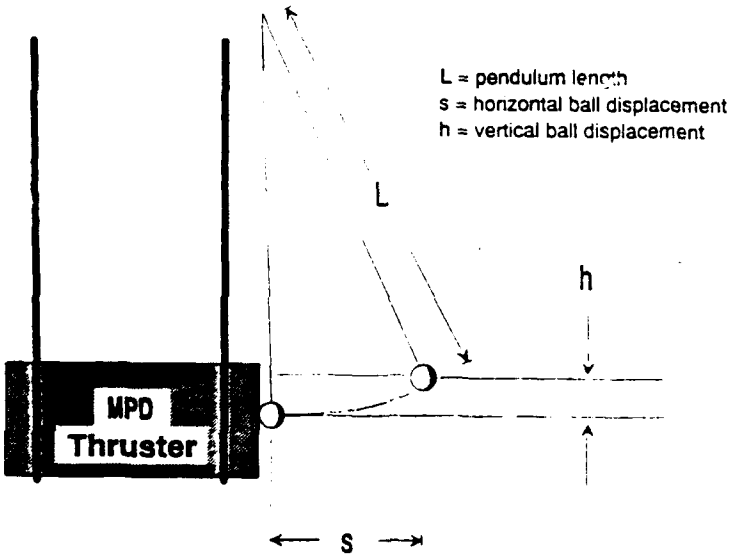

Figure 6a
Ball Impacting Stand

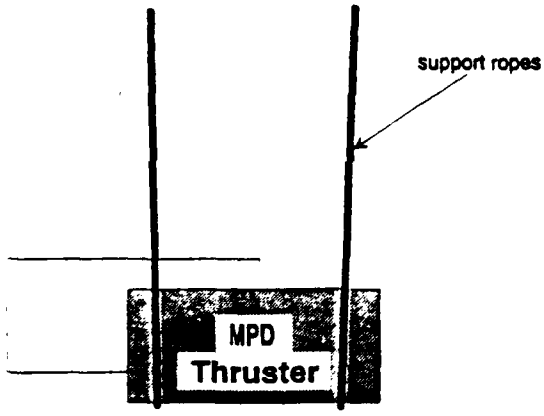

Figure 6b
MPD Pendulum

From conservation of momentum (inelastic collision), the equation is:

$$k(mV_{b1} + MV_{t1}) = mV_{b2} + MV_{t2}$$

Since the velocity of the thruster is zero before collision,

$$V_{t1} = 0 \qquad \text{Equation 2}$$

This reduces the conservation of momentum equation to:

$$kmV_{b1} = mV_{b2} + MV_{t2} \qquad \text{Equation 3}$$

Solving Equation 3 for velocity of ball after collision gives:

$$V_{b2} = \frac{kmV_{b1} - MV_{t2}}{m} \qquad \text{Equation 4}$$

From conservation of energy, we have the equation:

$$\frac{1}{2}kmV_{b1}^2 + \frac{1}{2}kMV_{t1}^2 = \frac{1}{2}mV_{b2}^2 + \frac{1}{2}MV_{t2}^2$$

Substituting in $V_{t1} = 0$ from Equation 2, this reduces to:

$$kmV_{b1}^2 = mV_{b2}^2 + MV_{t2}^2 \qquad \text{Equation 5}$$

Substituting Equation 4 into Equation 5 and solving for the velocity of the thruster after collision yields:

$$V_{t2} = V_{b1}\left[\frac{k + \sqrt{k\left(1 + \frac{m}{M}\right) - \frac{m}{M}k^2}}{\left(1 + \frac{M}{m}\right)}\right] \qquad \text{Equation 6}$$

When k=1 (elastic collision), Equation 6 reduces to:

$$V_{t2} = \frac{2V_{b1}}{\left(\frac{M}{m} + 1\right)} \qquad \text{Equation 7}$$

The total impulse imparted to the thruster, I, is:

$$I = M \triangle V$$

$$I = M \left(V_{t2} - V_{t1}\right)$$

or substituting in Equations 2 and 6:

$$I = MV_{b1}\left[\frac{k + \sqrt{k\left(1 + \frac{m}{M}\right) - \frac{m}{M}k^2}}{\left(1 + \frac{M}{m}\right)}\right] \qquad \text{Equation 8}$$

The velocity of the ball before impact can be determined by equating its potential energy before release to its kinetic energy at the bottom of its swing.

$$mgh = \frac{1}{2}mV_{b1}^2$$

Thus the total impulse imparted to the thruster is:

$$I = M\sqrt{2gh}\left[\frac{k + \sqrt{k\left(1 + \frac{m}{M}\right) - \frac{m}{M}k^2}}{\left(1 + \frac{M}{m}\right)}\right] \qquad \text{Equation 9}$$

where g is acceleration due to gravity, and h is the vertical distance the ball traveled from release to the bottom of its swing. Using trigonometric ratios (Fig. 6a), the height, h, can be equated to the length of the pendulum, L, and the horizontal displacement, s.

$$h = L - \sqrt{L^2 - s^2} \qquad \text{Equation 10}$$

Both L and s are much larger and much easier to measure to a greater degree of accuracy than h. Since g is known and m and L are measured for a given pendulum, it is only necessary to measure s to determine the impulse exchanged with the thruster.

PHYSICAL COMPONENTS

Total Impulse Stand

The primary impulse stand components are a machinist's dial indicator attached to the thruster, and a fixed metal support for the dial indicator (Fig. 7). The PLEPL used two dial indicators. The first one is a Chicago Dial Indicator Co. indicator measuring in thousandths of an inch (part number 2-C100-1000). It performed well, although there are uncertainties in how vacuum conditions affect the indicator spring lubricant and measurement rod. The second dial indicator is a Checker brand indicator and has a much smoother operation in air and in vacuum.

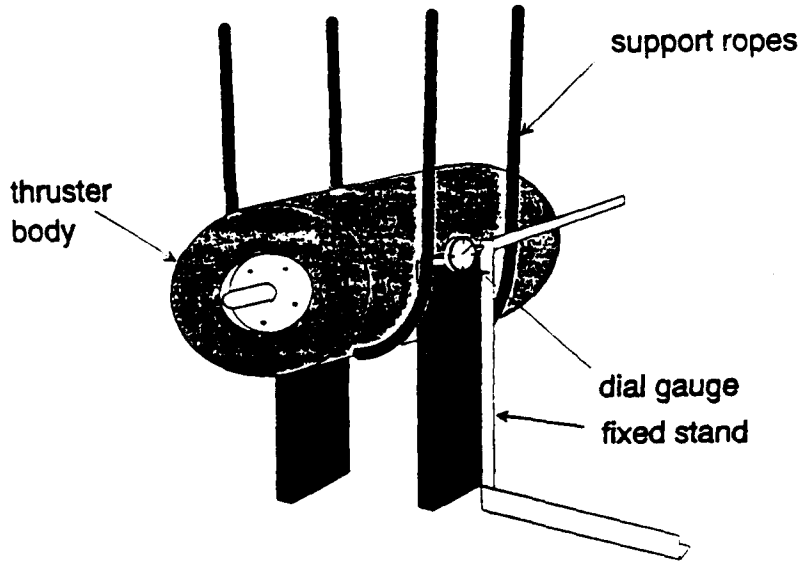

Figure 7
Impluse Stand

The fixed metal support is a plate attached to the vacuum chamber floor with a 1.0 inch Plexiglas insulation. The Plexiglas allows for smooth motion along the surface face. Repeated measurements with the Plexiglas covered support have proven consistent.

Video Recorder System

A video camera is located outside the vacuum chamber. The video camera is aimed through a view port window at approximately a 45 degree angle relative to the dial face. During testing, the dial deflections are viewed on a video monitor in the PLEPL control center and recorded on a video tape. The camera records at a speed of 1000 frames per second, which is sufficient to find the maximum deflection.

Calibration Components

The calibration components consist of a frame and attached solenoid, a rod for hanging calibration masses, and the masses (balls) themselves. The frame is an aluminum rectangular frame mounted on a flat base (Fig. 8). A solenoid device is attached to one leg of the frame to hold and release the balls. Also attached to the frame leg, behind the solenoid, is a measuring rule plate covered with graph paper. The rule plate serves as a positioning index to determine the initial horizontal displacement, s, of the ball from the thruster face.

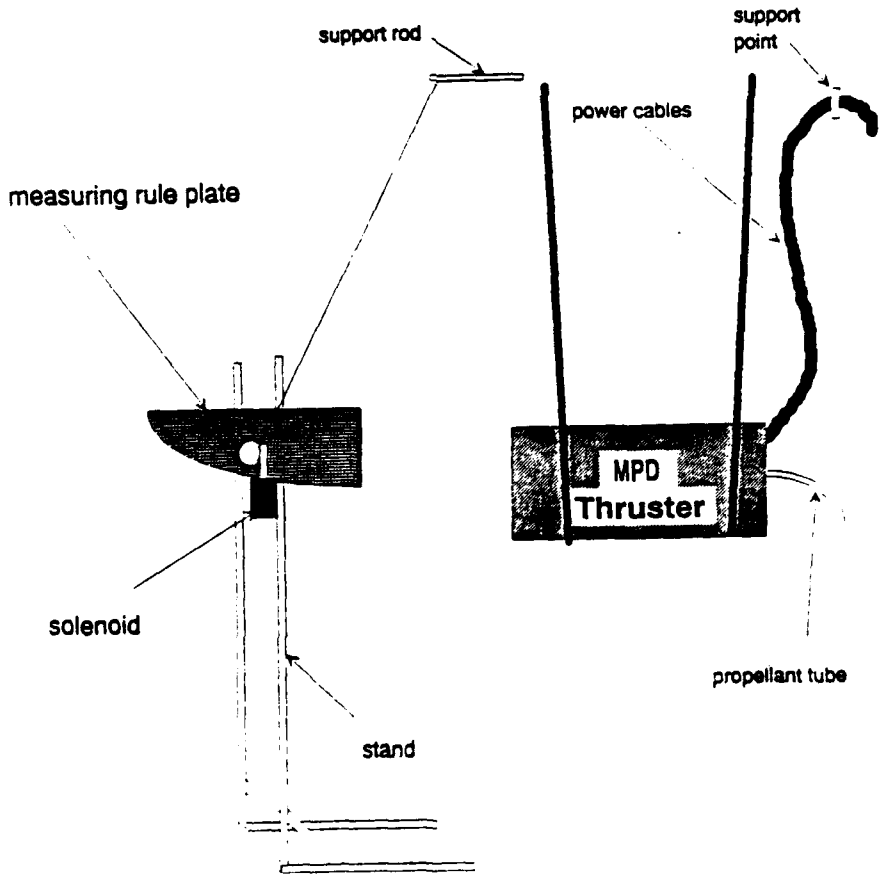

Figure 8
Calibration Components

The balls hang from an aluminum pipe rod (approximately 0.25 inch diameter). The rod is attached to the chamber ceiling and adjusted such that the balls barely touch the edge of the thruster face.

The final components in the calibration set are the pendulum ball masses. Three balls are used, with masses selected so that the impulse imparted to the thruster is on the same order as the impulse from a typical MPD test firing. Eyehole screws are set into the balls and a piano wire is attached. This allows a range below and above the expected MPD impulses for calibration purposes. The following table gives the values of the ball masses and wire lengths used.

Table 1. Ball Parameters

Ball	Mass (grams)	Length (meters)
#1	46.5 +/- 0.5	1.1748 +/- 0.01
#2	169.0 +/- 1.0	1.1684 +/- 0.01
#3	225.0 +/- 1.0	1.1862 +/- 0.01

Although the masses remain constant, there are some variations in wire length. This happens if wires break and have to be replaced or repaired, therfore the wire length must be remeasured. The length is measured from the top of the wire loop to the center of mass of the ball.

CALIBRATION PROCEDURE

Calibration is performed in an open (vented) vacuum chamber before and after a set of firings for a given thruster geometry. This permits checking variations in impulse measurements and gives an indication of impulse data uncertainty due to minor changes in experimental configuration.

Impulse Stand Calibration

The impulse stand calibration is a two person operation, with one person setting up in the chamber and another viewing the monitor, playing back the videotape, and recording the data.

Setup Procedures. Three different horizontal displacements, ranging from 10 centimeters to 50 centimeters, are used for each ball. The PLEPL has used 15 cm, 25 cm and 35 cm, roughly, in calibrations. For each ball, five identical drops are done at each displacement to ensure repeatability and statistical analysis. Forty-five data points are obtained in a typical calibra-

tion.

With the thruster in place, the calibration frame is placed in front of the thruster. The rod is adjusted so that the ball edge just touches the thruster face when the ball hangs motionless. The ball is also placed so that it strikes the flat part of the face. The measuring rule plate is adjusted to roughly the horizontal distance desired for testing. The exact distance does not matter, since the ball distance from the thruster is determined with the measuring rule. The triangular rule edge is brought within a centimeter from the thruster face. The distance is measured and added to the rule readings. When adjusting the measuring rule, care is taken to make sure it is parallel to the chamber floor and to the centerline of the thruster.

Finally, the solenoid is positioned to hold the ball, so that the ball swings freely and strikes the face of the thruster.

Calibration Procedure. Calibration begins with all elements in place. Four values are written down at each data point during stand calibration: the initial dial reading; the maximum displacement dial reading; the ball's initial horizontal displacement; and the ball being used. Horizontal displacements are read by looking at the edge of the ball against the measuring rule plate.

Once initial dial readings and horizontal displacements are recorded, the solenoid is activated and the ball released. When balls strike the face, they return to almost the same point from release (within 2 to 5 centimeters out of 15-35 centimeters or usually about 13 per cent). This gives a measure of k, the coefficient of restitution. After recording a portion of the collision (15 seconds after collision), the tape is stopped. The tape is advanced frame by frame to locate the maximum dial displacement. The best value of the dial displacement is ascertained together with an estimate of the uncertainty in the reading.

The calibration frame and the last ball are removed at calibration completion. The chamber door is shut and the vacuum chamber is ready for pump down. Once MPD thruster performance testing is over and the chamber is vented to atmosphere, the frame is brought back and the same calibration procedure is repeated.

Calibration Data Reduction and Analysis. The calibration data is reduced as follows: dial indicator readings are subtracted for absolute dial displacement; the corresponding total impulse imparted to the thruster for those displacements is calculated; the impulse due to the collision is found by using Equations 9 and 10; and a curve is found correlating impulse to dial displacements (with uncertainty included). Note that the particular correlation is valid for one set of thruster tests, i.e., one geometry. It is expected that impulse as a function of horizontal

displacement is a square root function, as shown in Figure 9.

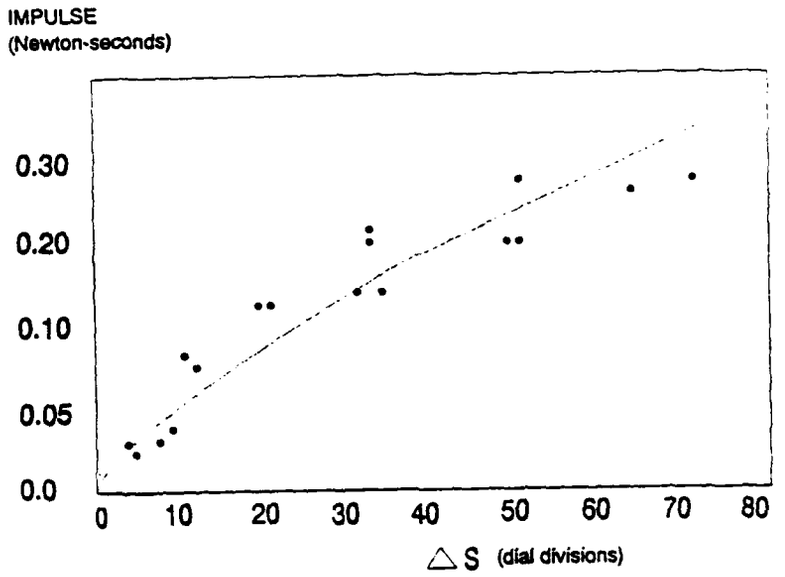

Figure 9
Impulse Calibration Curve

PULSED MPD TESTING

This section describes those key items involved in data collection pertaining to thrust and efficiency determination, and the procedure used in the PLEPL pulsed MPD in-house tests.

Thruster Operations

The half scale thruster is a copper cylinder (the anode) with a 2% thoriated tungsten cathode rod. A propellant tube and power cables attach at one end. A tungsten spark trigger is embedded in a boron nitride insulating plate inside the thruster. A large capacitor bank forms the pulse forming network (PFN). The PFN creates a square current pulse that is sent through the thruster. When the control center sends a fire signal, a valve opens releasing a gas propellant pulse. At the same time, the spark trigger releases a high voltage spark, which ionizes the gas in the thruster. Simultaneously, the PFN fires a high current electric pulse. This pulse creates the electric and magnetic fields in the thruster that interact to propel the ionized gas out of the thruster. The resulting thrust causes a dial indicator deflection which is recorded on video tape. At the same time, the thruster voltage and current are recorded on a digital oscilloscope (Fig. 10).

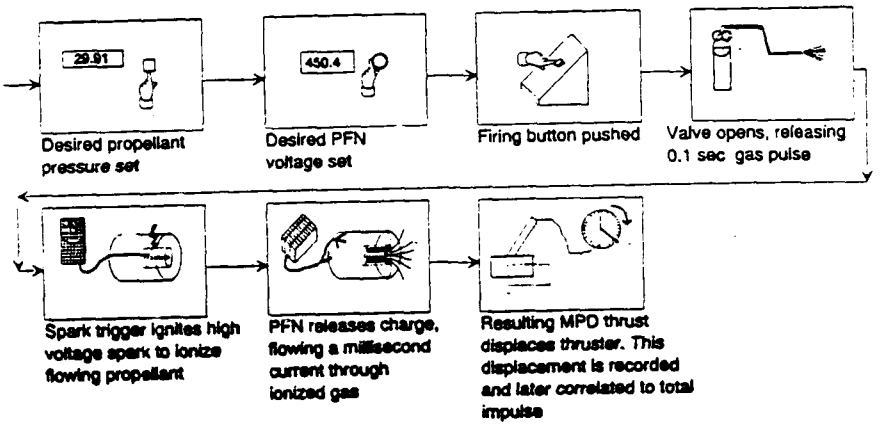

Figure 10
Thruster Firing Sequence

Cold Gas Tests

Before and after MPD thruster test firings, a series of cold gas tests are run to determine the cold gas impulse. In theory, the mass flow released through the gas valve should be constant. However, if the propellant line is twisted or the propellant feed holes into the thruster are stopped up, then there may be a change in mass flow. The cold gas tests indicate the variations in mass flow, which varies with different plenum pressures. As the plenum is filled with more gas, or as the temperature in the plenum rises, the pressure increases. This changes the mass flow rate. Finally, the PLEPL is interested in the MPD effects with respect to the impulse. Since the gas flow by itself causes impulse, the impulse due to MPD effects is found by subtracting the cold gas impulse from the measured impulse of an MPD firing.

The propellant system consists of a bottle of argon with tubing leading to a plenum located inside the chamber. Transducers measure plenum pressure and temperature. A valve driver controls the release of the gas pulse. Typical plenum pressures are 20 to 30 psia . The temperature is read from a thermocouple gauge connected to the propellant line at the argon bottle.

A Kistler force transducer (model 202A5/666M1) measures how long the plenum valve is open when gas is released. This data is collected on a Tektronix digital oscilloscope (model 11403). The curve generated is very nearly a square wave, with a tail dropping off exponentially. A method to approximate the pulse time is to integrate graphically and divide by the height of the nearly flat part of the curve, thus getting the pulse width of a perfect square wave with an equivalent area under the curve. Although a numerical quadrature of the curve data is possible, it is unnecessary (Fig. 11). A very simple graphical integration is to take the point of the drop (visually) where the area under the curve past the point is about equal to the area above the curve behind

the point. This area behind the point, if filled in, would complete the square wave. Typically, this is about the midpoint of the tail. Once this point is found, the pulse time can be read directly from the abscissa. The PLEPL has found that the gas pulse time is consistent, usually about 106 milliseconds.

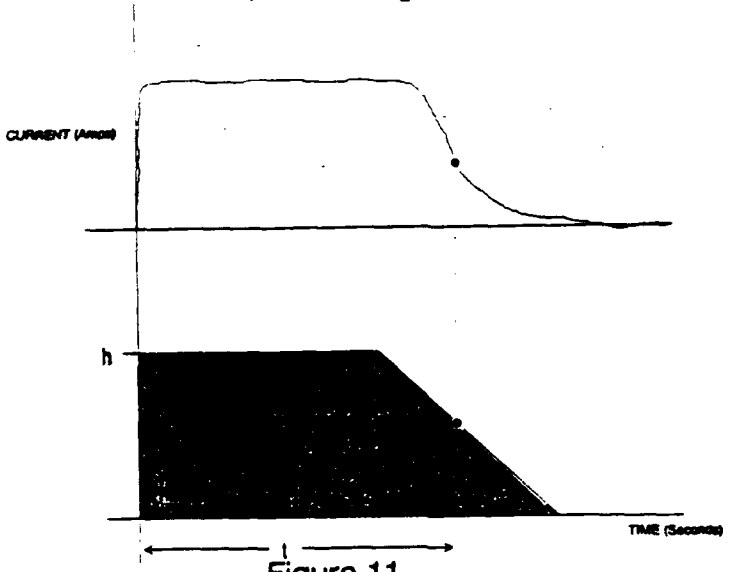

Figure 11
Graphical Integraton

The mass flow is calculated using the ideal gas law, PV=nRT, which is accurate for the low pressure, low density argon used in the PLEPL tests. The plenum is filled to the desired pressure, usually about 30 psia (sufficient time is allowed for the gauge readings to settle to a constant value). With the known volume, the initial plenum pressure and temperature are read from gauges. The cold gas pulse is fired and the pressure reading drops. Due to the mechanical inertia of the system, about ten seconds are allowed for the reading to settle to a constant value. The gauge is not allowed to settle too long, however, since the pressure goes up with temperature, which tends to rise over the term of an experiment (typically 1 degree Fahrenheit per half hour, during a four to five hour test period). From the final pressure recorded, the change in pressure is found and change in mass can be correlated. Dividing by the gas pulse time gives a quasi-steady state mass flow. The constants in the PLEPL mass flow calibrations are listed in Table 2.

Table 2. Mass Flow Cal Constants and Conversion Factors

Experimental Constants	
Plenum Volume	235.3 +/- 0.1 in^3
Gas Constant R	8.3144 J/mole*K
Mole Wt of Ar	39.94 g/mole
Conversion Factors	
$Inch^3$	1.6387064E-5 M^3
Psia	6.894757E3 N/m^2

The mass flow correlates linearly to initial plenum pressure (20 psi is about 1 g/sec and 30 psi is about 2 g/sec). The MPD tests are typically run at about 1.5 g/sec.

Concurrent with mass flow calibrations are cold gas impulse measurements, taken by recording dial indicator readings for each cold gas pulse. Typically, the displacements have been about 6 to 8 divisions of the dial indicator, although this is dependent on the alignment of the thruster and dial indicator. More importantly, the cold gas deflections have been approximately 25% of the total deflections of MPD thruster firings at high (600 V) voltages.

MPD Thrust Determination

From the impulse calibrations, the impulse from a firing can be correlated to total dial displacement. This impulse represents total impulse due to gas thrust and MPD thrust.

Thrust Calculations. Since the main interest is in thrust due to MPD effects, the impulse due to the gas thrust must be subtracted.

$$I_{tot} = I_{gas} + I_{MPD} \qquad \text{Equation 11}$$

The thrust due to MPD effects is the MPD impulse divided by the current pulse time taken from the oscilloscope. This is because the electromagnetic fields last only as long as the current is running.

$$\bar{T} = \frac{I_{tot} - I_{gas}}{t} \qquad \text{Equation 12}$$

Where T is the thrust due to MPD effects (in Newtons) and t is the current pulse time (in seconds). Specific impulse and electric power efficiency can be calculated using the following formulas (Ref. 11).

$$I_{sp} = \frac{\bar{T}}{\dot{m} g_o} \qquad \text{Equation 13}$$

$$\eta = \frac{I_{sp} T g_o}{2VJ} \qquad \text{Equation 14}$$

Here V is the voltage and J the current flowing through the thruster. The mass flow is m, and g is the standard acceleration due to gravity at sea level (9.8066 m/s^2). The efficiency gives a measure of how much of the electric power is transformed into thrust power.

Sample Calculation of Thrust. A sample of the impulse data taken so far gives an indication of how much a "direct" impulse measurement varies from the inelastic collision model impulse. The true impulse imparted to the thruster is difficult to measure, but as an approximation, the dial indicator displacement can be used as an order of magnitude measure of the thruster displacement. This, along with the calculated value of the thruster mass (from volume of the thruster and copper density) allow for an approximate measure of the thruster impulse. Table 3 shows the sample values used and the resulting impulses. As can be expected, the "direct" measurement is lower than the actual impulse imparted, which is due to friction and interference losses and is discussed in the next section.

Table 3. Example Thruster Data

Ball Data		Thruster Data	
Mass 0.169 kg Wire Length 119.4 cm		Mass 58.127 kg Rope Length 120 cm	
s (cm)	H (cm)	Dial Disp (cm)	H (cm)
14.3	0.859	0.043	7.7E-6
28.5	3.45	0.100	4.2E-5
38.0	6.21	0.136	7.7E-5
I (N-s)		I (N-s)	
0.115		0.071	
0.219		0.167	
0.280		0.226	

SOURCES OF ERRORS

There are a number of errors and uncertainties associated with the pendulum impulse stand, mass flow measurements and electrical measurements.

Thruster/ Ball Support Errors

Losses in energy occur due to friction in the calibration mass wires and the thruster ropes. A pendulum model assumes that the ropes are identical and aligned in parallel. Minor off-axis alignments cause the horizontal displacement to be less than the actual displacement. The off-axis alignment can cause extra, complex modes of thruster oscillations that subtract energy from translational motion. Loss in energy due to friction in calibration wires was found to be less than 0.5 percent in check-out tests.

The errors due to changes in system alignment are difficult to determine. However, the pre and post impulse stand calibration give some measure of the variation in the calibration system. As an example, during calibration system check-out, a roughly linear calibration curve was generated. The slope of the line was 0.00792 N-s/mil. After the stand was removed and placed back (more severe distortion than that caused by vacuum conditions or firings), calibration was repeated. The new slope measured was 0.00688 N-s/mil (13 percent change).

Dial Indication Errors

Misalignment of the dial indicator can cause a lower dial displacement reading than would normally be read. Ideally, the centerline of the thruster is normal to the support surface. To measure displacement along the centerline of the thruster, the rod should also be parallel to the thruster and normal to the support surface. Since both are not always possible, the main effort is in placing the rod normal to the support. This is justifiable for correlating impulse to indicated dial displacement since the actual distance traveled by the thruster is not easily measured.

Video Tape Errors

The largest errors affecting the accuracy of the impulse measurements are those associated with reading the dial indicator values from the recorded video tape. The tape records motion at certain time intervals. The probability is small that the true maximum is recorded. The PLEPL takes five measurements with the same ball in the same position, so that the errors in finding the maximum are averaged out. Tests taken with larger numbers of data indicate that five measurements usually result in average errors of less than 1 division.

Another problem associated with the video tape is that the pictures vary in clarity. Some are quite clear and are probably

indicative that a value very close to the true maximum has been obtained. These can be read to an accuracy of +/- 0.1 divisions. Others are blurred action shots that result in uncertainties ranging from +/- 0.2 divisions to +/- 1.5 divisions. Lighting and shadows also make readings difficult.

Other Stand Errors

Other possible effects on the calibration are magnetic force perturbations and aerodynamic drag on the balls. Although the potential for magnetic interference is great given the strong magnetic fields generated, tests indicate that they have had negligible effect on the impulse stand. Under vacuum conditions, the cathode was shorted to the anode to prevent the thruster from eroding while it was fired with no gas pulse. When the thruster was fired, magnetic fields similar to those from an actual firing were created. No motion was indicated on the dial face, demonstrating that magnetic perturbations do not affect impulse measurements on the stand.

A similar test was done to determine air drag effects. The calibration stand was set up and a ball was dropped several times, as is normal for calibration. The chamber was then pumped down to vacuum and the ball was placed on the holder using a remote positioning arm. The ball was dropped the same number of times and showed the same deflection as that for open air testing. This was as expected, given the small wire and ball sizes and velocities involved (relative to system mass). This experimental verification confirmed the fact that open air calibration is valid.

Concerns about the dial indicator interference were addressed by setting up the calibration stand and a measuring rule, and visually measuring the thruster displacement with and without the dial indicator attached. The thruster displacements were quite small, on the order of 1/32 of an inch. The thruster motion was slightly larger with the indicator removed, but how much larger could not be determined. It was not more than 3/64 inch total displacement.

Power cable interference was checked (with the dial indicator attached) in a similar fashion by dropping a ball with and without the power cable attached. The difference was approximately one division on the dial indicator (approximately 1/1000 inch). This indicates that the cable provides minimal resistance to thruster motion. With the small velocities involved, any linear damper is going to have a small resistive force. Thus, the cable acts as a very light damper, with almost no effect on measured thruster displacement.

Table 4. Measurement Uncertainties
(max indicates errors may be smaller,
% means error is percentage of value)

Item	Units	Range	Uncertainty
Ball Horiz Dist	cm	10-50	+/- 0.5
Dial Displacement	mils	5-60	+/- 1.5 max
Thruster Mass	kg	58.127	+5, -1
Plenum Pressure	psia	20-30	+/- 0.5
Plenum Temp	deg F	80-100	+/- 1
Vacuum Pressure	Torr	5E-5 - 5E-4	+/- 1%
Thruster Current	kA	0.8 - 30.0	+/- 0.001
Thruster Voltage	V	50 - 750	+/- 1
Gas Pulse Time	msec	106	+/- 0.1
Current Pulse Time	msec	1.5 - 2.5	+/- 0.01
Local Accel Gravity	m/sec	9.79366824	+/- 1.8E-6
Mass Flow	g/sec	1.0 - 2.0	+/- 1.2

Mass Flow Errors

The mass flow is a crucial datum. Mass flow must be known accurately and precisely to get realistic performance values. The mass flow system used in pulsed MPD testing was reasonably precise, but it did not allow an accurate mass flow measure. The thermocouple allows only an approximate temperature measure, since it was located outside of the chamber instead of on the plenum. The plenum-valve system made it very difficult to attain the same pressure for a test set. The mass flow directly depends on the plenum pressure. Difficulty in setting the exact same pressure was not an error in itself, but to speed up testing, a variation in pressure settings was accepted by the test team. This led to various mass flows being taken for different test cases. The "errors" arise in interpretation of the data. Which effects were due to different mass flow levels and which were due to plasmadynamic effects? It was impossible to tell. Finally, the mass flow was calculated by finding the pressure change before and after a gas pulse. The problem was that the pressure change was on the order of 0.2 psi. The plenum pressure gauge was selected for expected plenum pressures (order 30 psi), so that the gauge accuracy was on the order of 0.5 psi. Although pressure changes were taken, the accuracy of those measurements is uncertain, as is the absolute accuracy of the mass flow.

Well after the test matrix was conducted, an alternate mass flow calibration was devised for another project being run in the pulsed MPD facility. This technique consisted of flowing propellant into another plenum in place of the thruster. A highly accurate pressure gauge in that plenum measured the change in pressure due to a gas pulse. Since the pressure change could be measured very accurately, using the ideal gas law yielded the

mass flow out of the original plenum. Thus a correlation between the original plenum pressure and mass flow was attained. It turned out that the previous mass flow calibration curve (obtained using the old technique) was correct. Although the pressure gauge used in the old technique was used below its stated accuracy, the detected pressure changes were good enough to yield accurate calibration curves. The data taken with the old technique is probably correct in mass flow magnitude, but since the accurate calibration was taken long after the data was taken, the statements made in the previous paragraph must hold.

Voltage and Current Measurement Errors

Current and voltage measurements are needed for power efficiency calculations and for comparison of measured thrust to theoretical thrust. The voltage was measured by an attachment to the PFN circuit. Although in theory the location should give the correct thruster voltage (minus a minute drop through the power cables), in actuality the high currents involved may have influenced the voltage measurements. All the testing for this project was done with voltage probes attached to the PFN. Recently, the probes were reattached at the power feedthroughs entering the rear of the chamber. This resolved many odd current and voltage traces previously obtained with the old voltage measurement. Unfortunately, the complete test matrix had already been taken with the old location, resulting in erroneous voltage data being recorded. The extent of the uncertainty is not clear, but it may be as large as +/- 15 per cent.

Another concern with voltage measurement was impedance matching the thruster load and the PFN. This concept was not considered until the testing was over with. However, impedance matching is an important step in the MPD testing. If the thruster-PFN system is not properly matched, the voltage experiences a ringing or underdamped effect. Although this effect is not necessarily deleterious to the thruster, it does invalidate the performance results for comparison with other researcher's results. The only variable changeable in the MPD facility is the PFN inductance. Although it is not very convenient to change, the PFN inductance can be made to match almost any impedance. The impedance is a function of PFN current and capacitance, both of which vary with the level of PFN voltage. Voltage variation will require matching at various power levels.

The current was measured with Pearson coils. These coils are actually transformers that measure electric current in cables run through the coils. Although the coils are highly accurate, they do have a saturation limit. That theoretical limit is at a PFN voltage of about 350 volts. Since testing has been done at up to 750 volts, it is clear that much of the high power current measurements are erroneous. This explains the odd currents and voltage-current (V-I) traces at the high power levels. Another problem having a great bearing on performance measurement is the pulse time measurement. This time pulse is used to calculate the MPD thrust. Since the pulse time is on the order of a millisec-

ond, slight variations in the measure can lead to large variations in calculated thrust. The technique used to estimate the time pulse is described in the cold gas calibration section. With the current pulse trace tail varying in position, the "equal areas point" has varied quite a bit. The variation may have been due to Pearson coil saturation, or it may have been due to real effects. The end result has been comparatively large variations in current pulse time. In discussion with E.P. researchers, it was agreed that the best estimate of the pulse width is at the point where the pulse curve has dropped to 95 per cent of its maximum height. This would make the data taken at PLEPL more consistent.

SUMMARY OF RESULTS

Although the data requires more verification, it does provide trends and magnitudes of the pulsed MPD thruster performance. Unfortunately, the variations are difficult to attribute to specific factors. As previously discussed in the error section, we cannot tell whether a certain curve varies because of thruster geometry, differences in mass flow, improper calculation of pulse time, or other subtle changes in test configuration. The appendix contains samples of voltage-current traces (the most accurate data taken), thrust versus power (a few illustrative examples and a summary of best fit curves), specific impulse versus power, efficiency versus power, efficiency versus specific impulse, and thrust versus thruster volume.

Many researchers present MPD data in the above format, with the exception that some researchers compare performance versus current rather than power. The PLEPL results compared to other researcher's results generally indicate a worse efficiency for the PLEPL thruster. Whether this is due to low accuracy data, due to the PLEPL thruster design, or due to the test configuration is difficult to determine. The V-I curves did compare favorably with those reported in the literature.

The final item in the list of graphs, thrust versus thruster volume, is not a standard method of presenting data. The purpose of this graphical representation was to correlate geometric magnitude to thruster performance. The motivation for this is that MPD thrust is produced by the interaction of electric and magnetic fields. Both the magnitude and orientation of these fields determine the thrust produced. The fields' orientation is directly related to thruster geometry. To a first order approximation, the thruster volume (open space) between cathode and anode is the basic geometric variable (assuming that the anode and cathode shapes do not vary, but the electrode lengths vary). The three types of data points (dots, squares, and triangles) are an attempt to group mass flow ranges together.

The trends indicate that thrust is inversely proportional to thruster volume. This is a stronger effect as power levels grow higher. Assuming the data is accurate enough to make this assess-

ment (recall the discussion in the error section, especially on the thrust measurement and high current measurement), we can infer that for smaller volumes, more of the power goes into thrust generation. Perhaps for longer electrode lengths, plasma-dynamic instabilities form which reduce the power available for propellant acceleration. This result needs to be verified, but the implications are promising. For a given MPD thruster diameter, the smallest length (and hence weight) may be the best performing.

LESSONS LEARNED

A new propellant system has been designed for the MPD facility. This system uses a fast acting piezo-electric valve and a choked orifice to provide a precise and accurate flow control system. The flow through a choked orifice is solely a function of the upstream pressure. Thus instead of measuring a change in pressure, only the absolute pressure is needed. A highly accurate pressure gauge will give this performance. The fast acting valve will have a 2 millisecond open and close time, which is of the pulse time order. This allows a very rapid settling time for the mass flow and requires less total propellant mass ejected during a pulse. It also allows a quicker vacuum chamber pressure recovery time. A larger plenum with an attached thermocouple will allow smaller total pressure changes and a direct measure of the propellant temperature.

The voltage will be measured solely at the power feedthroughs leading to the thruster. Impedance testing will be accomplished to determine required PFN inductance, and future tests will involve matched impedance.

The data will only be taken below Pearson coil saturation limits. Future upgrades will include purchase of Pearson coils that can handle currents up to 40 kAmp with little saturation. Pulse time widths will be taken at the 95 per cent drop off point.

Thruster impulse measurements have been impeded by thruster mass. The thruster was designed for machining ease and not for optimal experimental configuration. A near term upgrade will be to design a much lighter thruster with the same dimensions of interest. This way, the thrust pulses will cause larger displacements that can be more easily measured. A similar pendulum measurement system will be used, but a redesign will eliminate many of the old system uncertainties. The displacement will be measured with a LVDT or the acceleration will be measured with an accelerometer, thus giving a direct thrust measurement. The calibration will also involve a similar concept, but the calibration frame will be made sturdier and an improved ball release mechanism will be used.

Other questions remain regarding the pulsed MPD facility. A magnetic field characterization would be helpful in understanding

possible chamber interactions with the thruster. Effects of thruster warm-up on thruster performance also need to be investigated. And finally, some thermocouple measurements on heat distribution over the thruster might also be helpful in overall understanding.

FUTURE EXPERIMENTS

The data taken thus far has pointed the way toward an improved MPD thruster design. However, with the problems encountered with the facility, a data verification must be run with the improved facility. The verification will consist of a detailed repetition of data for a given thruster geometry and will give a measure of the accuracy of the previous data. In addition, an abbreviated test matrix will be run, repeating several of the previous electrode combinations. This test matrix will be designed using the Taguchi method to get maximum performance information with the minimum number of test runs.

Another area of investigation will be in the use of a pre-ionization plenum. Part of the motivation for this investigation is based on an incident which occurred during the initial test matrix. The boron nitride backplate came loose during a test firing. The thruster motion caused the plate to edge forward. Since the plate is embedded deep in the thruster, this motion was not apparent to the researchers. But the sudden jump in thruster performance was instantly noticed by the test team. What had previously been ordinary thrust levels and current pulse shapes became nearly double thrust levels and pulse curves that closely resembled an idealized square wave. There wasn't time to further investigate this, so the PLEPL will investigate a pre-ionization plenum at a later date.

A possible explanation for improved performance with a pre-ionization plenum is that the PLEPL MPD uses an embedded wire to create the spark that breaks down the propellant. This spark is asymmetrically distributed through the MPD cathode channel, as propellant flows and expands to a vacuum. Since the plasma is sensitive to initial conditions, asymmetries may create instabilities that reduce MPD performance. The pre-ionization plenum would provide a small holding area for better propellant ionization. This ionized propellant would uniformly enter the main MPD channel, where symmetric fields accelerate the propellant. This conjecture needs to be verified with a detailed experiment.

ERROR ANALYSIS

In experiments two types of errors propagate to cause an uncertainty in the final results (Ref. 12 and 13): systematic errors and random errors. Systematic errors are those that occur due to faulty calibration. Random errors arise from the inability to make totally accurate measurements from one observation to another. The precision of an experiment depends on the uncer-

tainty due to the random errors. This section discusses the estimates in random errors.

Assuming a Gaussian distribution in the experimental values about an average value, the uncertainty in determining the average value is proportional to the standard deviation of the distribution. The mean value of the distribution and the "true" value may not be equal. However, as can be shown in statistical theory, there is a 95 percent probability that the difference between the "true" value and the mean value is less than the uncertainty given by the standard deviation. This defines the uncertainty in the results. The definition does not give a value for the uncertainty, but it does allow a method for calculating the uncertainty of the results, given the uncertainties in the parameters that are used in the mathematical model.

If the model that describes the system has at least two parameters,

$$x = F(u, v, \ldots)$$

and the most probable value of the result, $\vec{X}$, is given by,

$$x = F(\bar{u}, \bar{v}, \ldots)$$

The uncertainty in X (ignoring cross terms) , , is given by

$$\sigma_x^2 = \sigma_u^2\left[\frac{\delta x}{\delta u}\right]^2 + \sigma_v^2\left[\frac{\delta x}{\delta v}\right]^2 + \ldots \qquad \text{Equation 15}$$

or for Equation 9, the uncertainty in impulse becomes

$$\sigma_I^2 = \sigma_M^2\left[\frac{\delta I}{\delta M}\right]^2 + \sigma_m^2\left[\frac{\delta I}{\delta m}\right]^2 + \sigma_g^2\left[\frac{\delta I}{\delta g}\right]^2 + \sigma_L^2\left[\frac{\delta I}{\delta L}\right]^2 + \sigma_s^2\left[\frac{\delta I}{\delta s}\right]^2 + \sigma_k^2\left[\frac{\delta I}{\delta k}\right]^2 \qquad \text{Equation 16}$$

In Equation 16, the σ's are the values listed in the uncertainty section of Tables 1 and 4. The values of the partial derivatives are listed in Appendix A. With the parameter uncertainties determined, a computer program calculates the uncertainty in each impulse calculated, given the measured parameter values.

CONCLUSION

The PLEPL has conducted a preliminary experiment in the establishment of MPD performance for different electrode length combinations. Data collected has given us an understanding of general trends in thruster performance, but limitations in experimental capability have prevented the use of this data in an absolute sense. The most valuable outcome of this project has been a much better understanding of MPD research requirements for the PLEPL staff. The pulsed MPD facility can now be upgraded to gather accurate MPD thruster performance data.

REFERENCES

1. Jahn, R.G., Physics of Electric Propulsion, McGraw-Hill, 1968.

2. Kaplan, David I.; Jahn, R.G.; Performance Characteristics of Geometrically Scaled MPD Thrusters, MAE 1492, Princeton University, Feb 1982.

3. Mead, F.B.; Jahn, R.G.; Scaling of MPD Thrusters, International Electric Propulsion Conference Paper 79-2075, Oct 30 - Nov 1, 1979, Princeton, New Jersey.

4. Kaplan, David I.; Jahn, R.G.; Performance Characteristics of Geometrically Scaled MPD Thrusters, MAE 1492, Princeton University, Feb 1982.

5. King, D.Q.; Jahn, R.G.; Clark, K.E.; Magnetoplasmadynamic Channel Flow for Design of Coaxial MPD Thrusters, MAE 1552, Princeton University.

6. Phillips, T.; Bell, K.; 100 Lbf ACS Engine Evaluation Program Facility Checkout Tests, AFRPL-TR-79-01, AFRPL, Edwards AFB, Aug 79.

7. Kaplan, David I.; Jahn, R.G.; Performance Characteristics of Geometrically Scaled MPD Thrusters, MAE 1492, Princeton University, Feb 1982.

8. Mead, F.B.; Jahn, R.G.; Scaling of MPD Thrusters, International Electric Propulsion Conference Paper 79-2075, Oct 30 - Nov 1, 1979, Princeton, New Jersey.

9. Gilland, J.H.; Kelly, A.J.; Jahn, R.G.;MPD Thruster Scaling, International Electric Propulsion Conference Paper AIAA-87-0997, May 11-13, 1987, Colorado Springs, Colorado.

10. Sears, F.W.; Zemansky, M.W.; Young, H.D.; University Physics, Addison-Wesley Publishing Co, Reading, Mass, 1983.

11. Kaplan, David I.; Jahn, R.G.; Performance Characteristics of Geometrically Scaled MPD Thrusters, MAE 1492, Princeton University, Feb 1982.

12. Bevington, Philip R., Data Reduction and Error Analysis for the Physical Sciences, McGraw-Hill, New York, 1969.

13. Hogg, R.V.; Tanis, E.A.; Probability and Statistical Inference, MacMillen, New York, 1983.

APPENDIX A
Partial Derivatives for Uncertainty in Mass Flow

$$\dot{m} = \frac{\Delta p \, v \, M}{R \, T \, \tau_g}$$

Δp = Change in Plenum Pressure
v = Plenum Volume
M = Molecular Weight
R = Universal Gas Constant
T = Temperature
τ_g = Gas Pulse Time

$$\frac{\delta \dot{m}}{\delta p} = \frac{vM}{RT\tau_g} \qquad \frac{\delta \dot{m}}{\delta v} = \frac{pM}{RT\tau_g} \qquad \frac{\delta \dot{m}}{\delta M} = \frac{pv}{RT\tau_g}$$

$$\frac{\delta \dot{m}}{\delta R} = -\frac{pvM}{R^2 T\tau_g} \qquad \frac{\delta \dot{m}}{\delta T} = -\frac{pvM}{RT^2\tau_g} \qquad \frac{\delta \dot{m}}{\delta \tau_g} = -\frac{pvM}{RT\tau_g^2}$$

APPENDIX B

Partial Derivatives for Uncertainty in Impulse

Let $\alpha = \sqrt{k\left(1+\frac{m}{M}\right) - \frac{m}{M}k^2}$

$\beta = 1 + \frac{M}{m}$

$\gamma = \sqrt{L - \sqrt{L^2 - s^2}}$

m = ball mass

M = thruster mass

L = string length

s = horizontal distance

k = coefficient of restitution

g = acceleration of gravity

$$I = \frac{M\sqrt{2g}\,\gamma\left[k+\alpha\right]}{\beta}$$

$$\frac{\delta I}{\delta m} = \frac{M\sqrt{2g}\,\gamma}{\beta}\left\{\frac{M(k+\alpha)}{m^2\beta} + \frac{k(k-1)}{2M\alpha}\right\}$$

$$\frac{\delta I}{\delta M} = \frac{\sqrt{2g}\,\gamma}{\beta}\left\{k+\alpha - \frac{M(k+\alpha)}{m\beta} + \frac{m\,k(k-1)}{2M\alpha}\right\}$$

$$\frac{\delta I}{\delta L} = \frac{M\sqrt{2g}\left(1 - \frac{L}{\sqrt{L^2-s^2}}\right)(k+\alpha)}{2\beta\gamma}$$

$$\frac{\delta I}{\delta s} = \frac{Ms\sqrt{2g}\,(k+\alpha)}{2\beta\gamma\sqrt{L^2-s^2}}$$

$$\frac{\delta I}{\delta k} = \frac{\gamma M\sqrt{2g}\left(1 + \frac{1+\frac{m}{M}(1-2k)}{2\alpha}\right)}{\beta}$$

$$\frac{\delta I}{\delta g} = \frac{M(k+\alpha)\gamma}{\beta\sqrt{2g}}$$

APPENDIX C

Partial Derivatives for Uncertainty in Thrust, Specific Impulse, and Efficiency

Thrust, T I = Total Impulse

τ_J = Current Pulse Time

$$T = \frac{I}{\tau_J}$$

$$\frac{\delta T}{\delta \tau_J} = -\frac{I}{\tau_J^2} \qquad \frac{\delta T}{\delta I} = -\frac{1}{\tau_J}$$

Specific Impulse, I_{sp} $\dot{m}$ = Mass Flow

$g_\circ$ = Gravitational Acceleration

$$I_{sp} = \frac{T}{\dot{m} g_\circ}$$

$$\frac{\delta I_{sp}}{\delta T} = \frac{1}{\dot{m} g_\circ} \qquad \frac{\delta I_{sp}}{\delta \dot{m}} = -\frac{T}{\dot{m}^2 g_\circ} \qquad \frac{\delta I_{sp}}{\delta g_\circ} = -\frac{T}{\dot{m} g_\circ^2}$$

Efficiency, η V = Thruster Voltage

J = Thruster Current

$$\eta = \frac{I_{sp} T g_\circ}{2VJ}$$

$$\frac{\delta \eta}{\delta I_{sp}} = \frac{T g_\circ}{2VJ} \qquad \frac{\delta \eta}{\delta T} = \frac{I_{sp} g_\circ}{2VJ} \qquad \frac{\delta \eta}{\delta g_\circ} = \frac{I_{sp} T}{2VJ}$$

$$\frac{\delta \eta}{\delta V} = -\frac{I_{sp} T g_\circ}{2V^2 J} \qquad \frac{\delta \eta}{\delta J} = -\frac{I_{sp} T g_\circ}{2VJ^2}$$

APPENDIX D
Test Matrix

Note: Lengths are in centimeters. Date indicates the day testing began on an anode–cathode combination.

Date	Cathode	Anode
6 Sep 89	3.2	3.2
8 Sep 89	8.4	8.4
12 Sep 89	3.4	8.4
15 Sep 89	13.4	13.4
4 Oct 89	8.4	13.4
11 Oct 89	3.4	13.4
2 Nov 89	18.4	18.4
9 Nov 89	13.4	18.4
21 Nov 89	8.4	18.4
27 Nov 89	3.4	18.4
29 Nov 89	3.4	20.4
1 Dec 89	8.4	20.4
6 Dec 89	13.4	20.4
8 Dec 89	18.4	20.4
13 Dec 89	20.4	20.4
11 Jan 90	3.4	3.4

APPENDIX E

Sample Voltage, Currents Traces, and V–I Characteristics

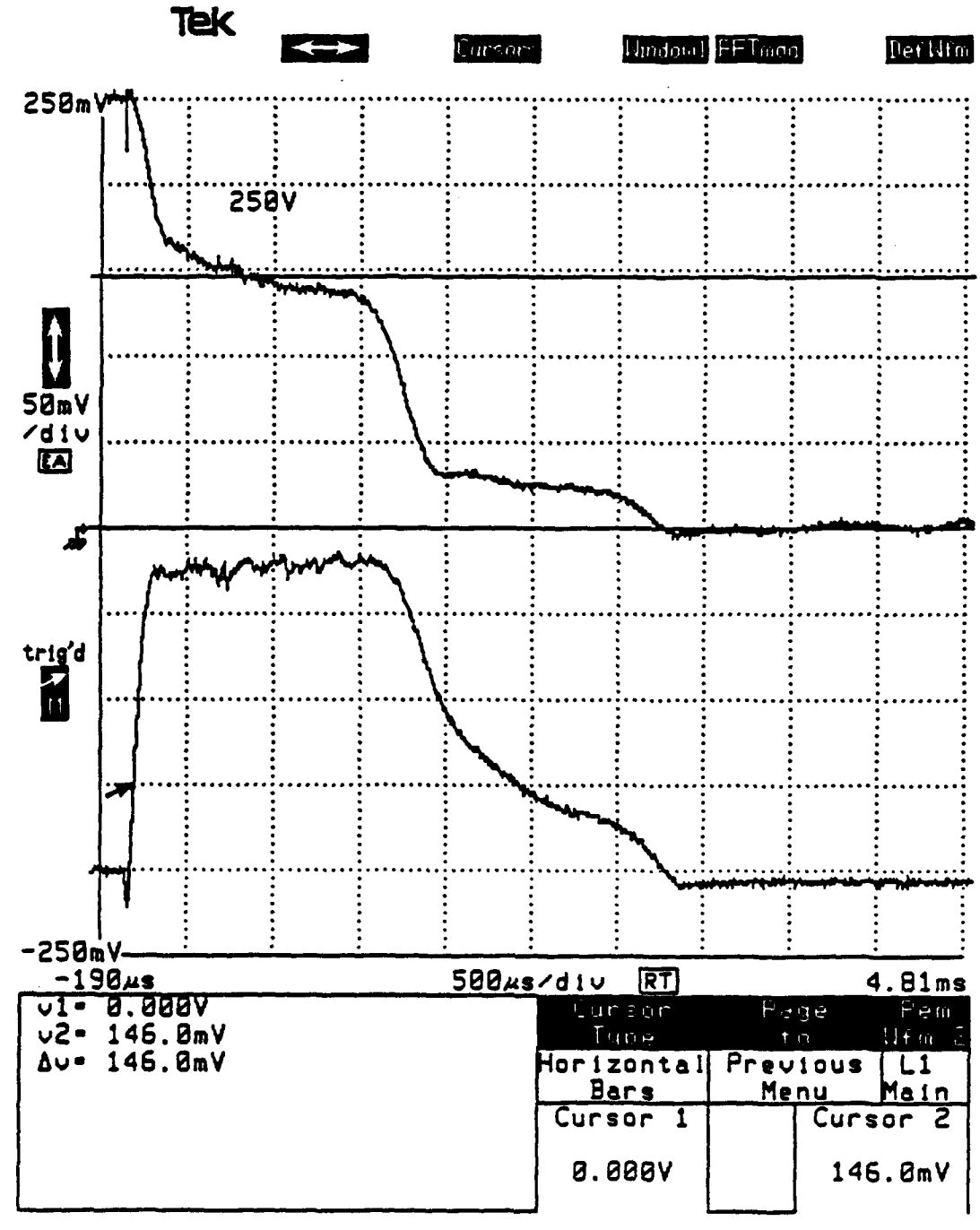

Voltage Trace

Current Trace

Typical (Good) Firing

– Note Square Wave Shape of Current Pulse

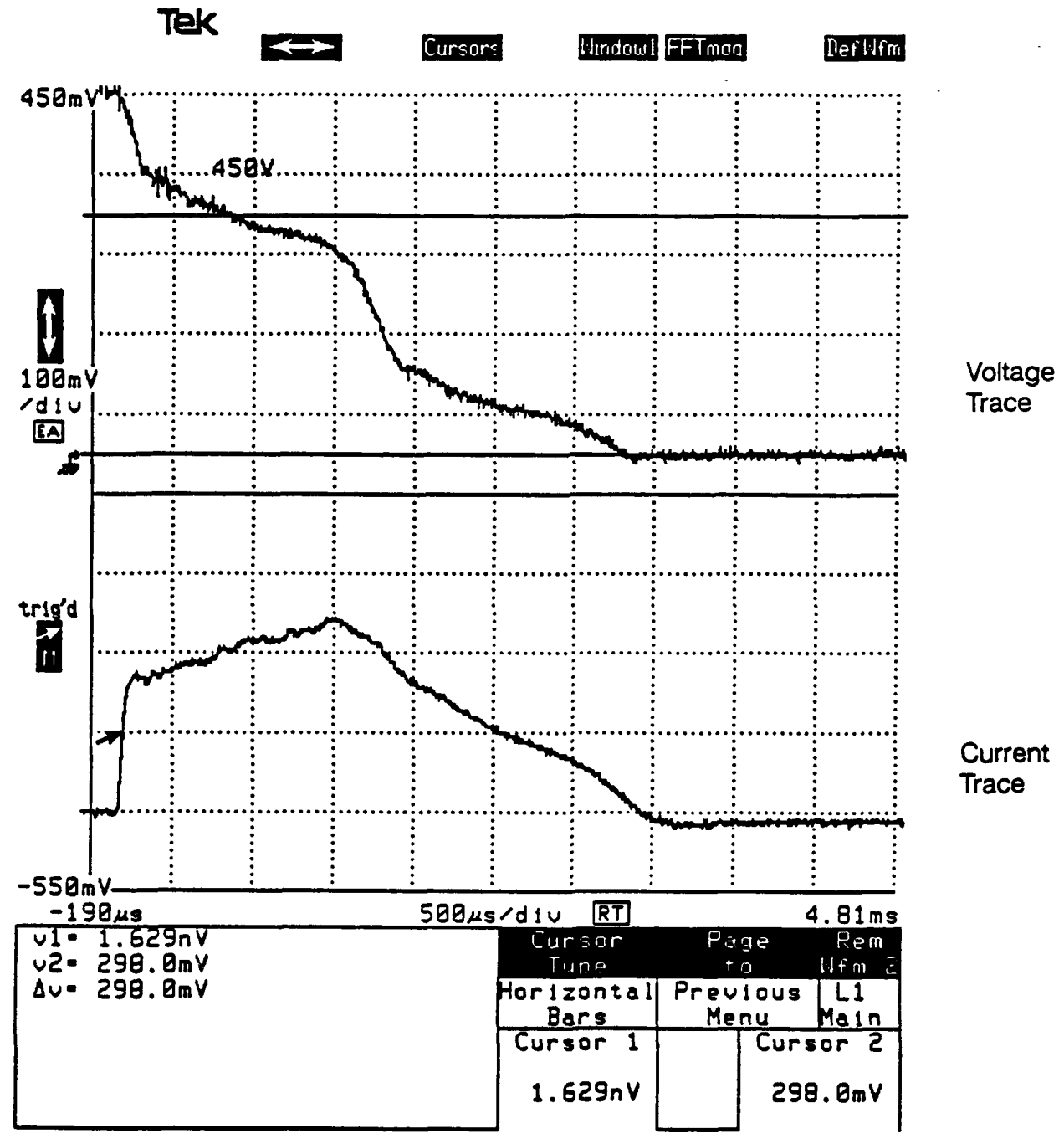

"Bad" Firing
– Note Drawn Out, Misshapen Current Pulse

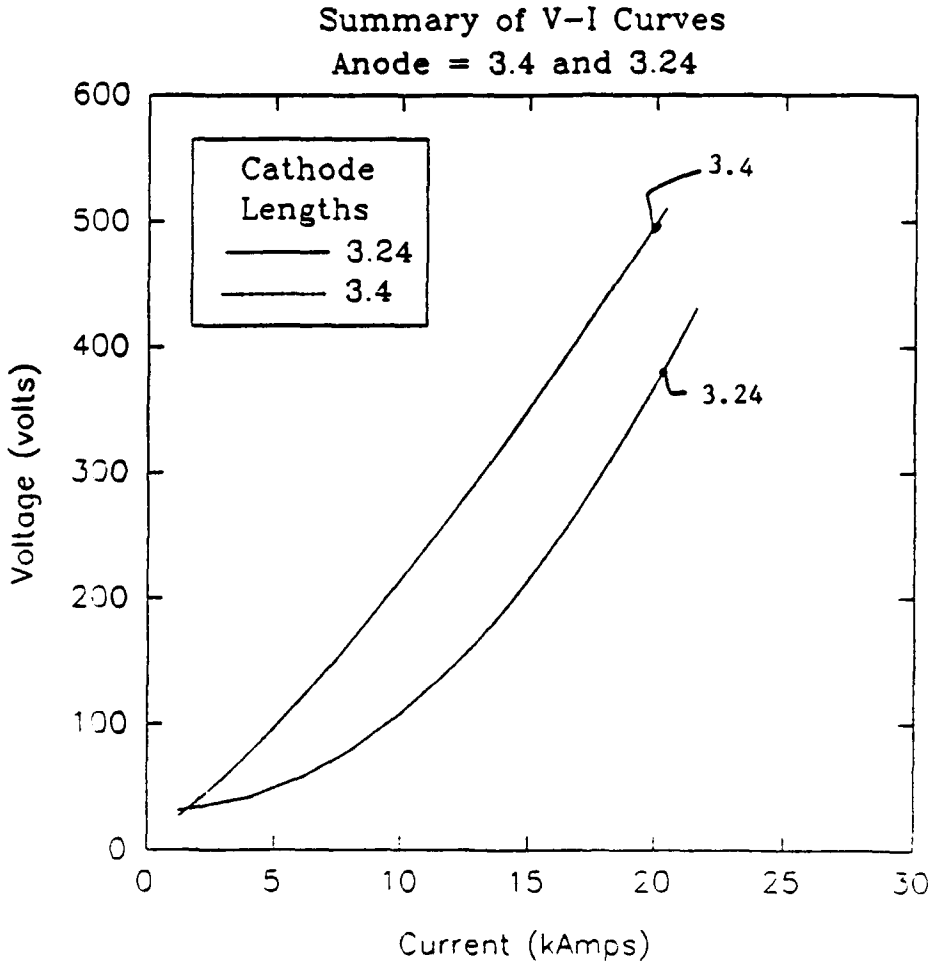
Summary of V-I Curves
Anode = 3.4 and 3.24
Cathode
Lengths
3.24
3.4
3.4
3.24
Voltage (volts)
600
500
400
300
200
100
0
0
5
10
15
20
25
30
Current (kAmps)

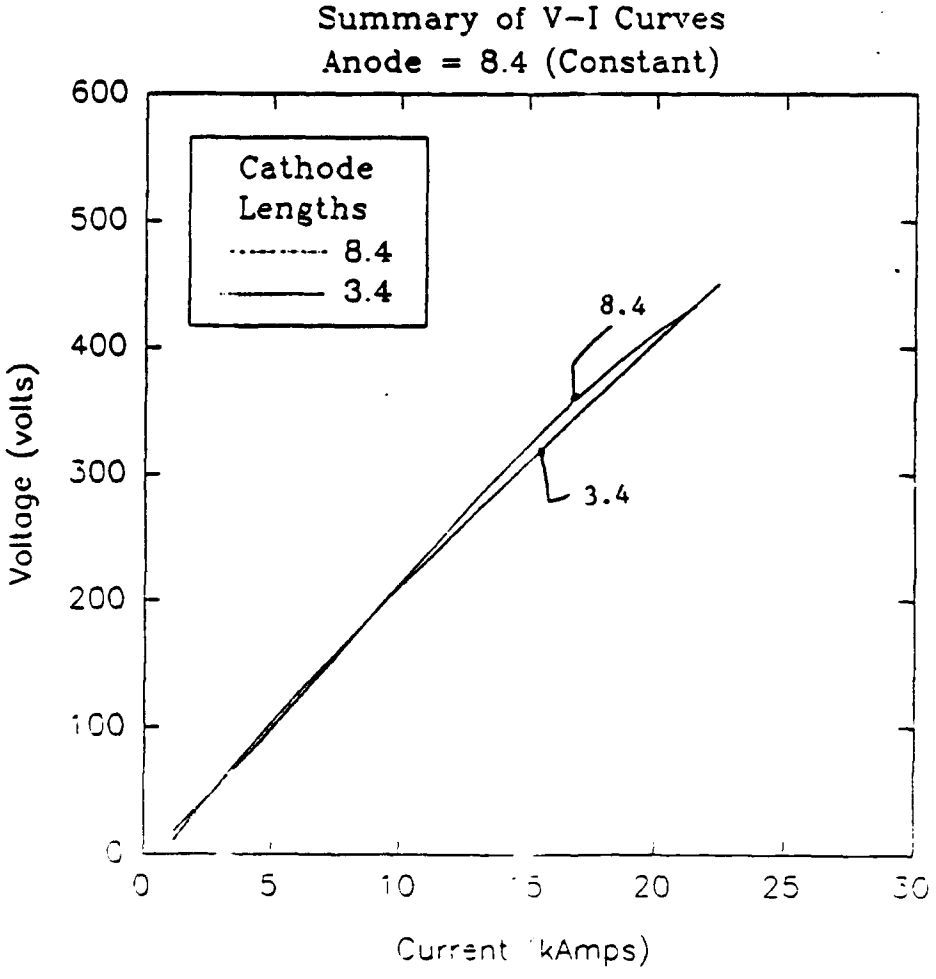
Summary of V-I Curves
Anode = 8.4 (Constant)
Cathode
Lengths
8.4
3.4
8.4
3.4
Voltage (volts)
600
500
400
300
200
100
0
0
5
10
15
20
25
30
Current (kAmps)

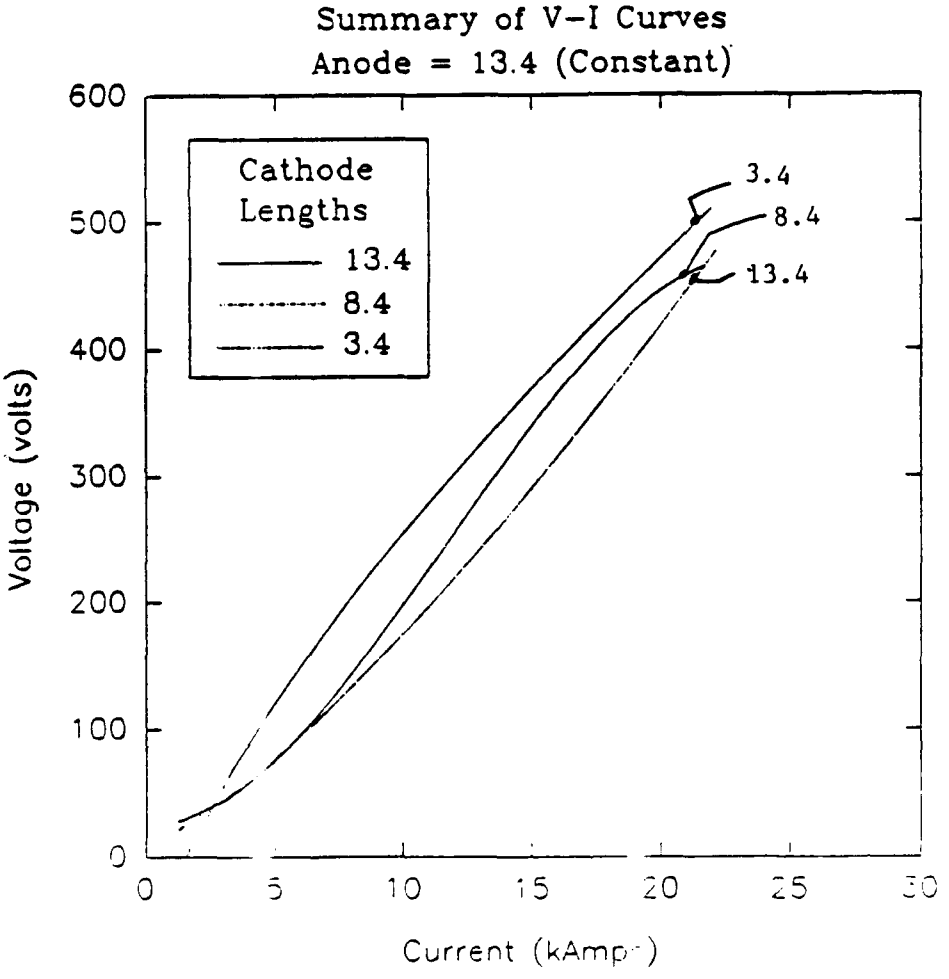
Summary of V-I Curves
Anode = 13.4 (Constant)
Cathode Lengths
13.4
8.4
3.4
3.4
8.4
13.4
Voltage (volts)
600
500
400
300
200
100
0
0
5
10
15
20
25
30
Current (kAmp)

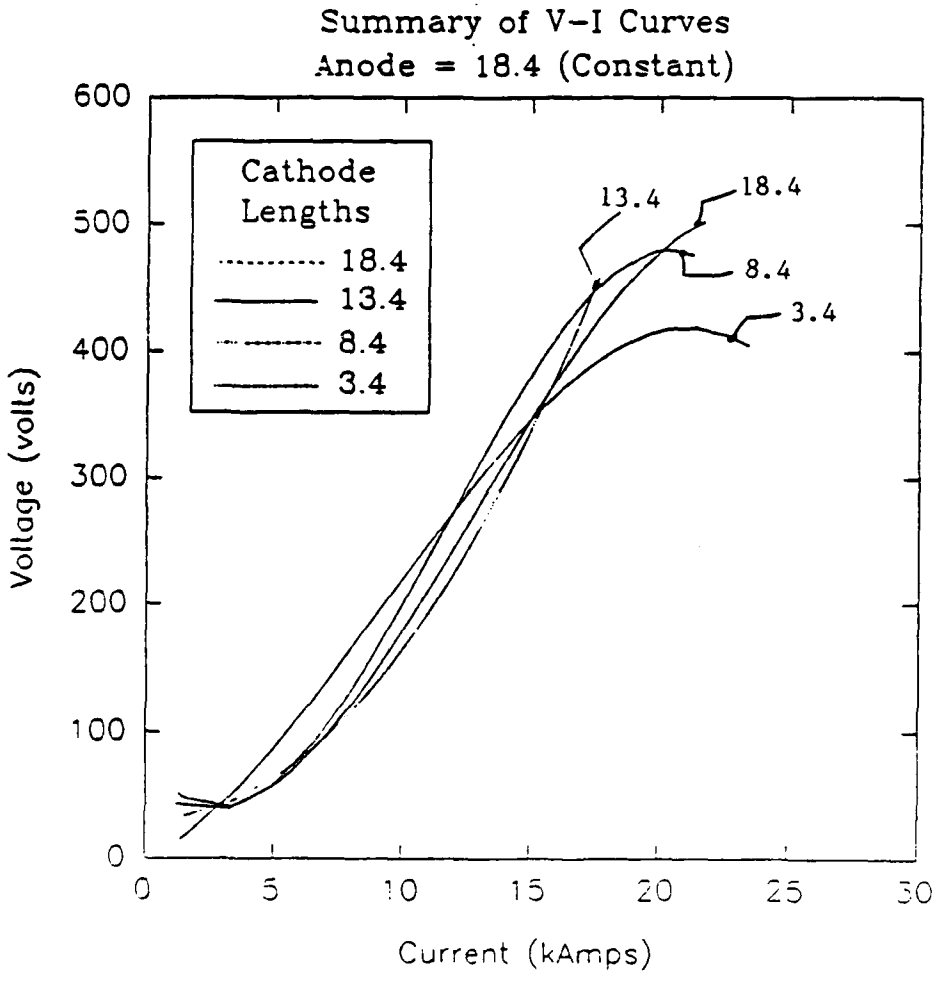
Summary of V-I Curves
Anode = 18.4 (Constant)
Cathode Lengths
18.4
13.4
8.4
3.4
13.4
18.4
8.4
3.4
Voltage (volts)
Current (kAmps)
0
100
200
300
400
500
600
0
5
10
15
20
25
30

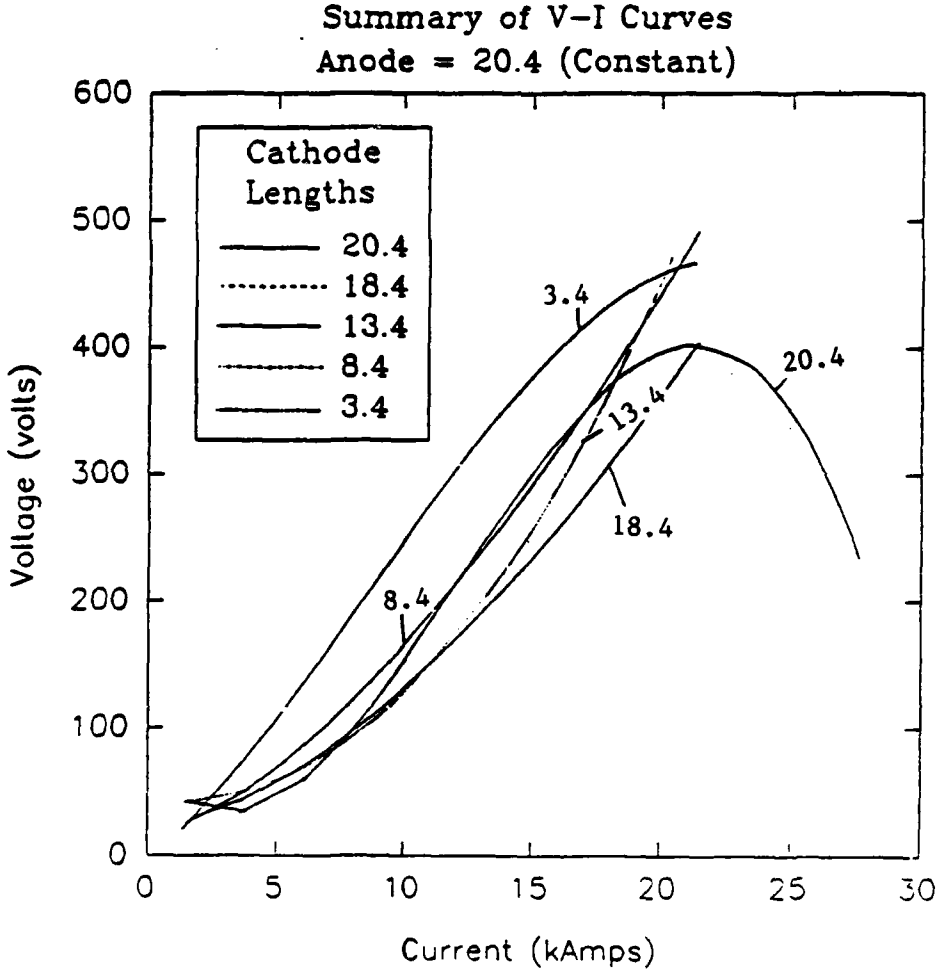
Summary of V–I Curves
Anode = 20.4 (Constant)
Cathode Lengths
20.4
18.4
13.4
8.4
3.4
Voltage (volts)
Current (kAmps)
0
100
200
300
400
500
600
0
5
10
15
20
25
30

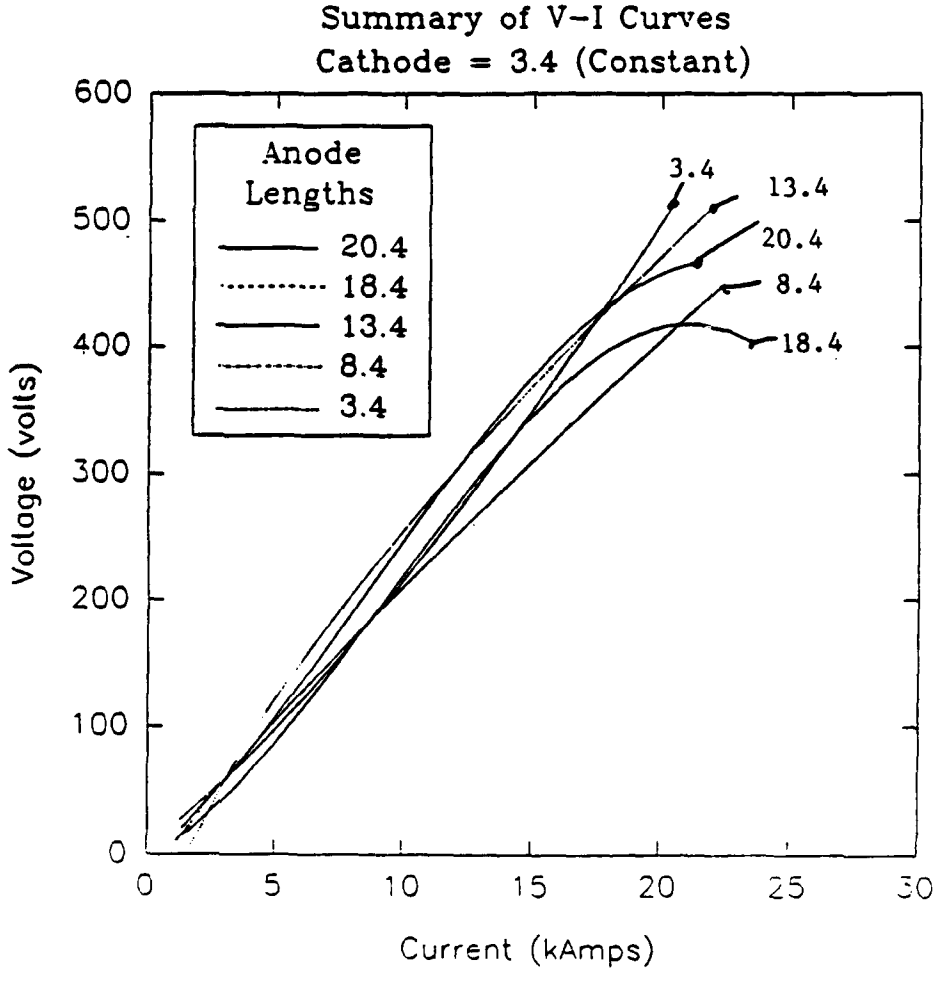
Summary of V-I Curves
Cathode = 3.4 (Constant)
Anode Lengths
20.4
18.4
13.4
8.4
3.4
3.4
13.4
20.4
8.4
18.4
Voltage (volts)
Current (kAmps)
0
100
200
300
400
500
600
0
5
10
15
20
25
30

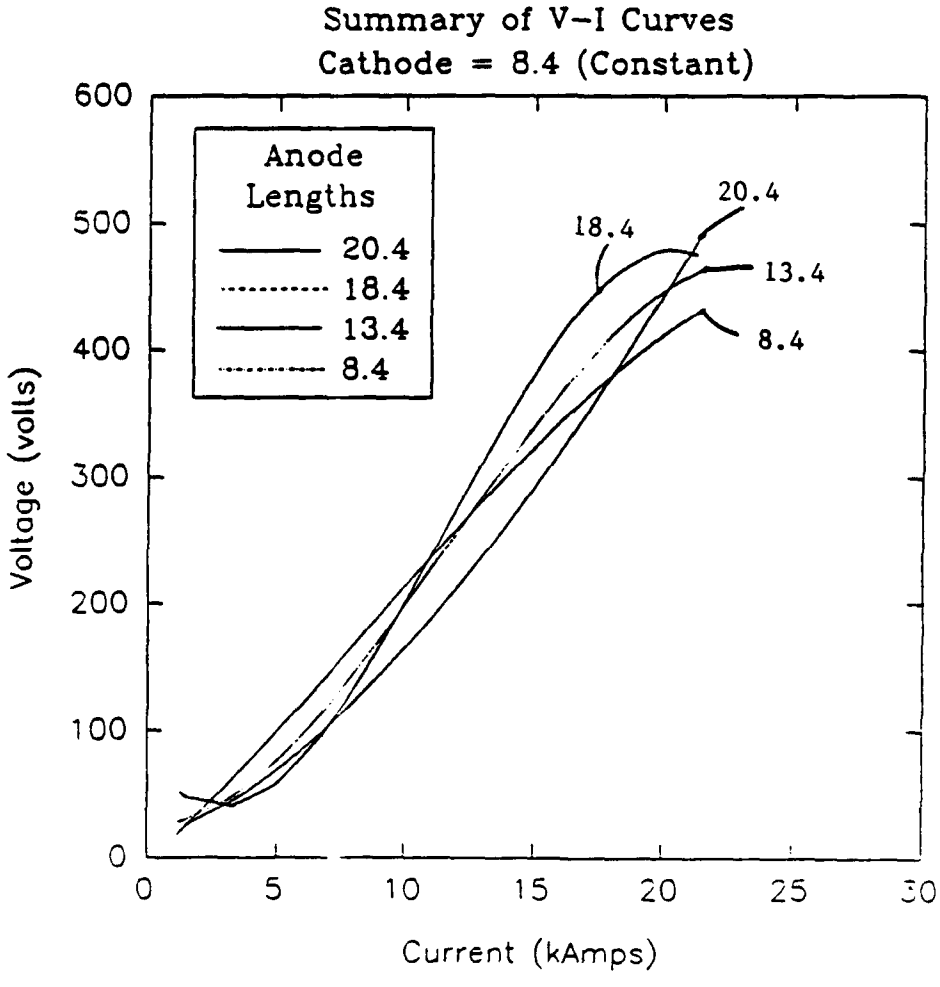
Summary of V–I Curves
Cathode = 8.4 (Constant)
Anode
Lengths
20.4
18.4
13.4
8.4
20.4
18.4
13.4
8.4
Voltage (volts)
Current (kAmps)
600
500
400
300
200
100
0
0
5
10
15
20
25
30

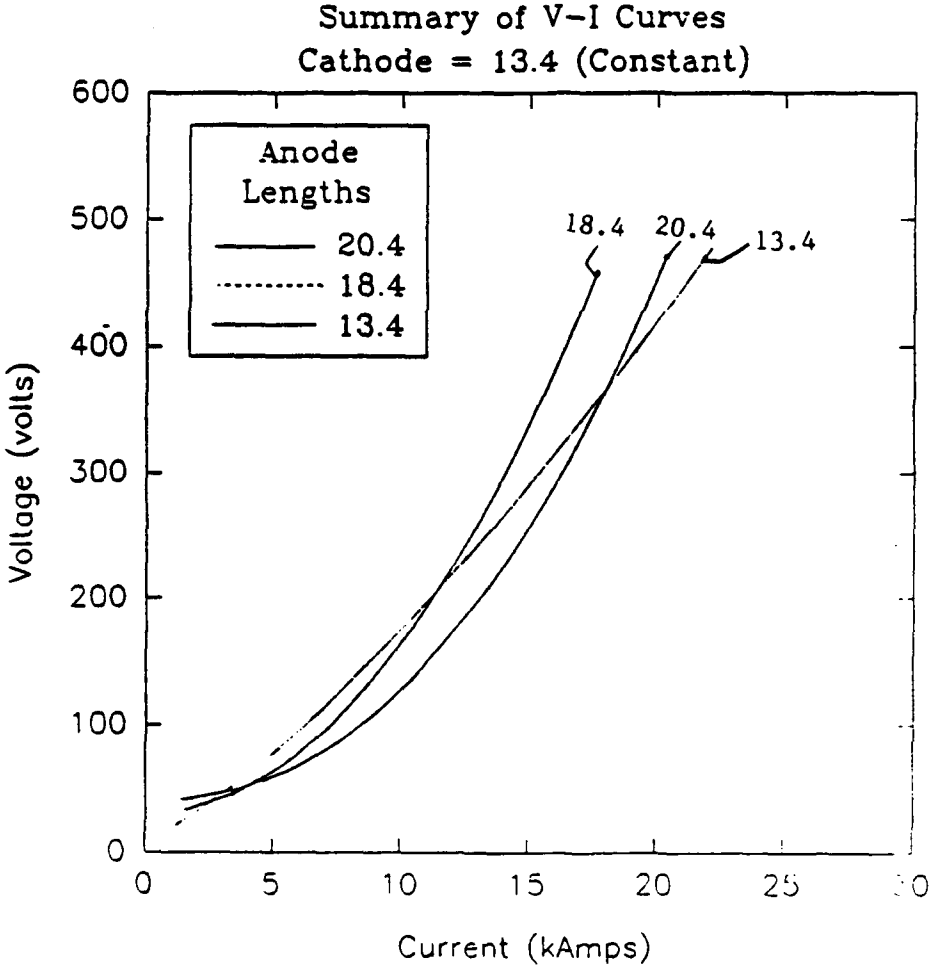
Summary of V-I Curves
Cathode = 13.4 (Constant)
Anode
Lengths
20.4
18.4
13.4
18.4
20.4
13.4
Voltage (volts)
Current (kAmps)
600
500
400
300
200
100
0
0
5
10
15
20
25

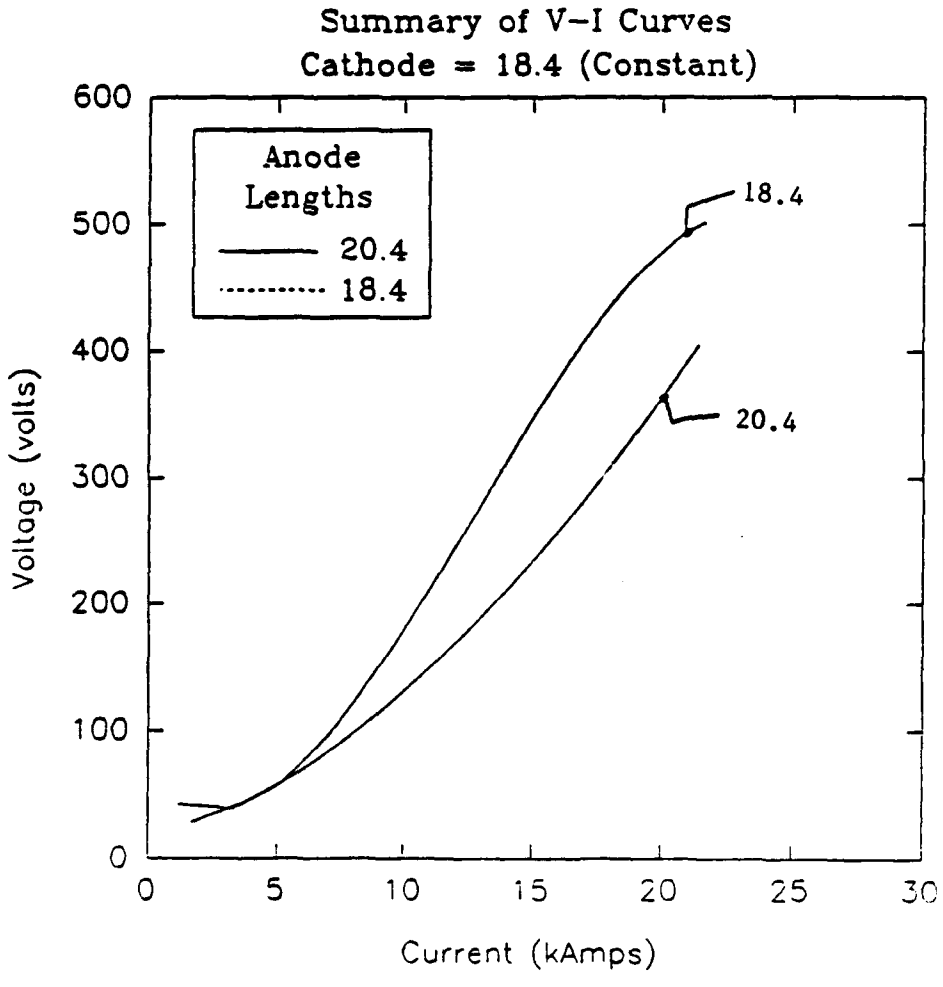
Summary of V–I Curves
Cathode = 18.4 (Constant)
Anode
Lengths
20.4
18.4
18.4
20.4
Voltage (volts)
Current (kAmps)
600
500
400
300
200
100
0
0
5
10
15
20
25
30

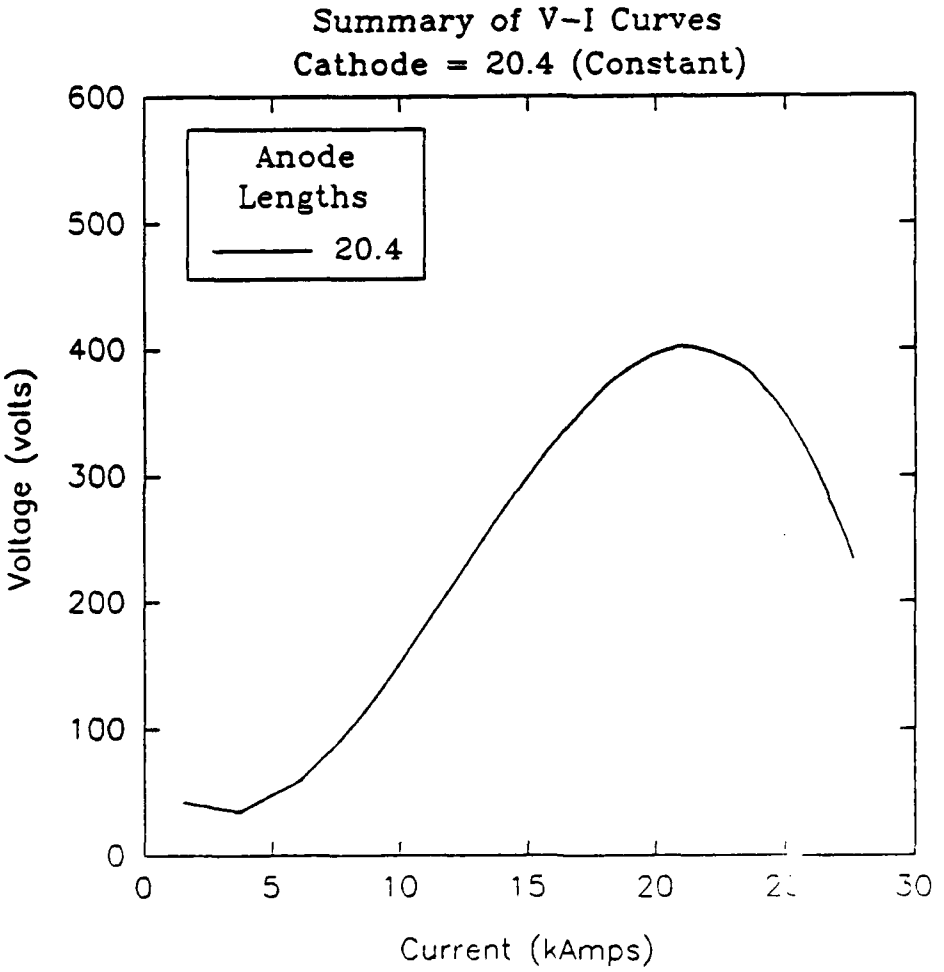
Summary of V-I Curves
Cathode = 20.4 (Constant)
Anode
Lengths
20.4
600
500
400
300
200
100
0
Voltage (volts)
0
5
10
15
20
30
Current (kAmps)

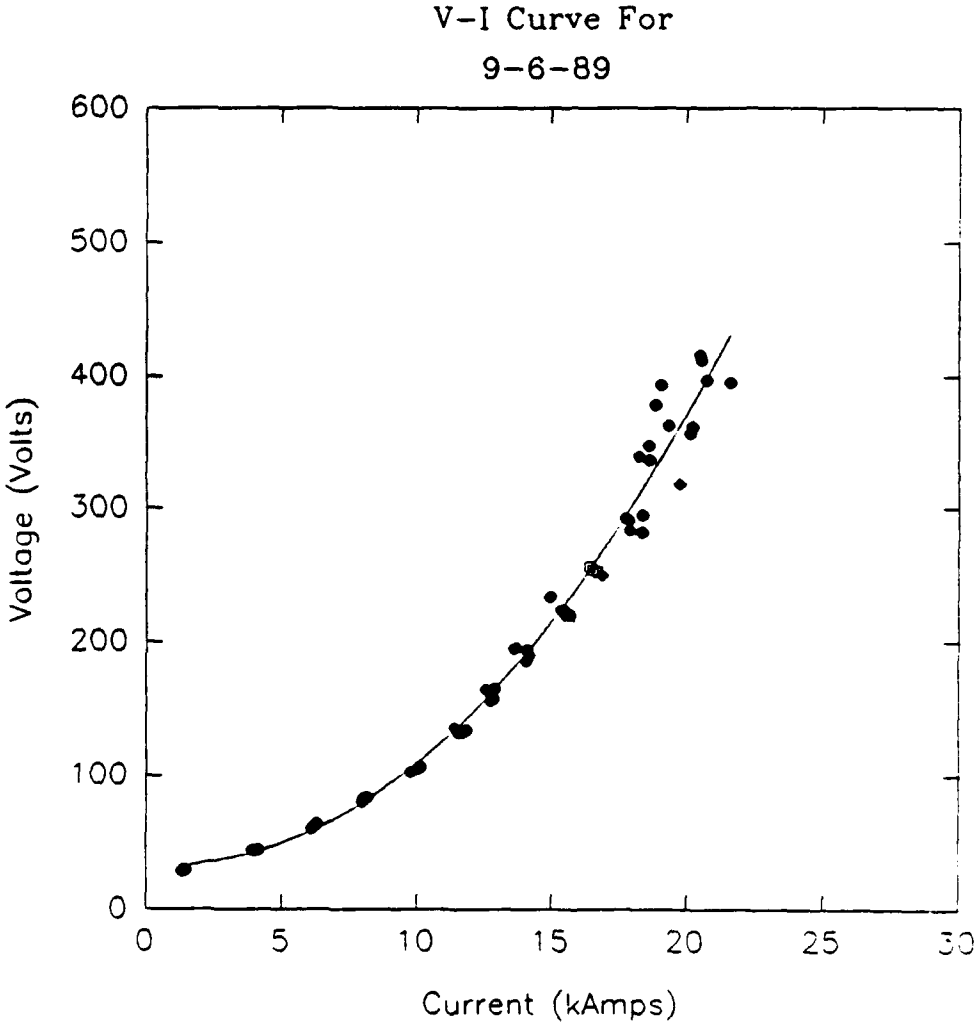
V-I Curve For
9-6-89
600
500
400
300
200
100
0
Voltage (Volts)
0
5
10
15
20
25
30
Current (kAmps)

C: 3.24 A:3.24

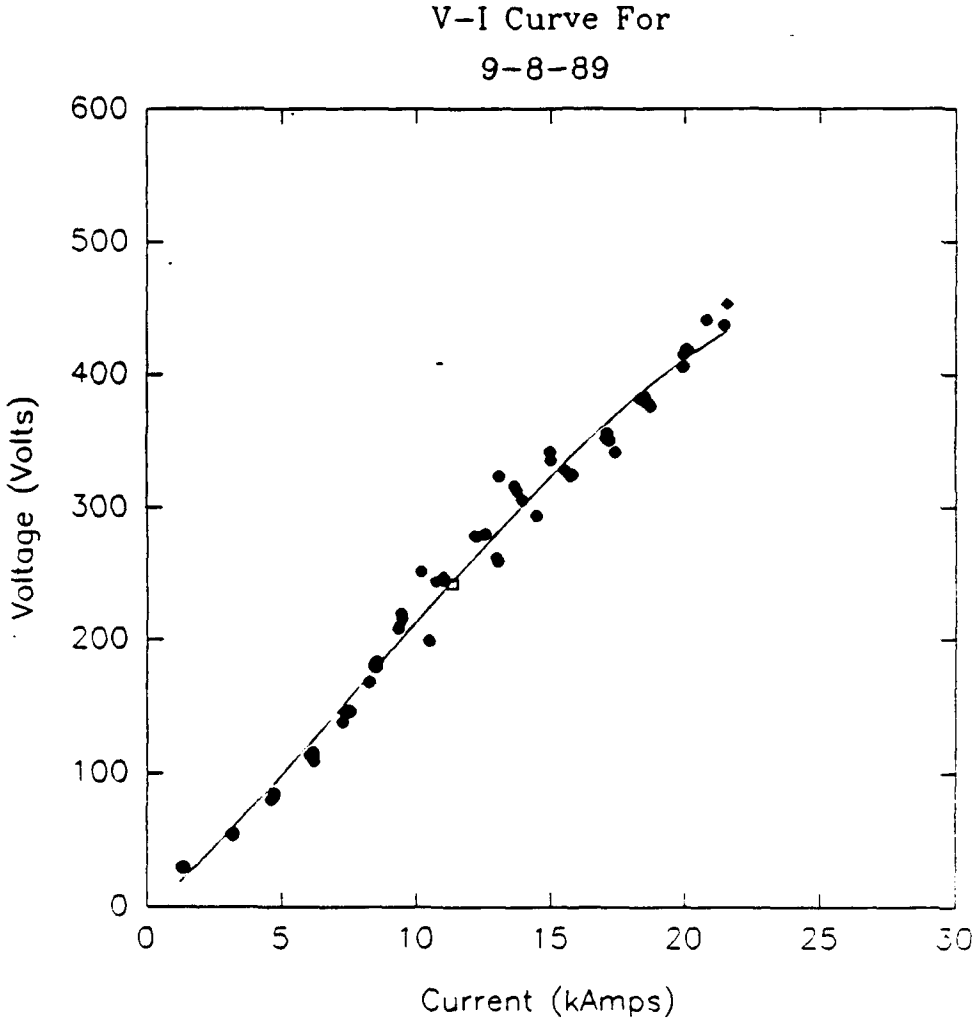
V-I Curve For
9-8-89
600
500
400
300
200
100
0
Voltage (Volts)
0
5
10
15
20
25
30
Current (kAmps)

C: 8.4 A: 8.4

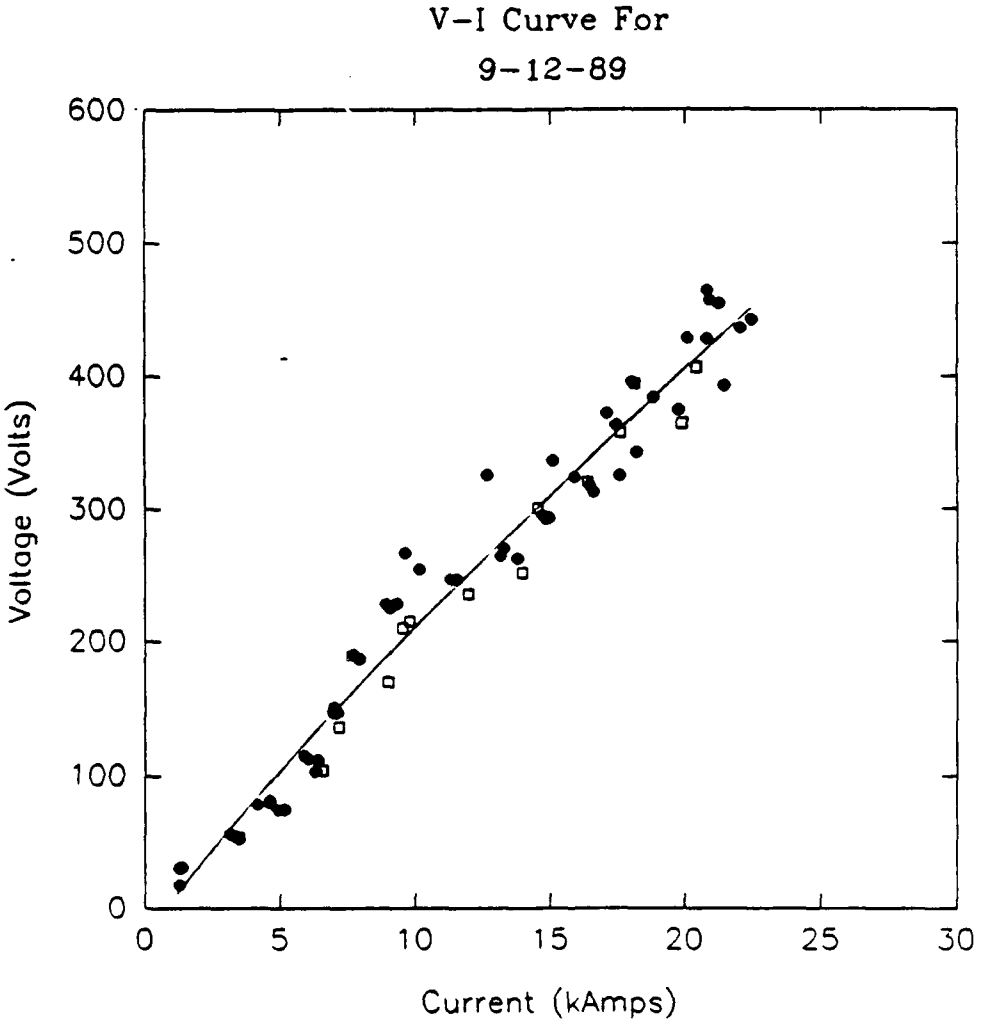
V-I Curve For
9-12-89
600
500
400
300
200
100
0
Voltage (Volts)
0
5
10
15
20
25
30
Current (kAmps)

C: 3.4 A: 8.4

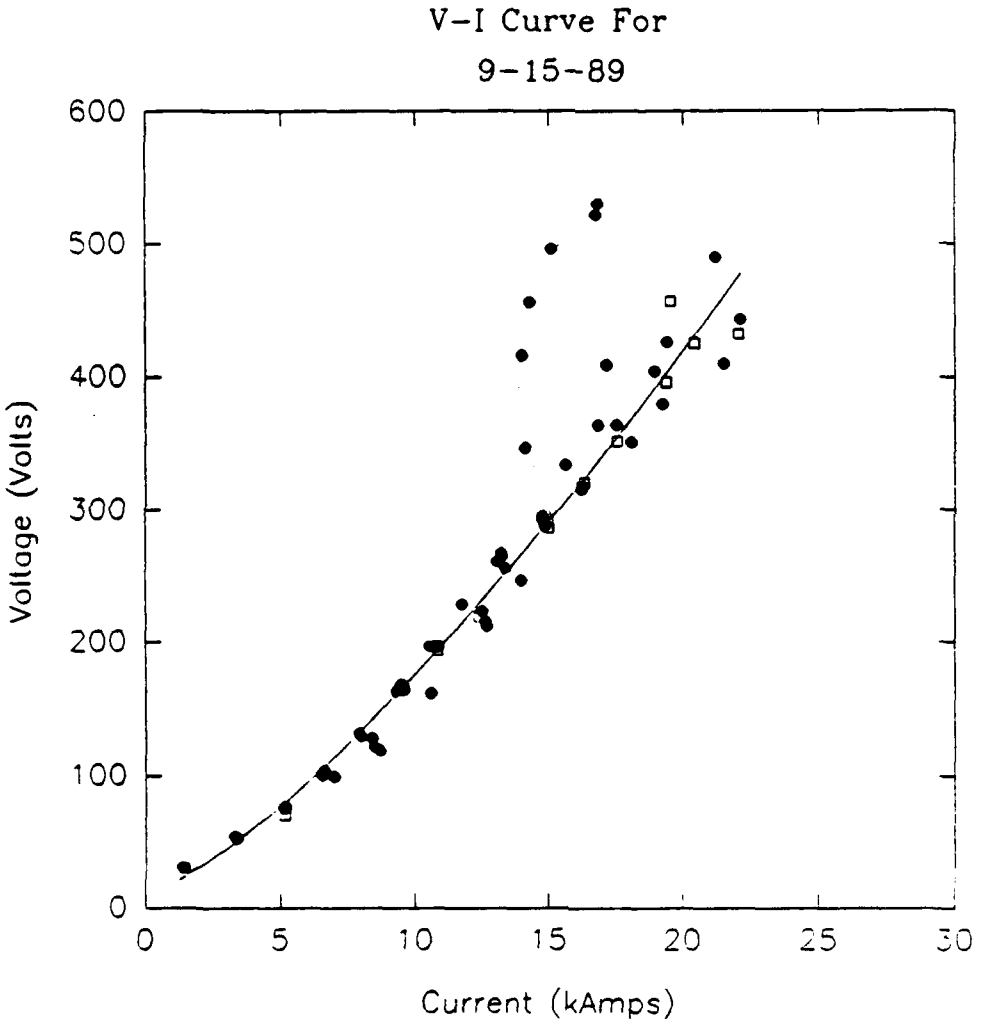
V-I Curve For
9-15-89
Voltage (Volts)
600
500
400
300
200
100
0
0
5
10
15
20
25
30
Current (kAmps)

C: 13.4 A: 13.4

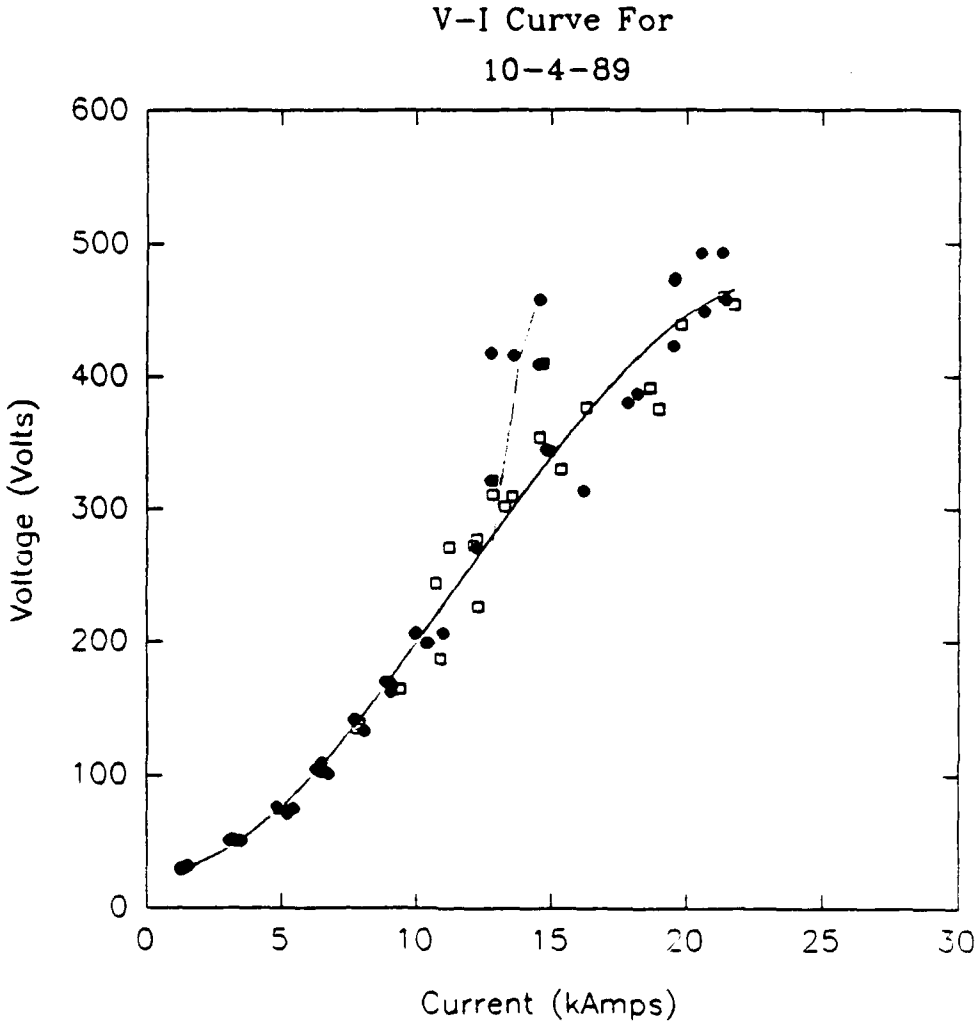
V-I Curve For
10-4-89
Voltage (Volts)
600
500
400
300
200
100
0
0
5
10
15
20
25
30
Current (kAmps)

C: 8.4 A: 13.4

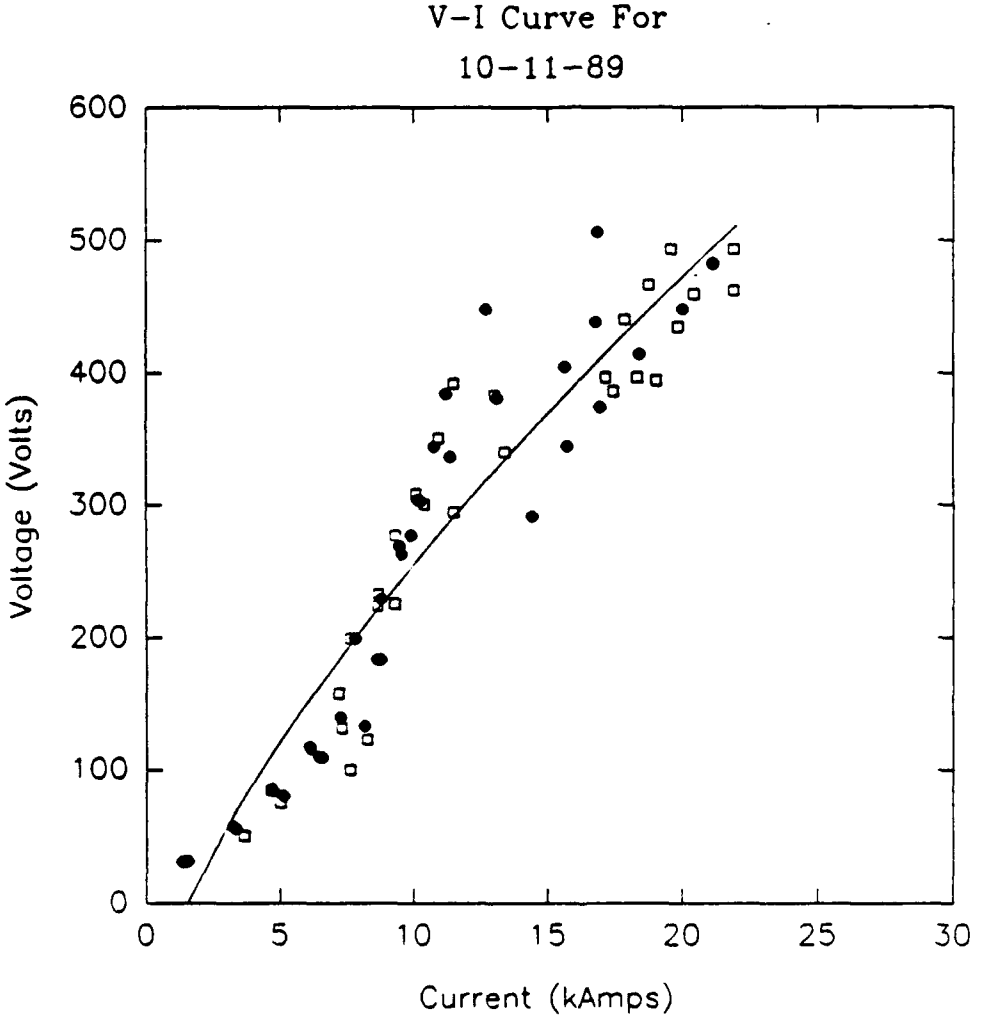
V-I Curve For
10-11-89
Voltage (Volts)
600
500
400
300
200
100
0
0
5
10
15
20
25
30
Current (kAmps)

C: 3.4 A: 13.4

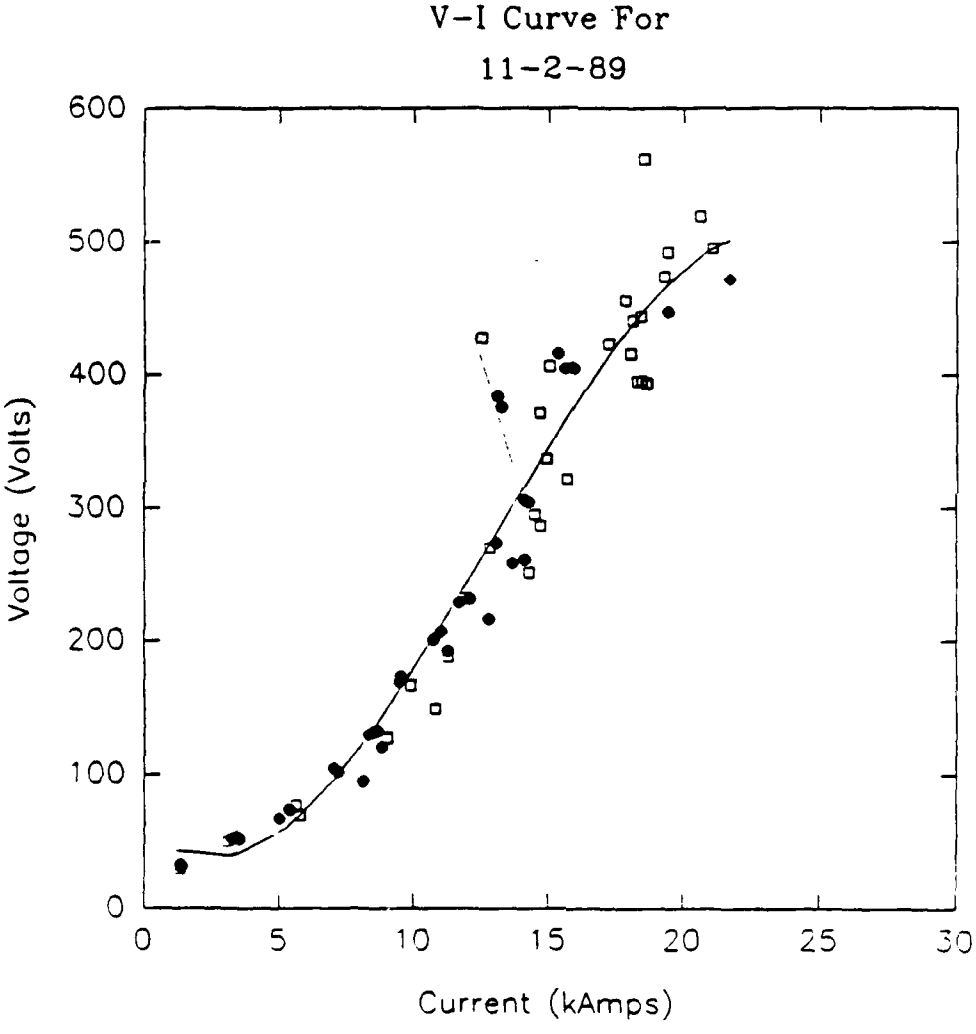
V-I Curve For
11-2-89
600
500
400
300
200
100
0
Voltage (Volts)
0
5
10
15
20
25
30
Current (kAmps)

C: 18.4 A: 18.4

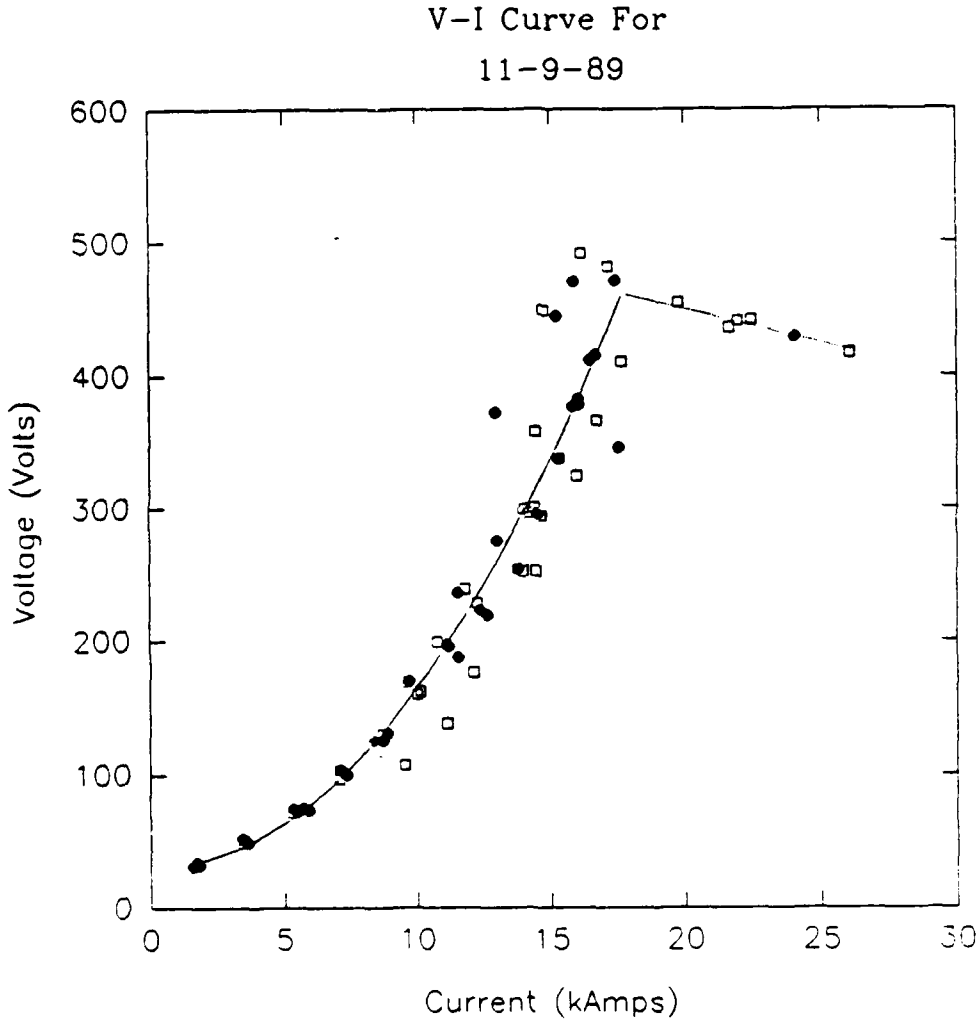
V-I Curve For
11-9-89
600
500
400
300
200
100
0
Voltage (Volts)
0
5
10
15
20
25
30
Current (kAmps)

C: 13.4 A: 18.4

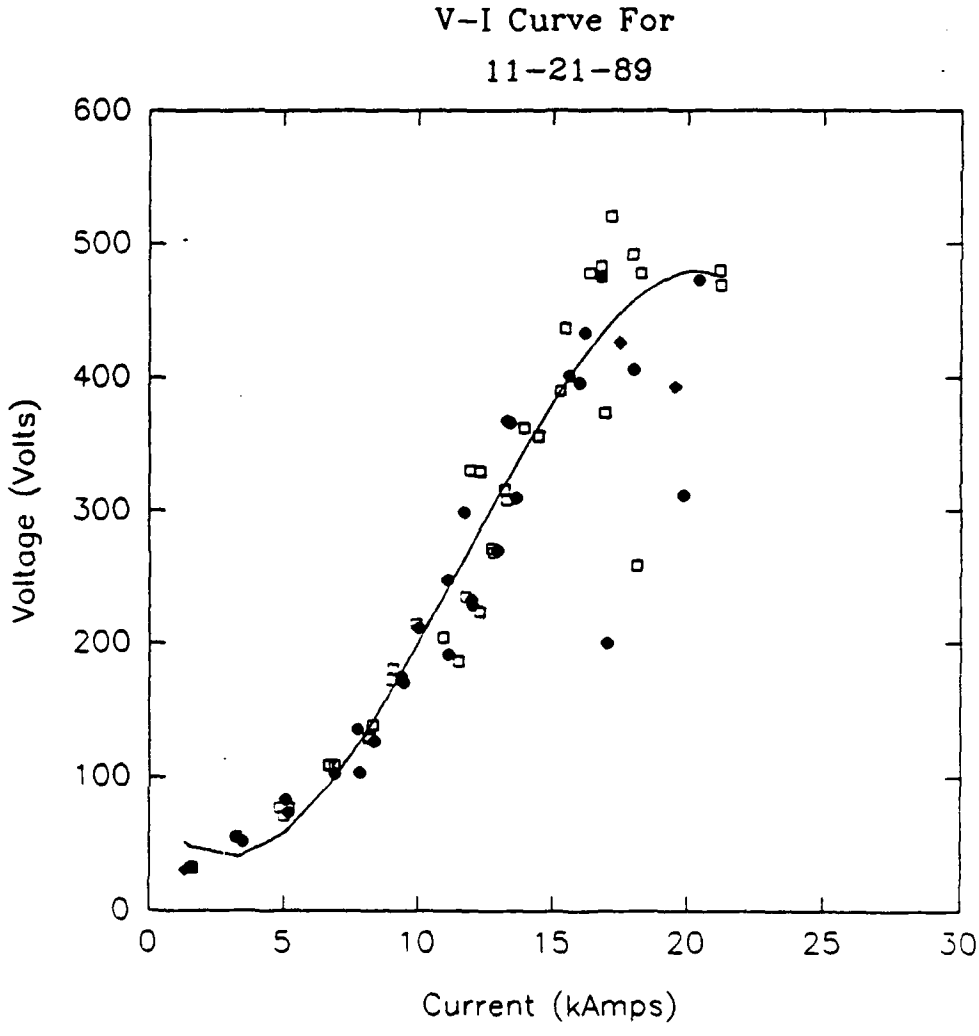
V-I Curve For
11-21-89
600
500
400
300
200
100
0
Voltage (Volts)
0
5
10
15
20
25
30
Current (kAmps)

C: 8.4 A: 18.4

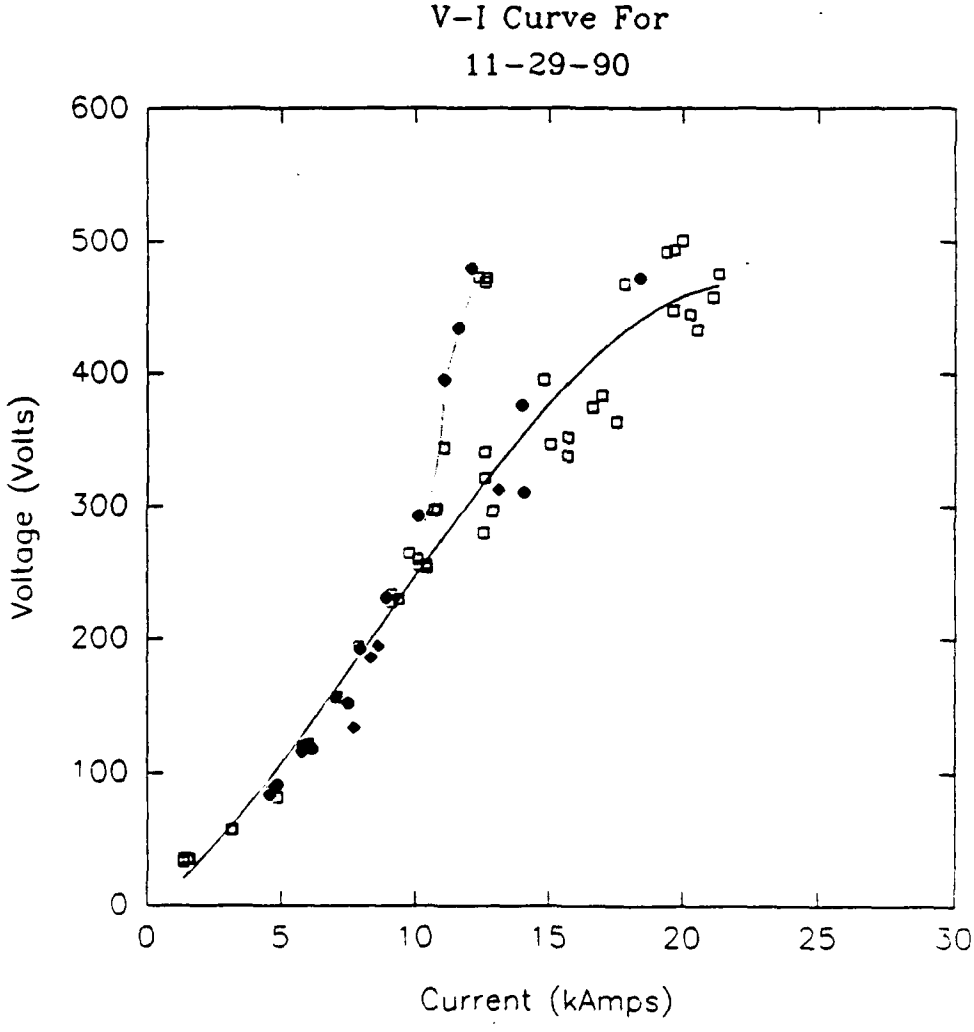
V-I Curve For
11-29-90
Voltage (Volts)
600
500
400
300
200
100
0
0
5
10
15
20
25
30
Current (kAmps)

C: 3.4 A: 20.4

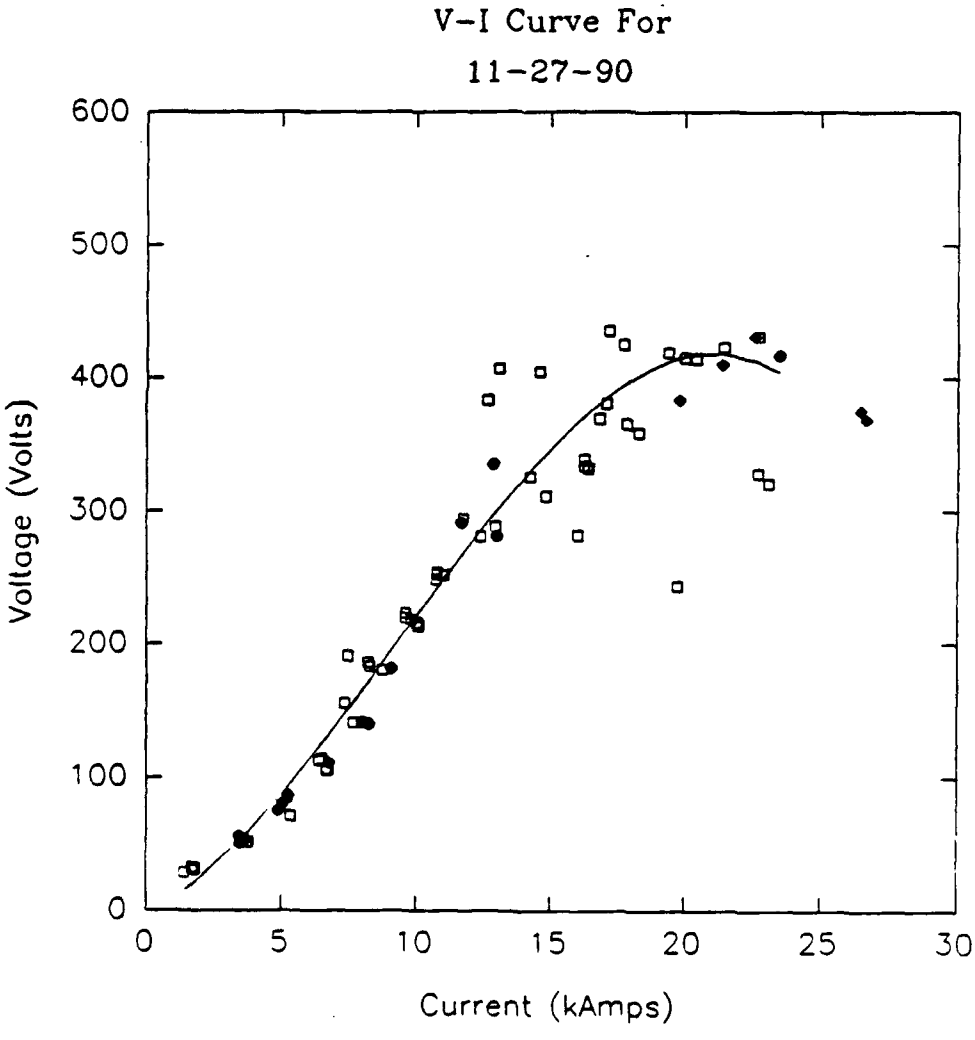
V-I Curve For
11-27-90
600
500
400
300
200
100
0
Voltage (Volts)
0
5
10
15
20
25
30
Current (kAmps)

C: 3.4 A: 18.4

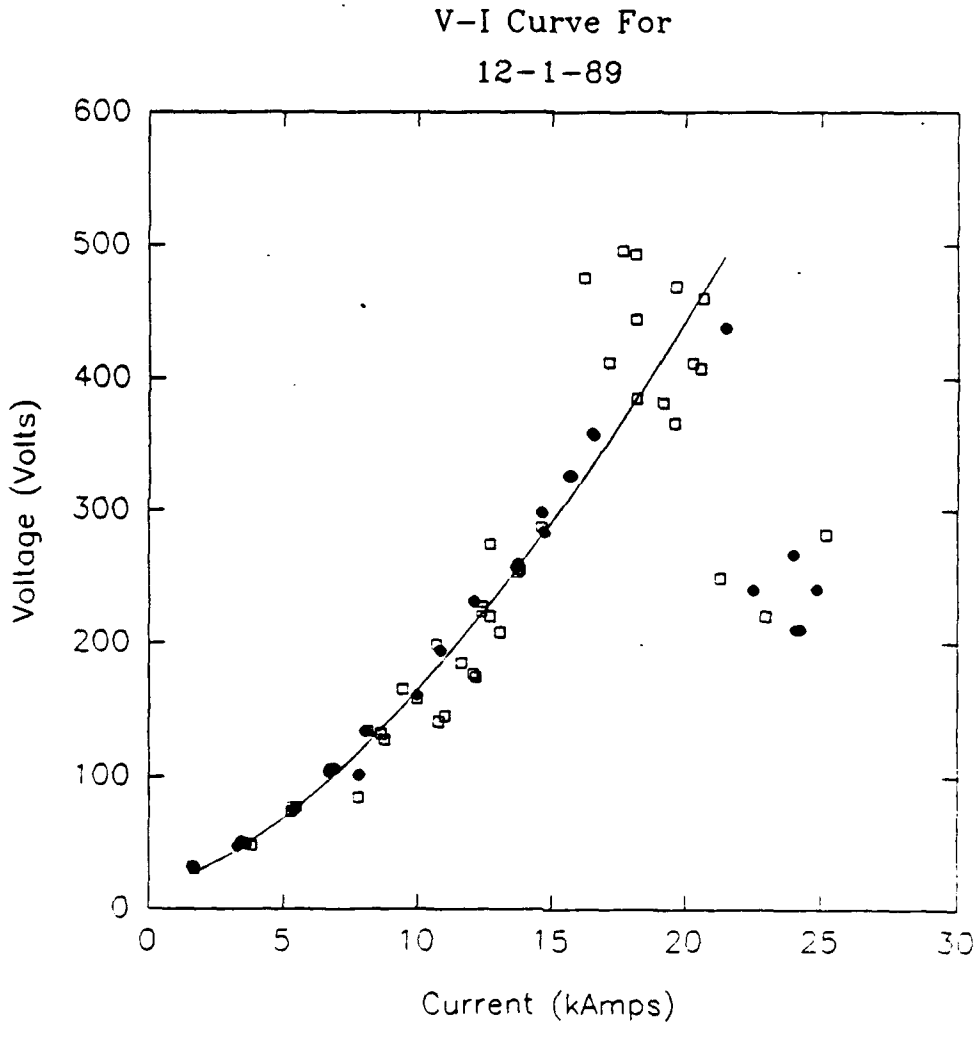
V-I Curve For
12-1-89
600
500
400
300
200
100
0
Voltage (Volts)
0
5
10
15
20
25
30
Current (kAmps)

C: 8.4 A: 20.4

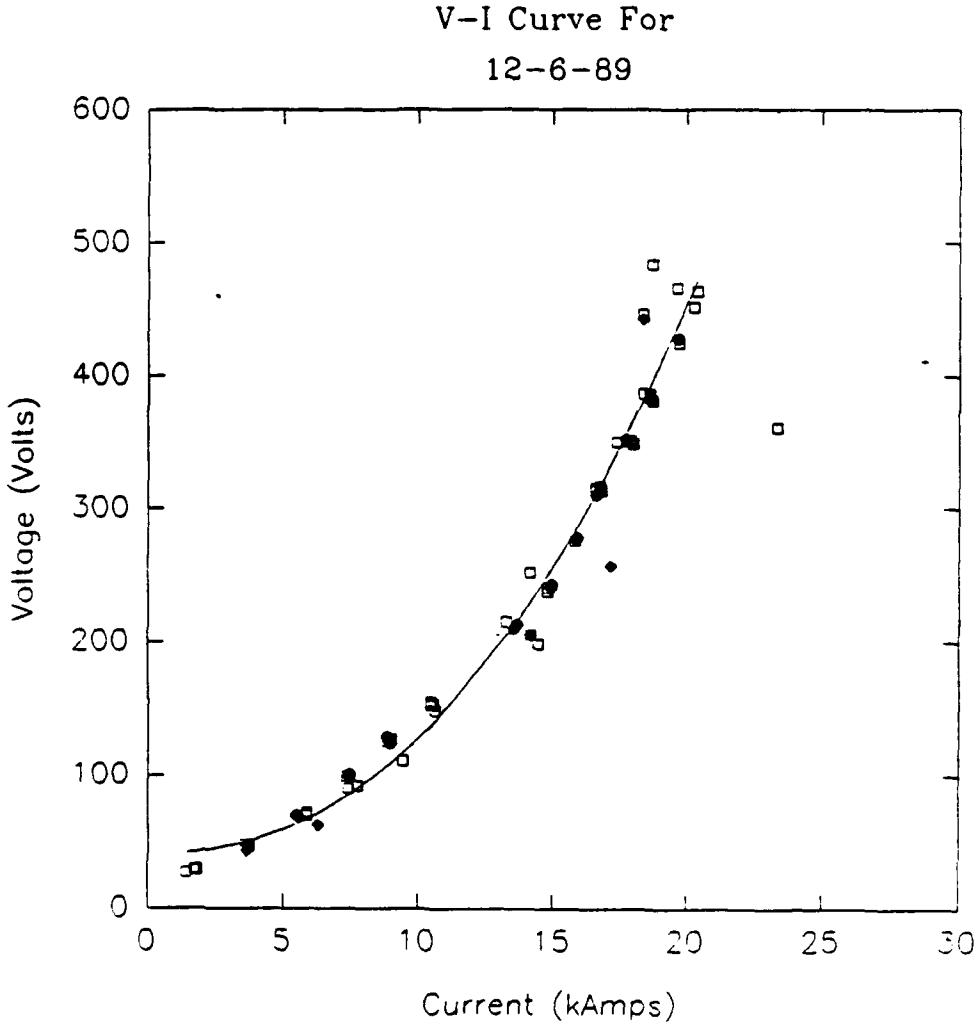
V-I Curve For
12-6-89
600
500
400
300
200
100
0
Voltage (Volts)
0
5
10
15
20
25
30
Current (kAmps)

C: 13.4 A: 20.4

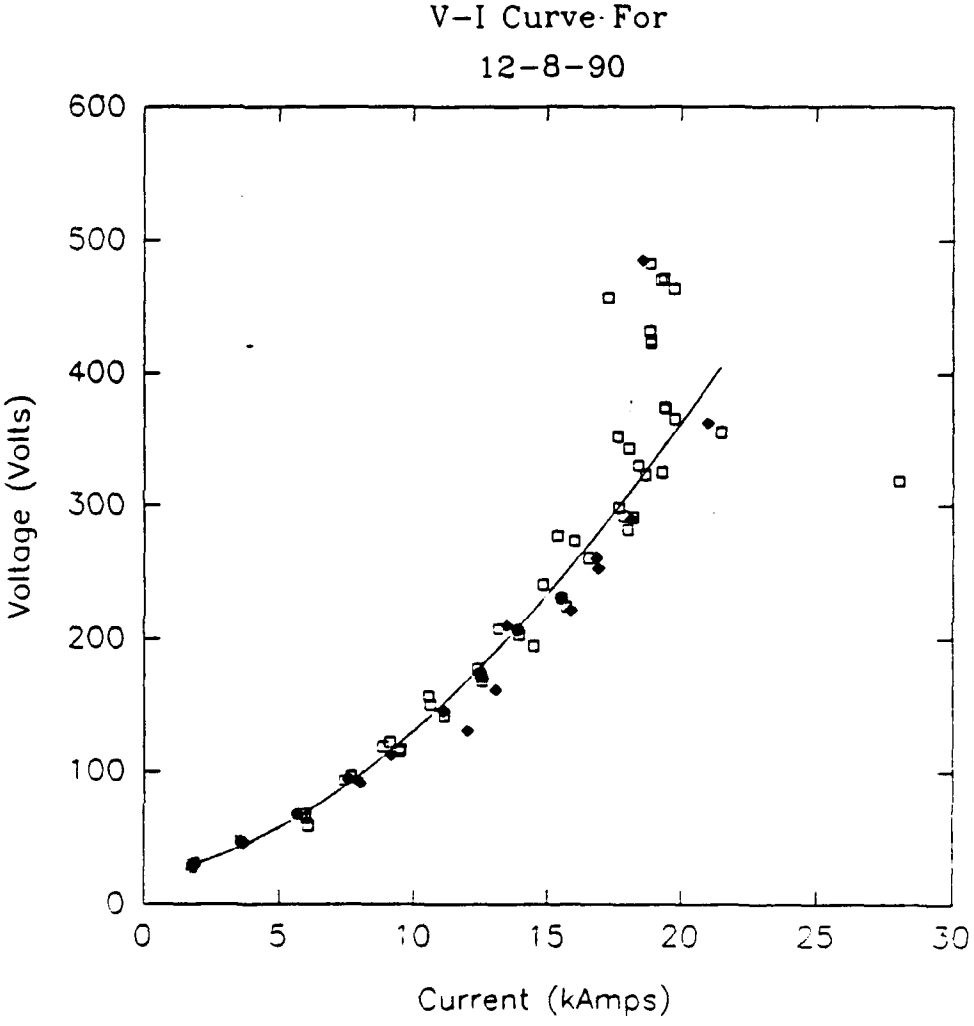
V-I Curve For
12-8-90
600
500
400
300
200
100
0
Voltage (Volts)
0
5
10
15
20
25
30
Current (kAmps)

C: 18.4 A: 20.4

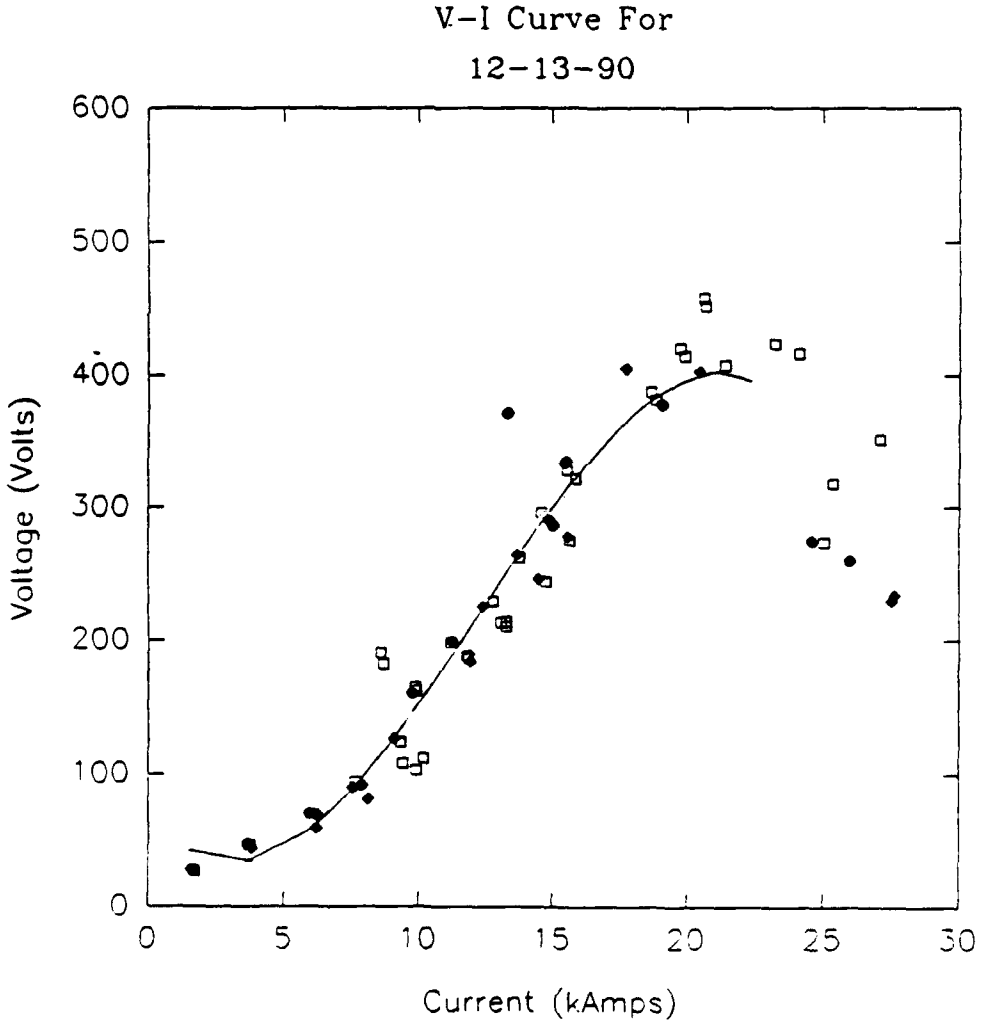
V-I Curve For
12-13-90
600
500
400
300
200
100
0
Voltage (Volts)
0
5
10
15
20
25
30
Current (kAmps)

C: 20.4 A: 20.4

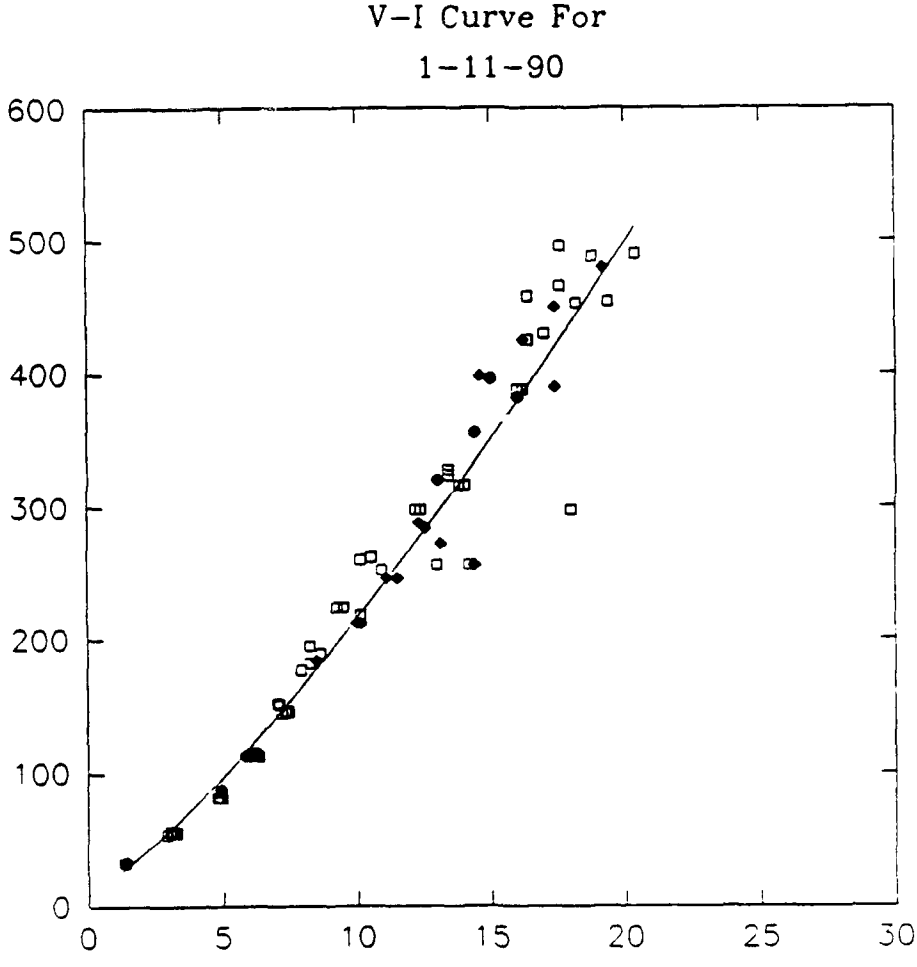

C: 3.4 A: 3.4

Appendix F

Thrust vs. Power, Specific Impulse vs. Power, Efficiency vs. Power, Specific Impulse vs. Efficiency, Thrust vs Thruster Volume

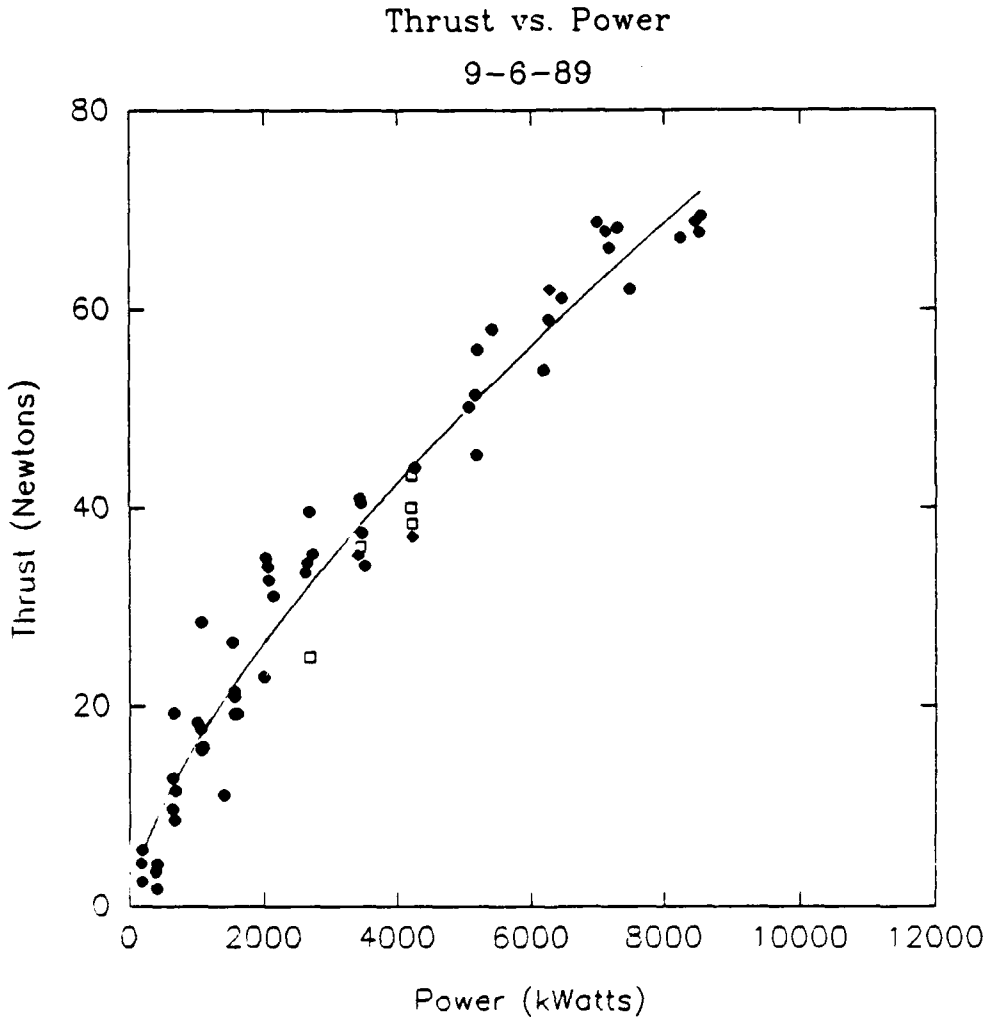
Thrust vs. Power
9-6-89
Thrust (Newtons)
Power (kWatts)
0
20
40
60
80
0
2000
4000
6000
8000
10000
12000

C: 3.24 A: 3.24

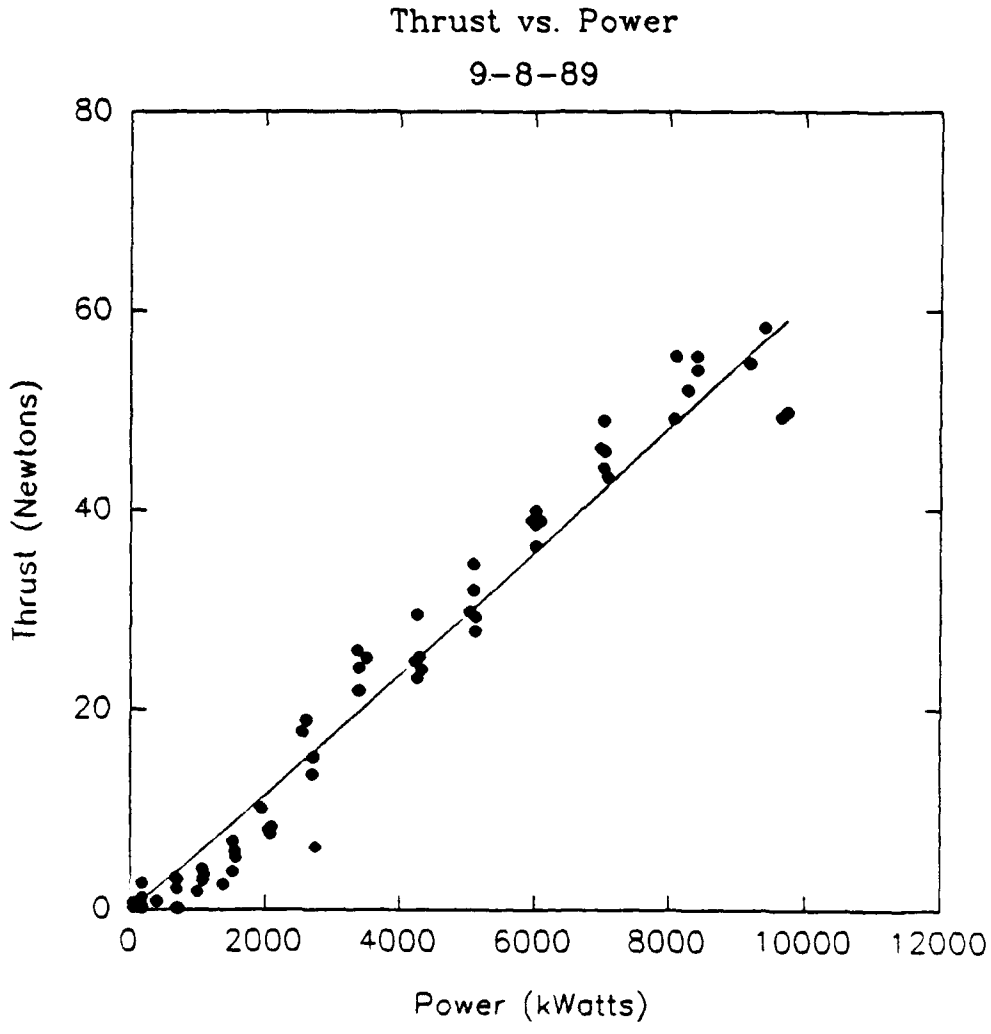
Thrust vs. Power
9-8-89
Thrust (Newtons)
80
60
40
20
0
0
2000
4000
6000
8000
10000
12000
Power (kWatts)

C: 8.4 A: 8.4

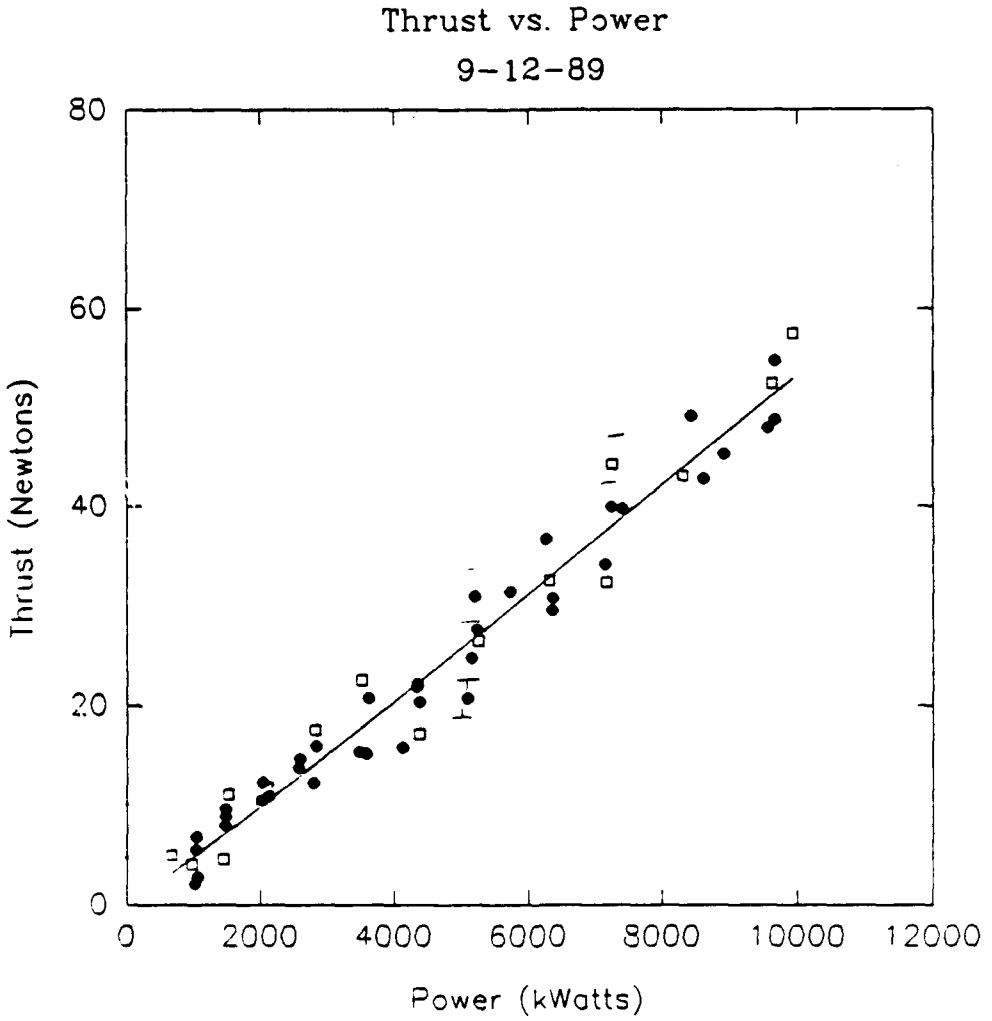
Thrust vs. Power
9-12-89
Thrust (Newtons)
Power (kWatts)
0
20
40
60
80
0
2000
4000
6000
8000
10000
12000

C: 3.4 A: 8.4

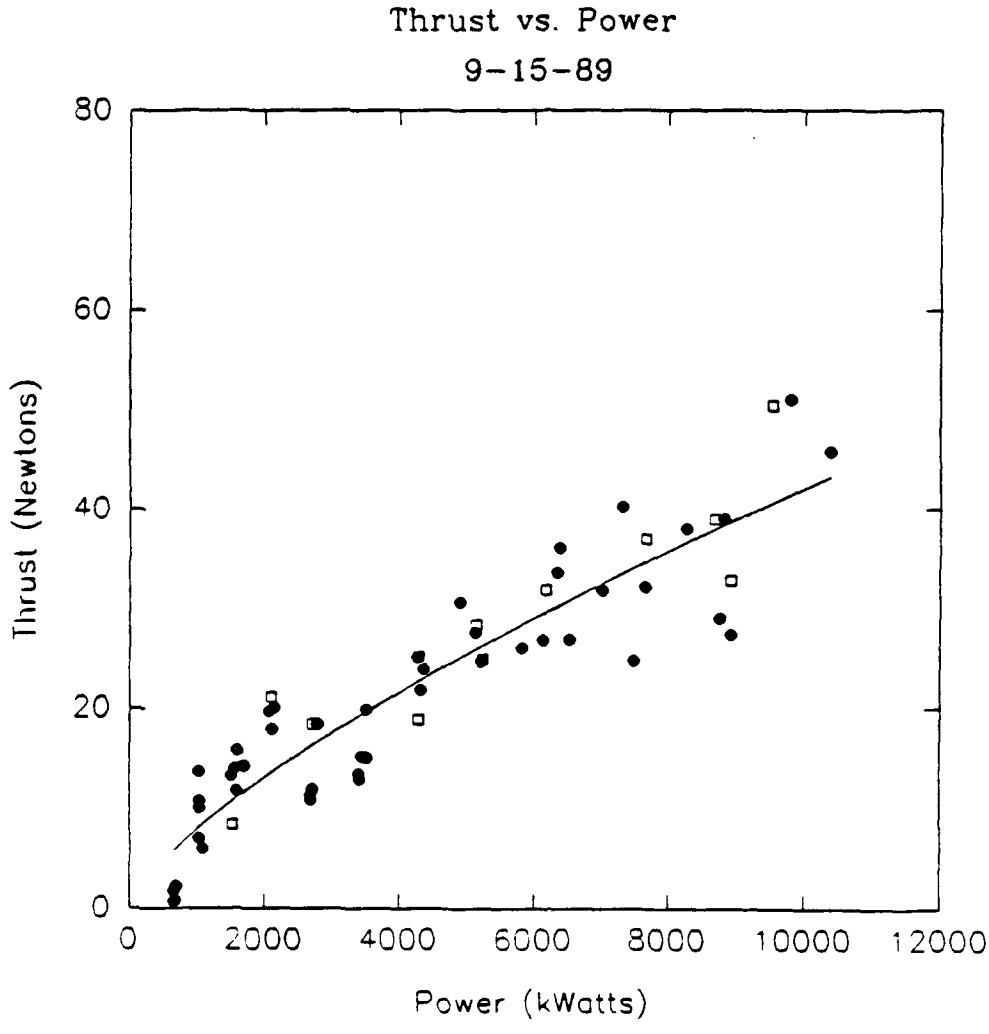

C: 13.4 A: 13.4

● 1.3 – 1.7
□ 1.7 – 2.0
◆ 2.0 – 2.3

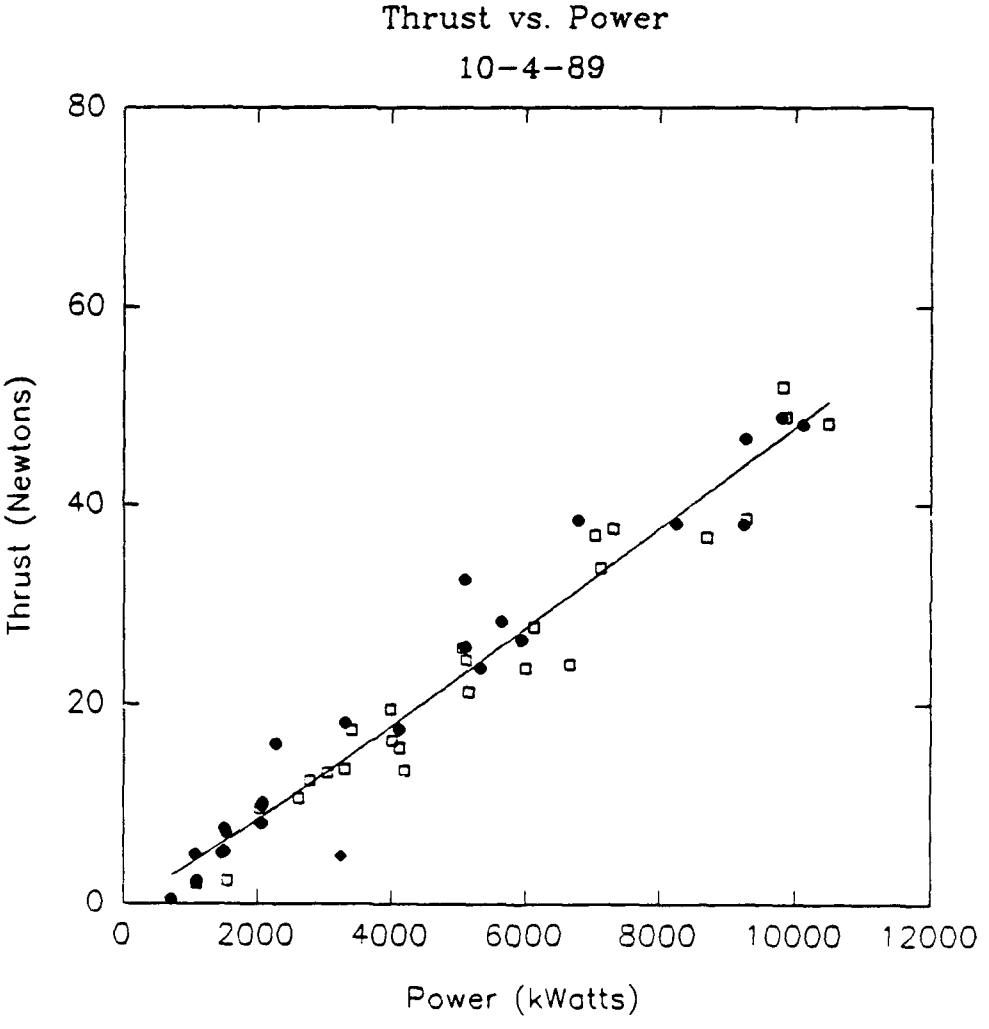
Thrust vs. Power
10-4-89
Thrust (Newtons)
Power (kWatts)
0
20
40
60
80
0
2000
4000
6000
8000
10000
12000

C: 8.4 A: 13.4

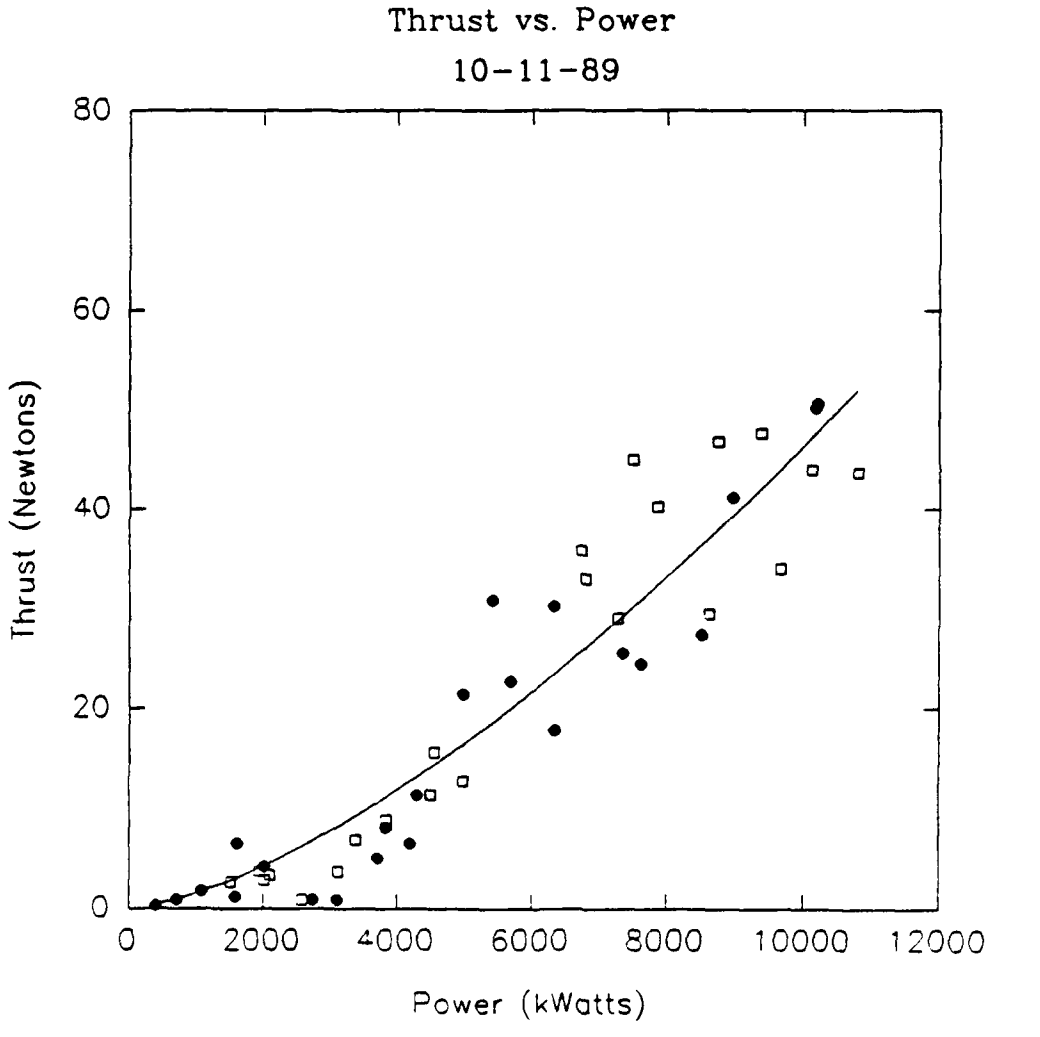
Thrust vs. Power
10-11-89
Thrust (Newtons)
80
60
40
20
0
0
2000
4000
6000
8000
10000
12000
Power (kWatts)
● 1.3 – 1.7
□ 1.7 – 2.0
C: 3.4 A: 13.4

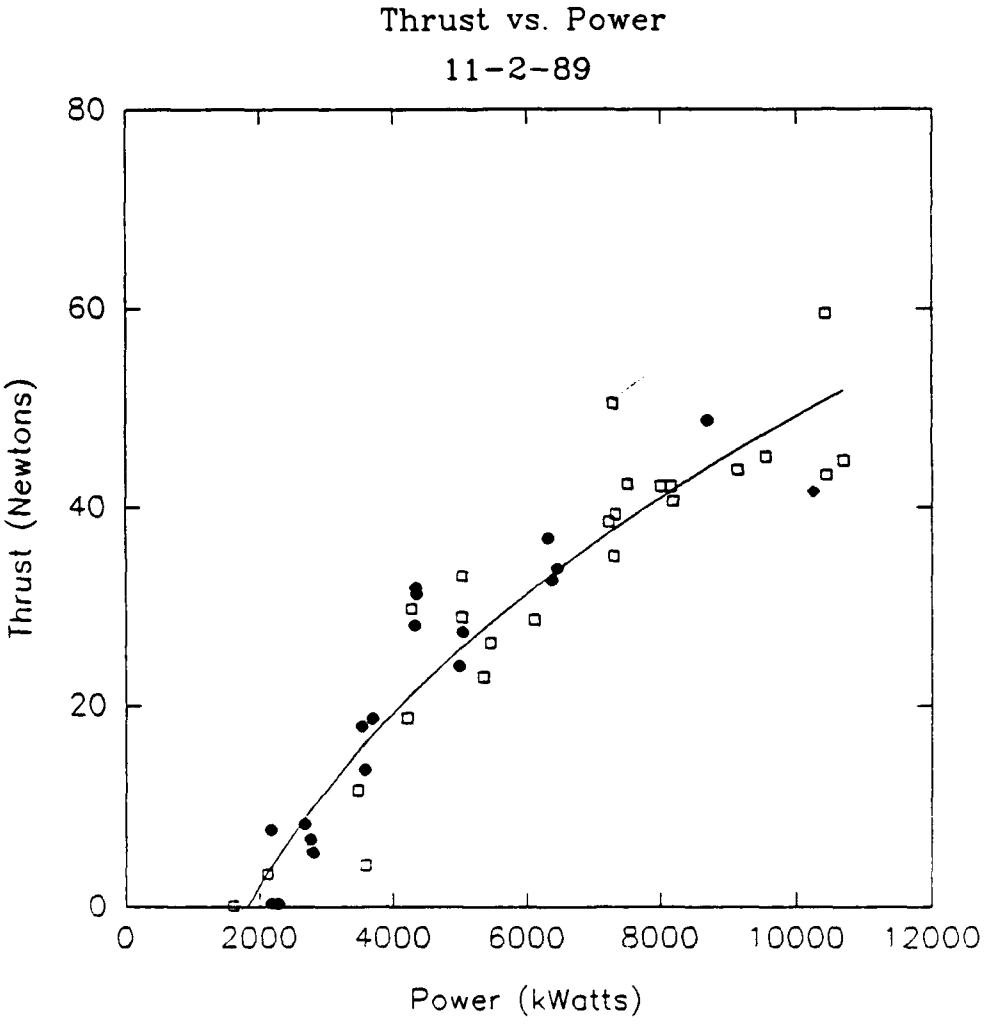
Thrust vs. Power
11-2-89
Thrust (Newtons)
Power (kWatts)
0
20
40
60
80
0
2000
4000
6000
8000
10000
12000

C: 18.4 A: 18.4

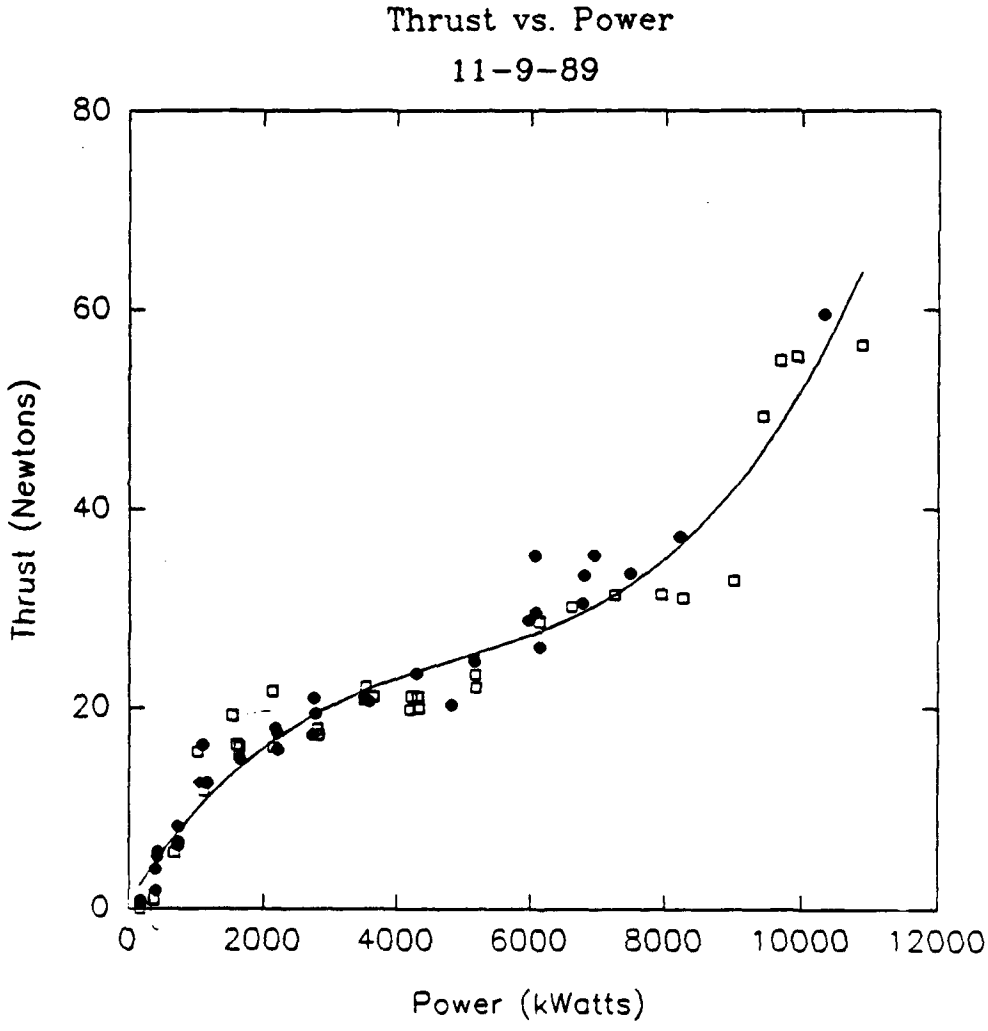
Thrust vs. Power
11-9-89
Thrust (Newtons)
80
60
40
20
0
0
2000
4000
6000
8000
10000
12000
Power (kWatts)

C: 13.4 A: 18.4

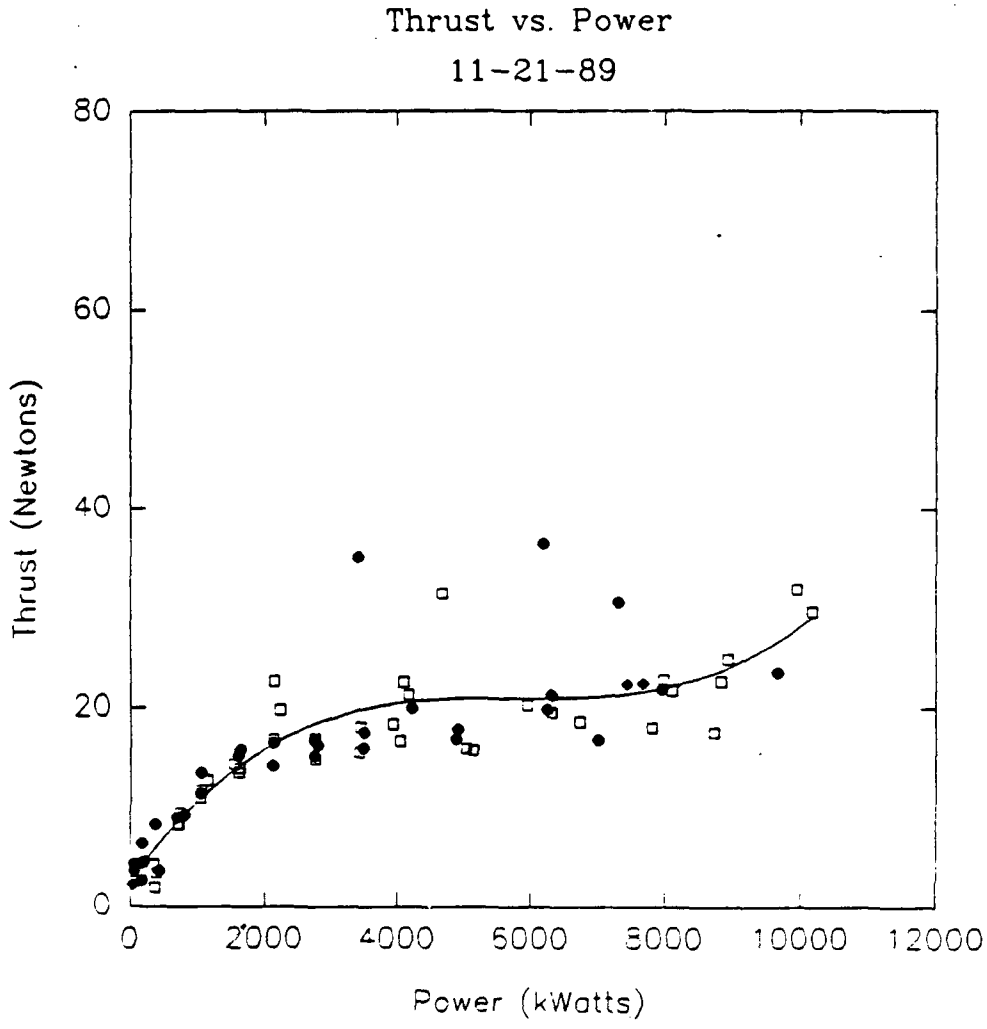
Thrust vs. Power
11-21-89
Thrust (Newtons)
80
60
40
20
0
0
2000
4000
6000
8000
10000
12000
Power (kWatts)

C: 8.4 A: 18.4

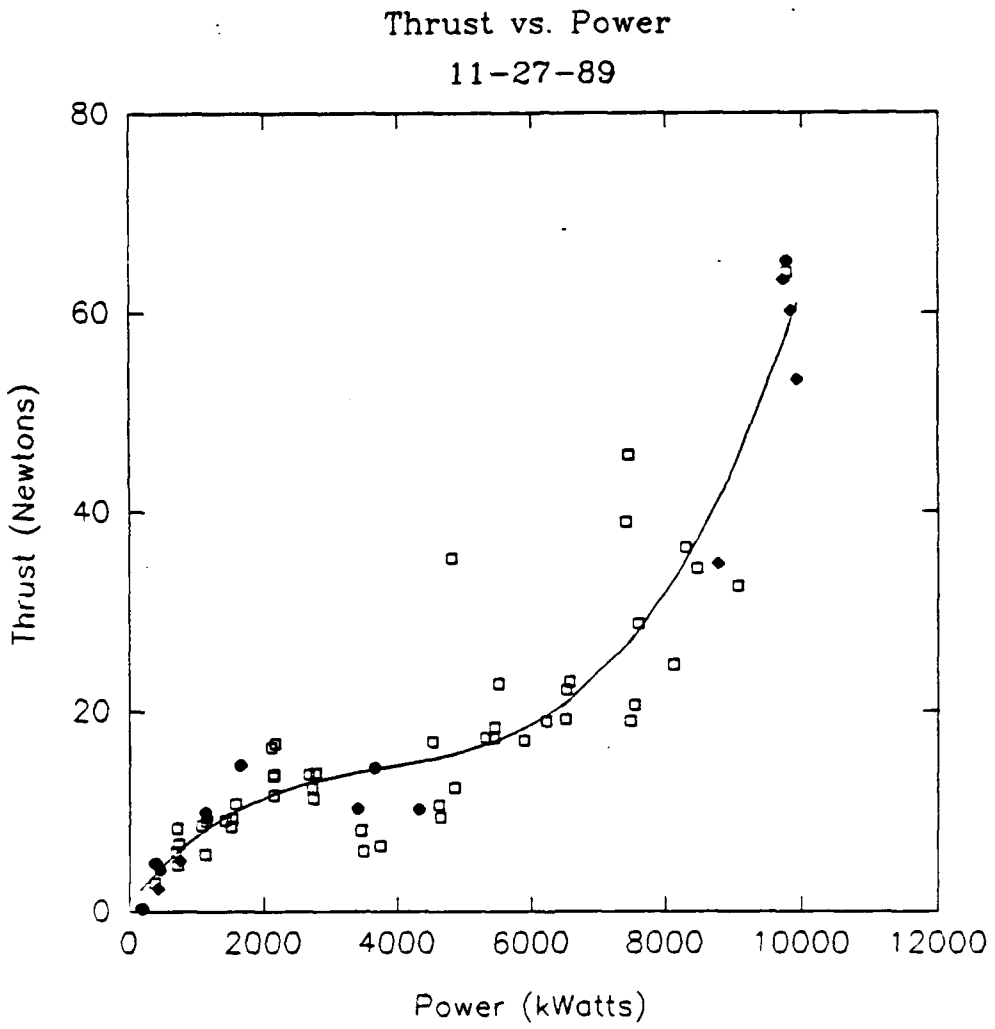
Thrust vs. Power
11-27-89
Thrust (Newtons)
Power (kWatts)
0
20
40
60
80
0
2000
4000
6000
8000
10000
12000

C: 3.4 A: 18.4

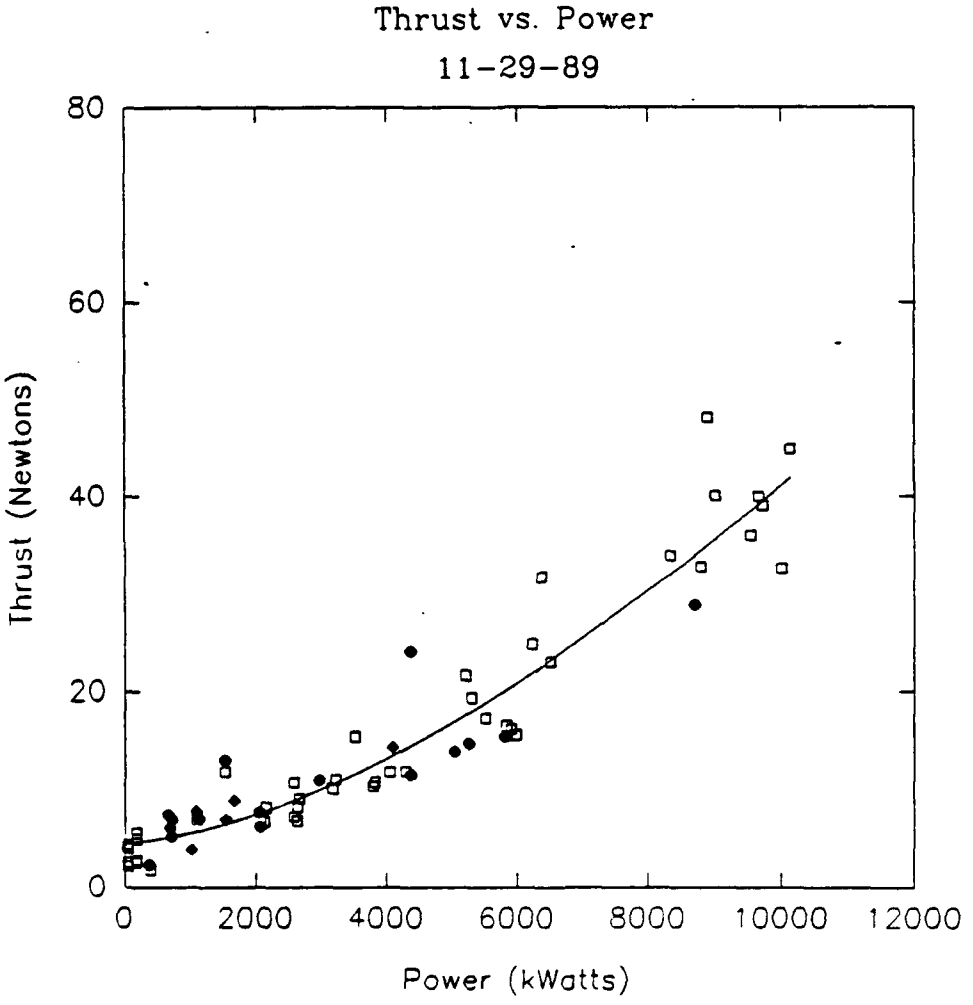
Thrust vs. Power
11-29-89
Thrust (Newtons)
Power (kWatts)
0
20
40
60
80
0
2000
4000
6000
8000
10000
12000

C: 3.4 A: 20.4

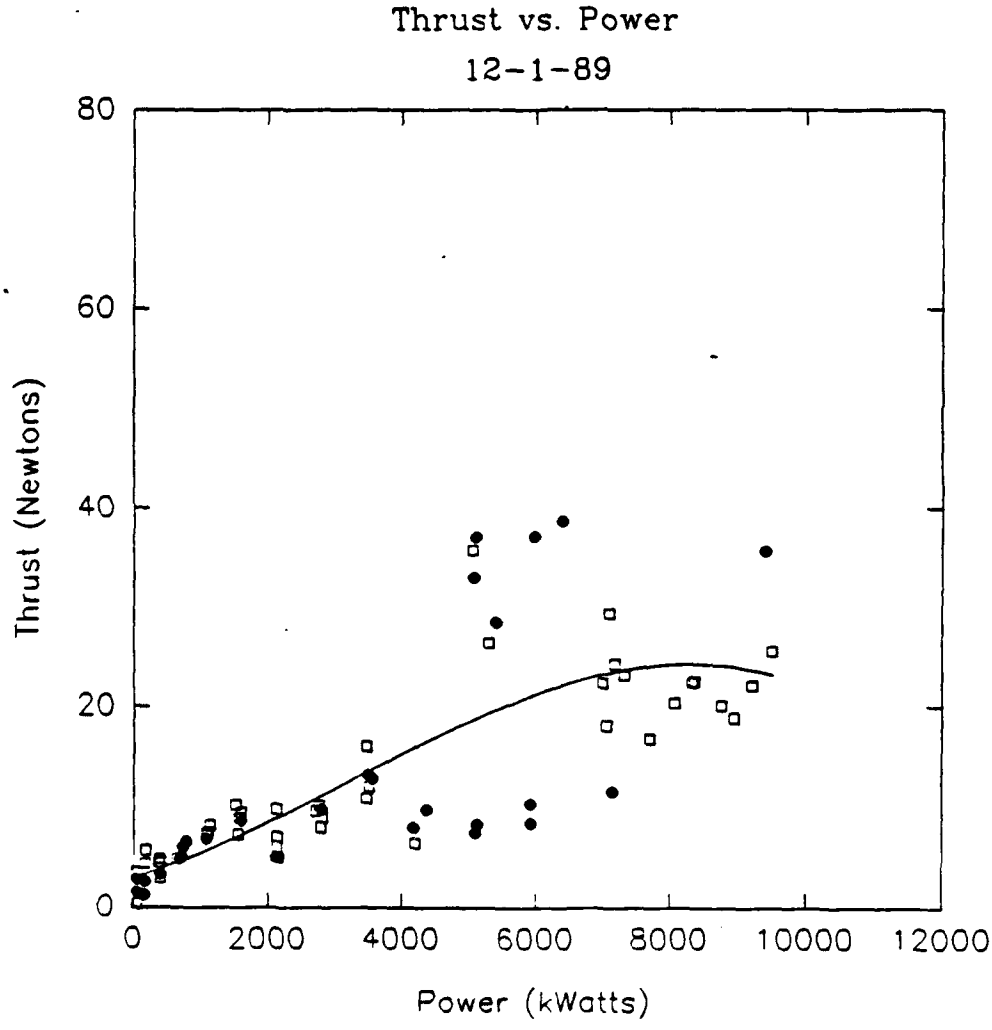
Thrust vs. Power
12-1-89
Thrust (Newtons)
80
60
40
20
0
0
2000
4000
6000
8000
10000
12000
Power (kWatts)

C: 8.4 A: 20.4

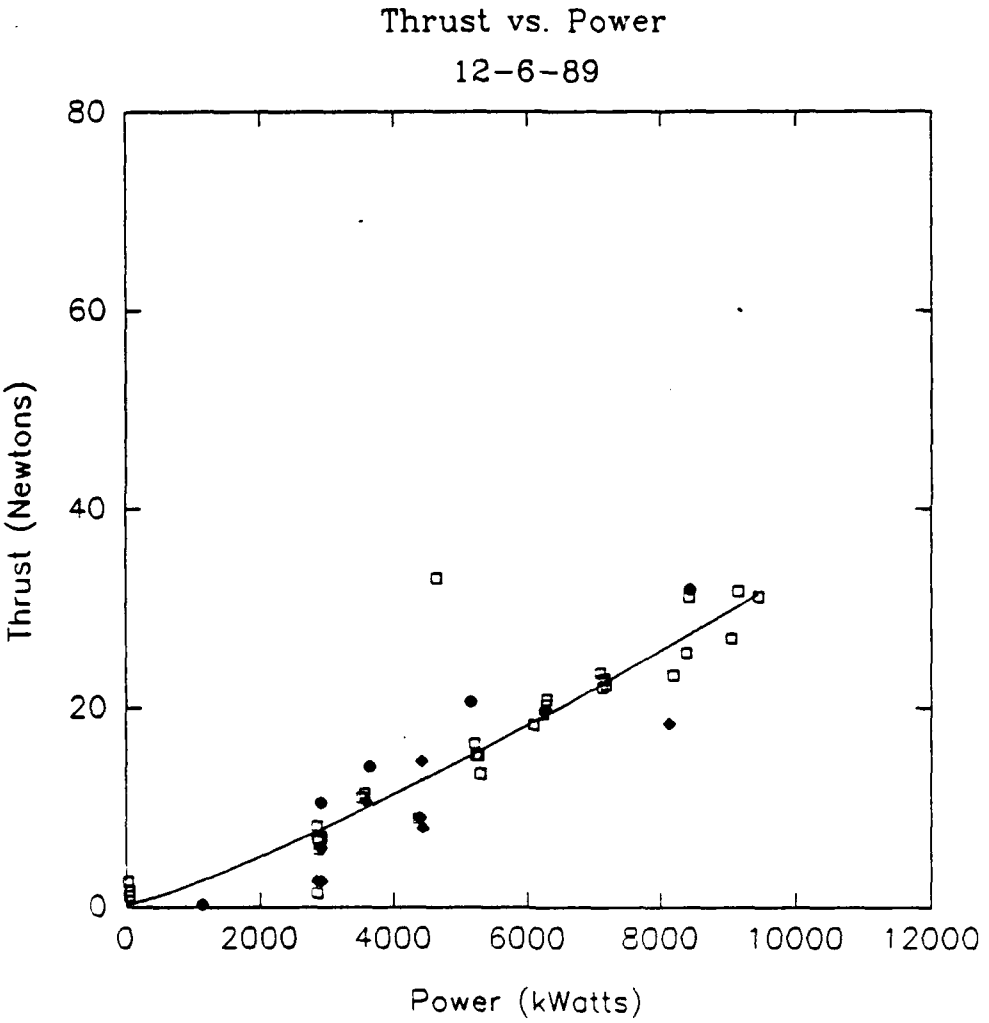
Thrust vs. Power
12-6-89
Thrust (Newtons)
80
60
40
20
0
0
2000
4000
6000
8000
10000
12000
Power (kWatts)

C: 13.4 A: 20.4

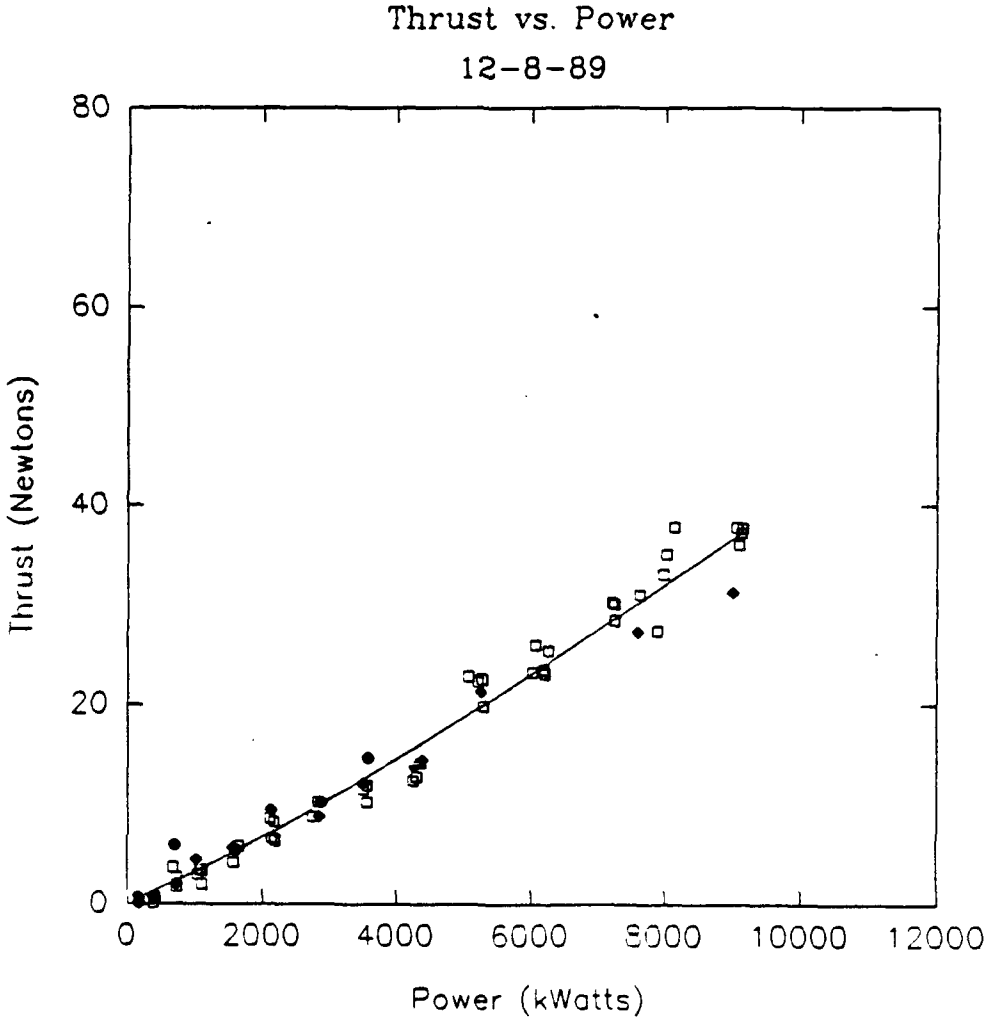
Thrust vs. Power
12-8-89
Thrust (Newtons)
80
60
40
20
0
0
2000
4000
6000
8000
10000
12000
Power (kWatts)

C: 18.4 A: 20.4

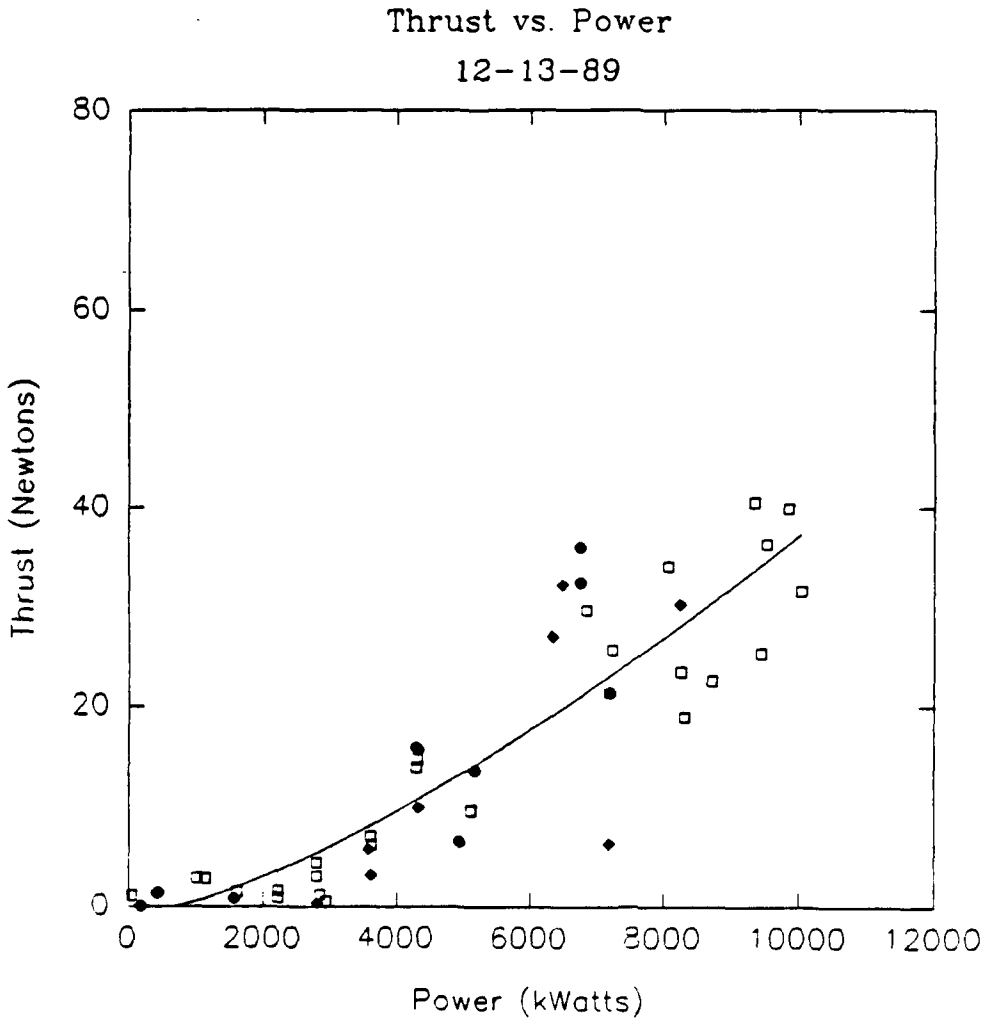
Thrust vs. Power
12-13-89
Thrust (Newtons)
80
60
40
20
0
0
2000
4000
6000
8000
10000
12000
Power (kWatts)

C: 20.4 A: 20.4

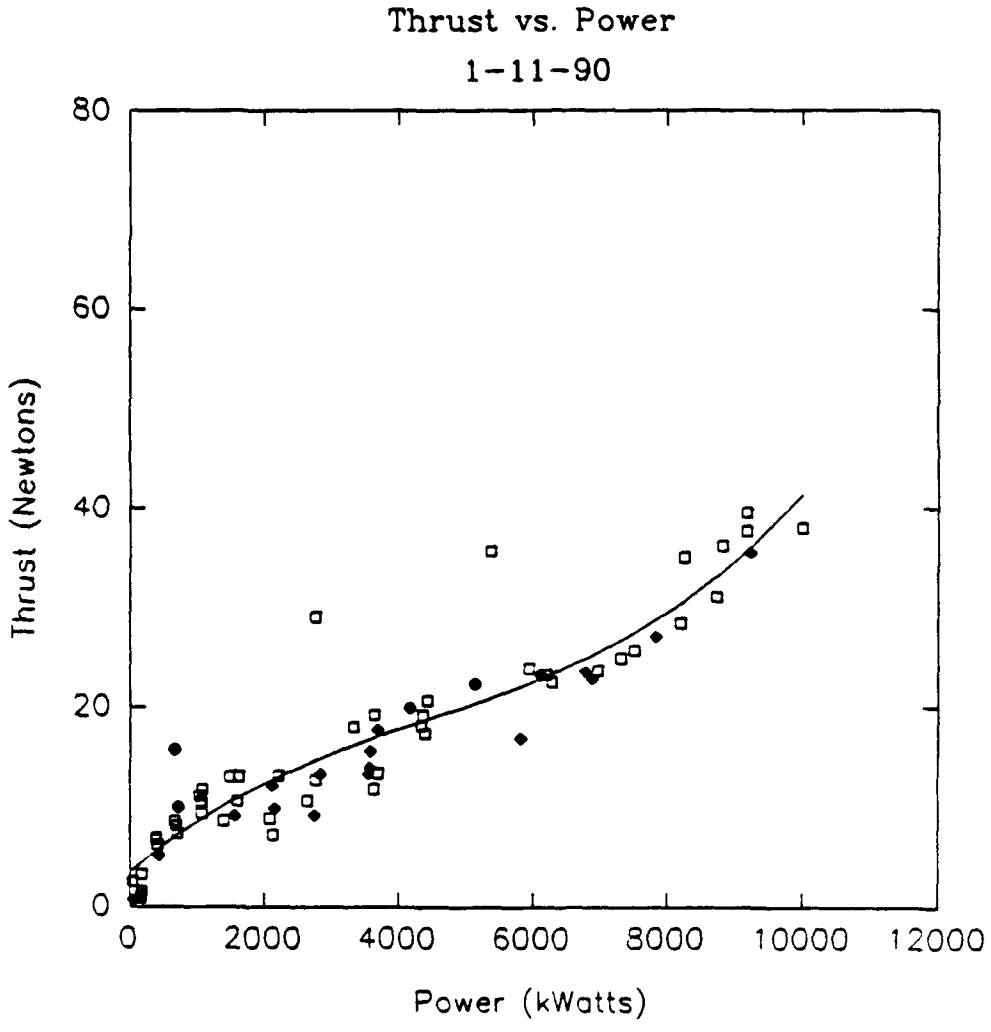
Thrust vs. Power
1-11-90
Thrust (Newtons)
Power (kWatts)
0
20
40
60
80
0
2000
4000
6000
8000
10000
12000

C: 3.4 A: 3.4

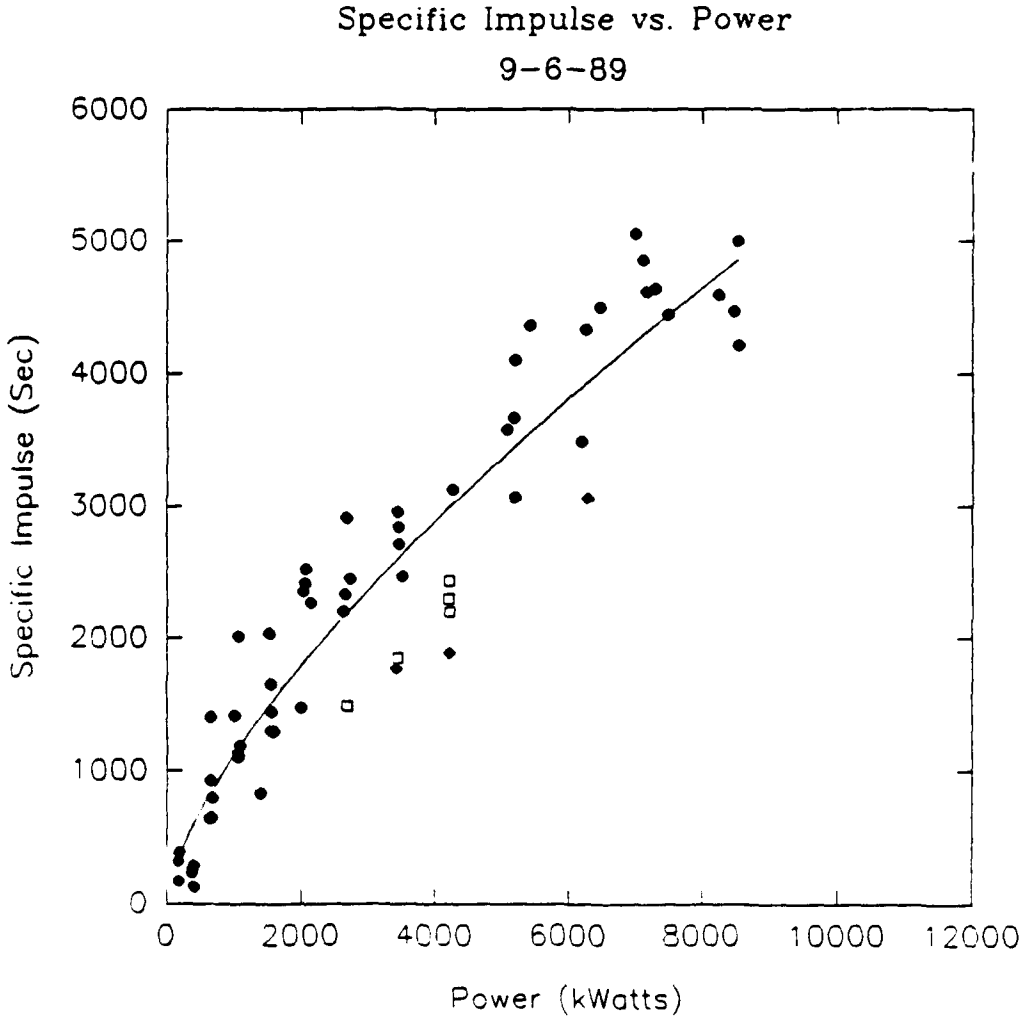
Specific Impulse vs. Power
9-6-89
Specific Impulse (Sec)
6000
5000
4000
3000
2000
1000
0
0
2000
4000
6000
8000
10000
12000
Power (kWatts)

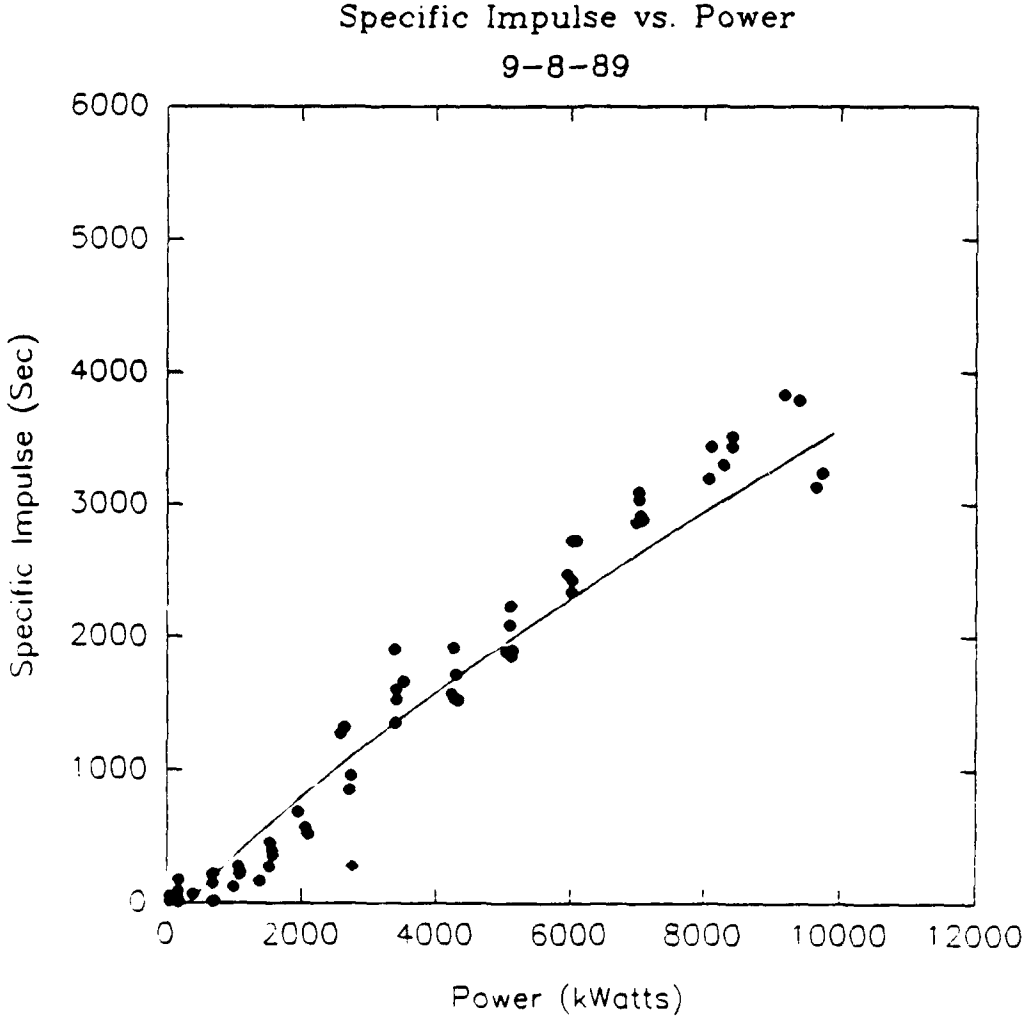
Specific Impulse vs. Power
9-8-89
Specific Impulse (Sec)
6000
5000
4000
3000
2000
1000
0
0
2000
4000
6000
8000
10000
12000
Power (kWatts)

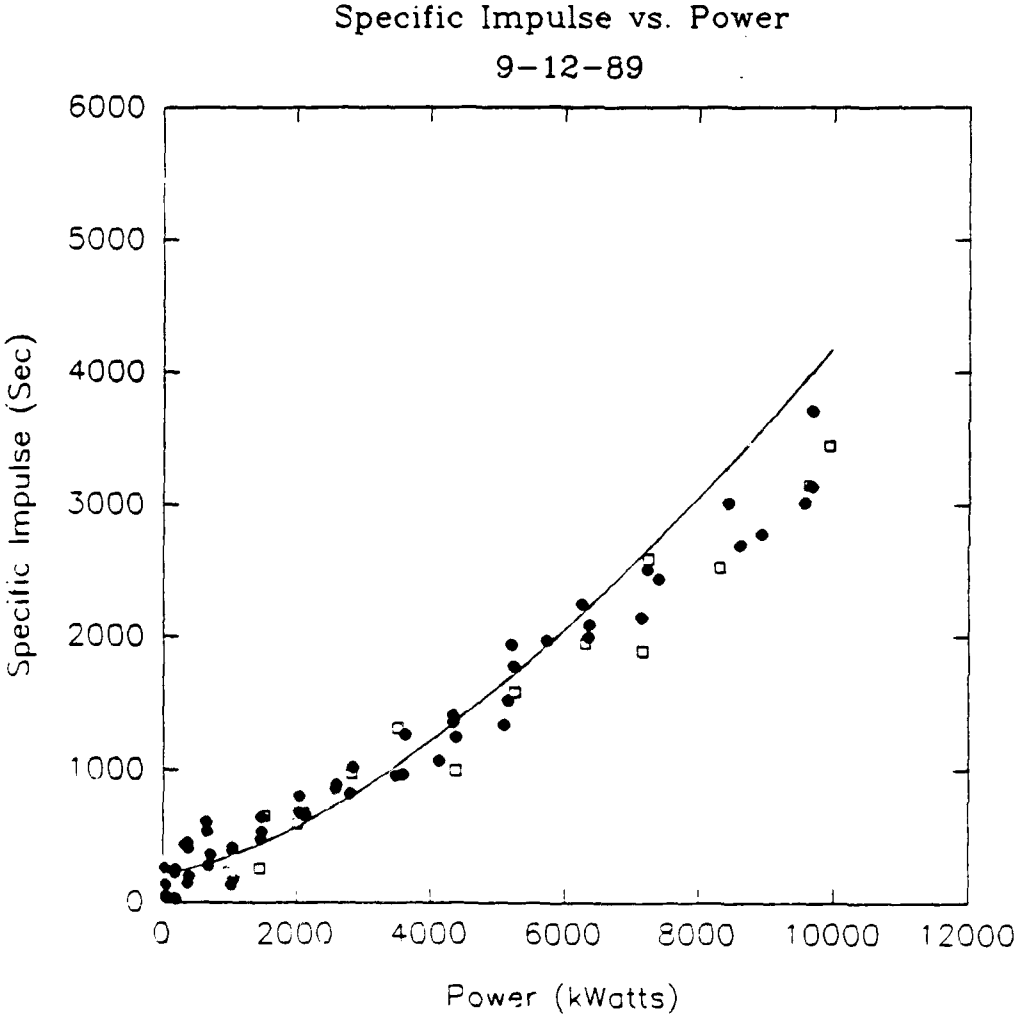
Specific Impulse vs. Power
9-12-89
Specific Impulse (Sec)
6000
5000
4000
3000
2000
1000
0
0
2000
4000
6000
8000
10000
12000
Power (kWatts)

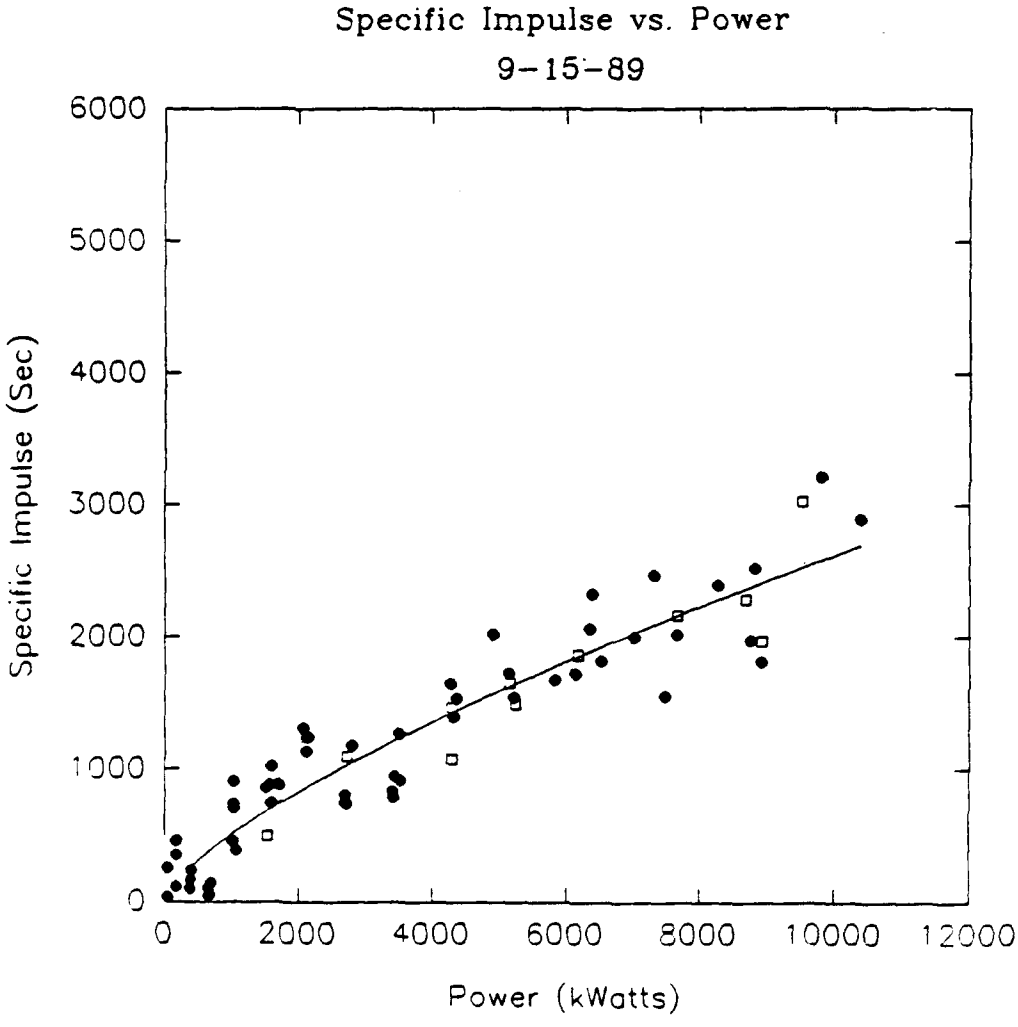
Specific Impulse vs. Power
9-15-89
Specific Impulse (Sec)
6000
5000
4000
3000
2000
1000
0
0
2000
4000
6000
8000
10000
12000
Power (kWatts)

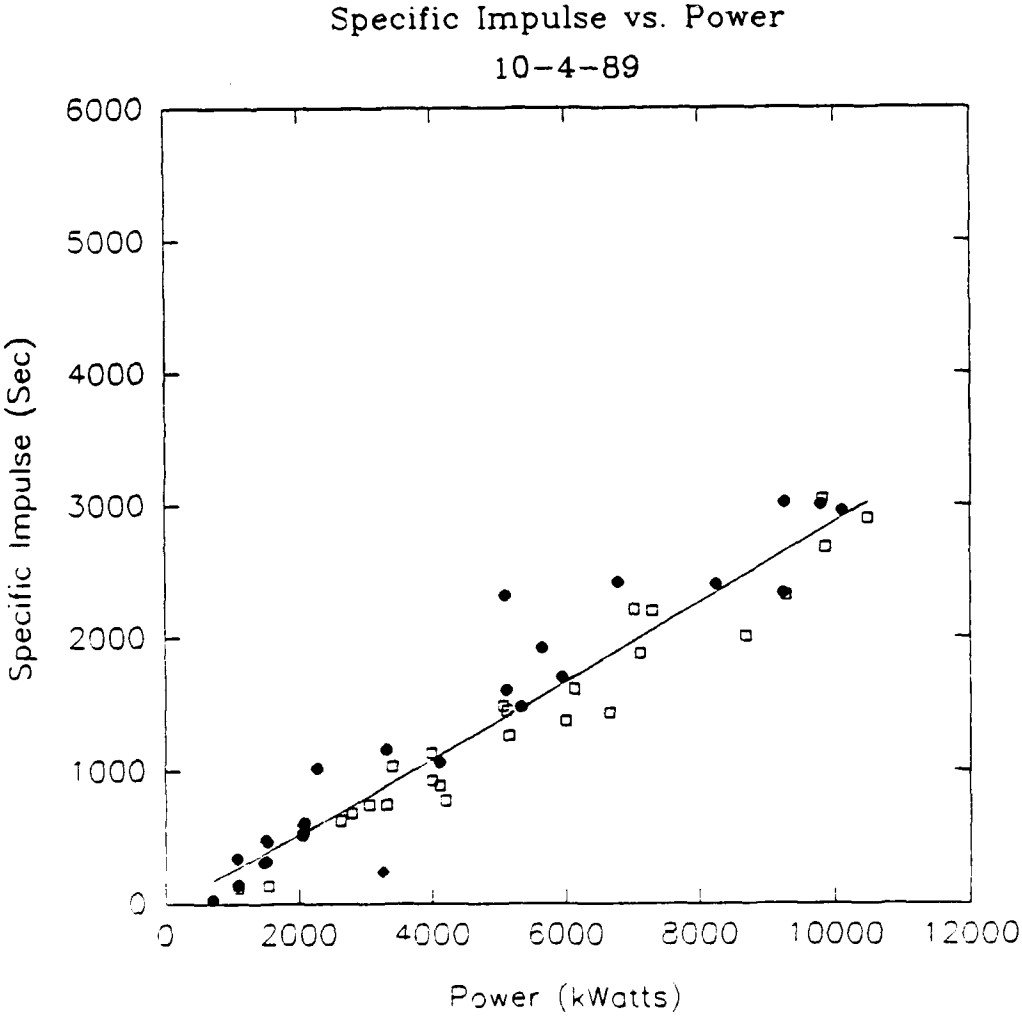
Specific Impulse vs. Power
10-4-89
Specific Impulse (Sec)
6000
5000
4000
3000
2000
1000
0
0
2000
4000
6000
8000
10000
12000
Power (kWatts)

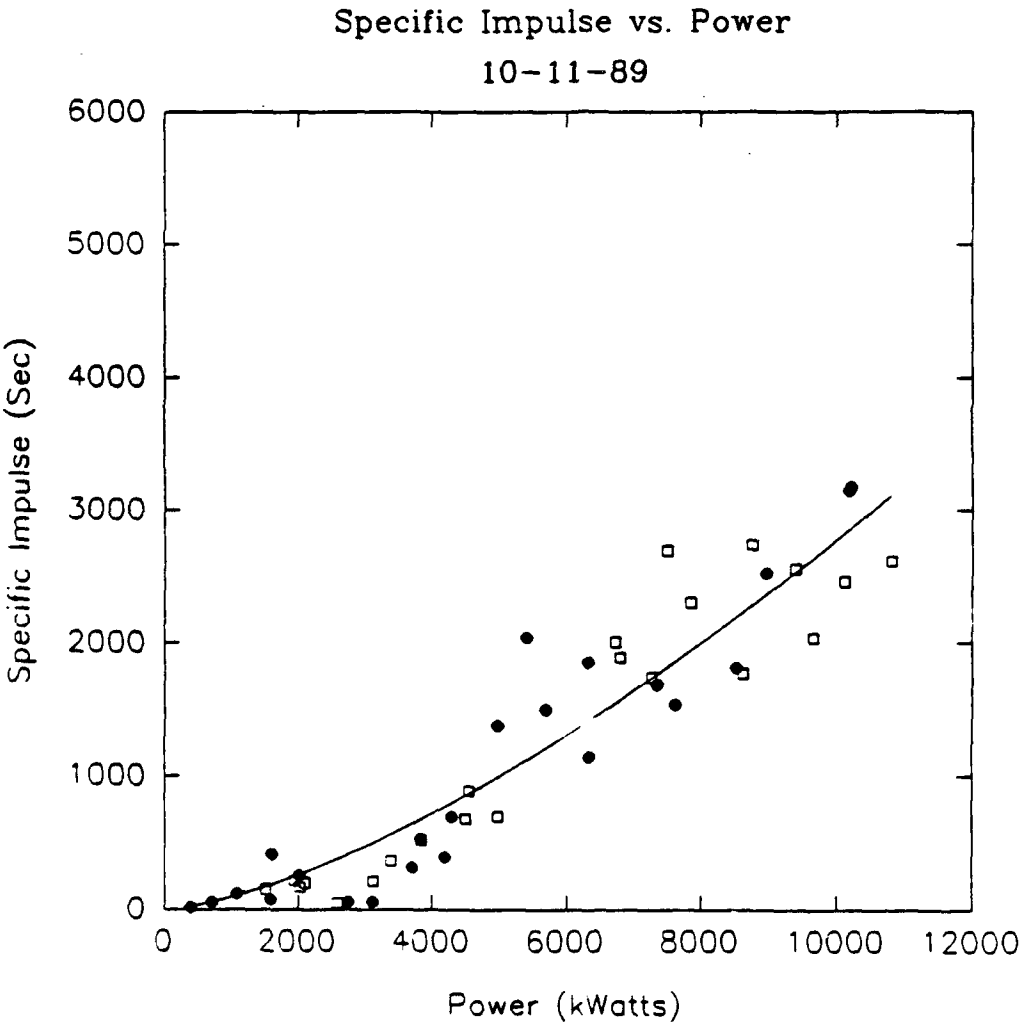
Specific Impulse vs. Power
10-11-89
Specific Impulse (Sec)
6000
5000
4000
3000
2000
1000
0
0
2000
4000
6000
8000
10000
12000
Power (kWatts)

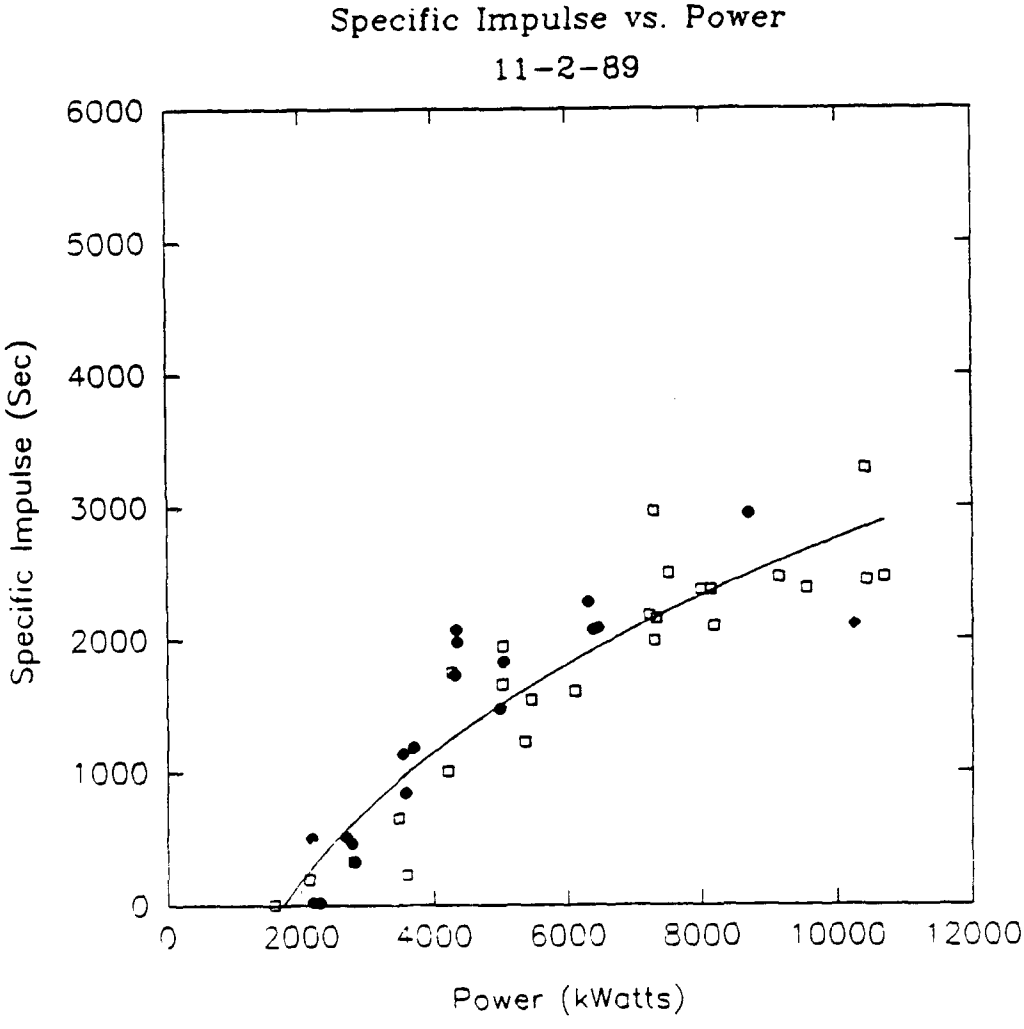
Specific Impulse vs. Power
11-2-89
Specific Impulse (Sec)
6000
5000
4000
3000
2000
1000
0
0
2000
4000
6000
8000
10000
12000
Power (kWatts)

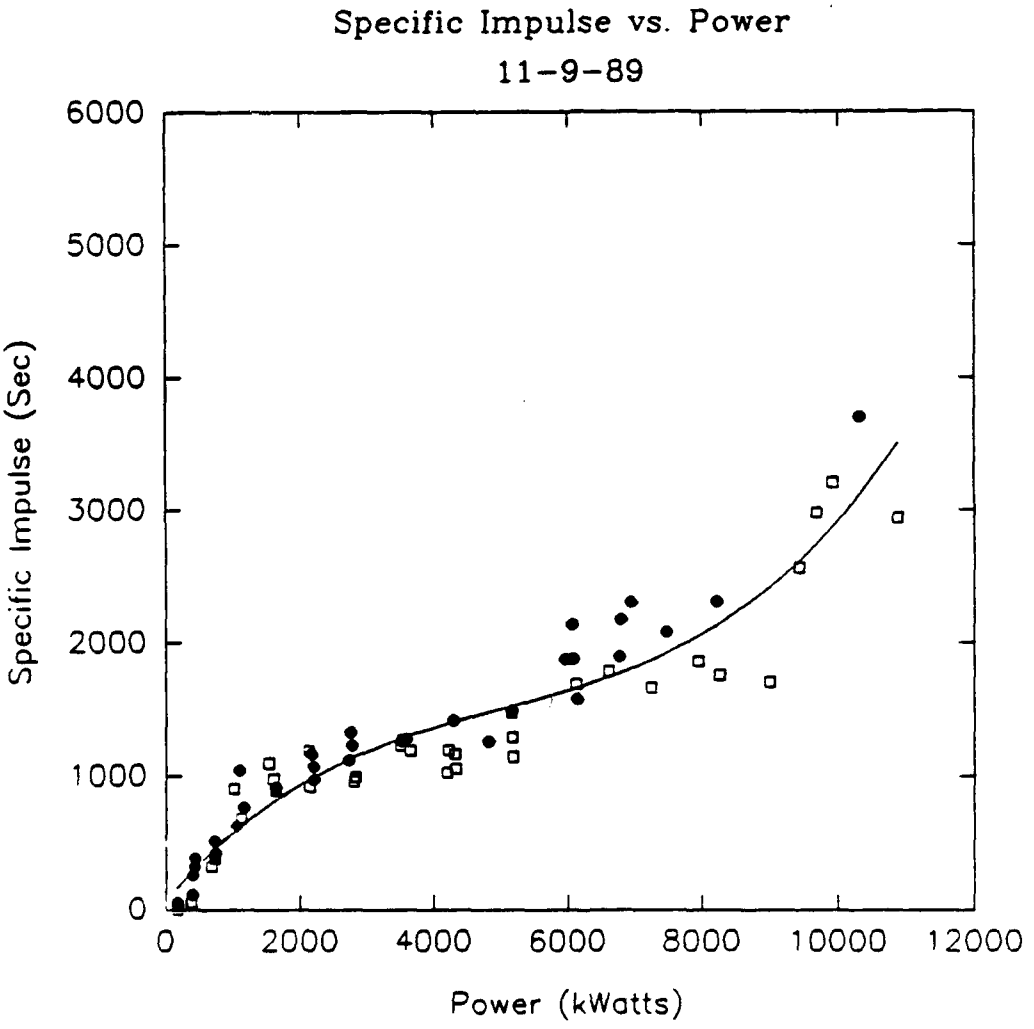
Specific Impulse vs. Power
11-9-89
Specific Impulse (Sec)
6000
5000
4000
3000
2000
1000
0
0
2000
4000
6000
8000
10000
12000
Power (kWatts)

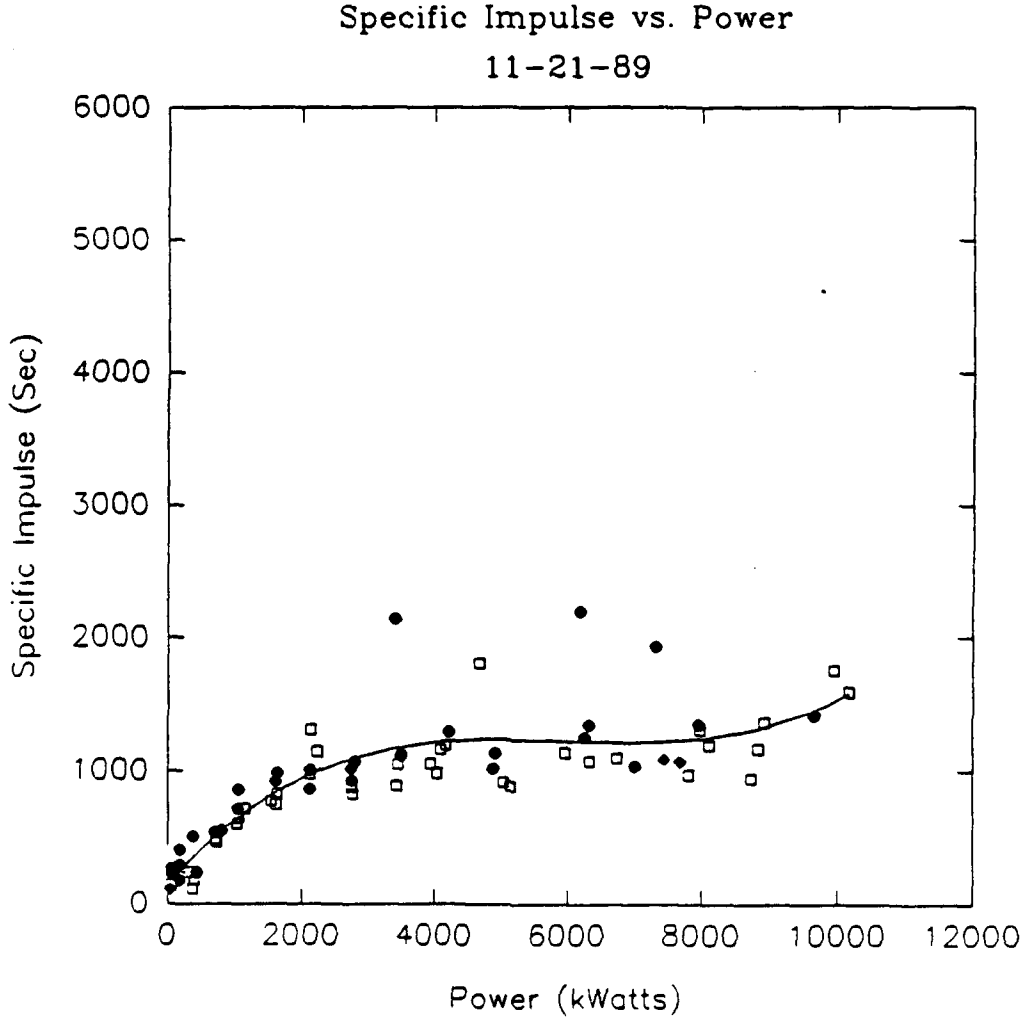
Specific Impulse vs. Power
11-21-89
Specific Impulse (Sec)
6000
5000
4000
3000
2000
1000
0
0
2000
4000
6000
8000
10000
12000
Power (kWatts)

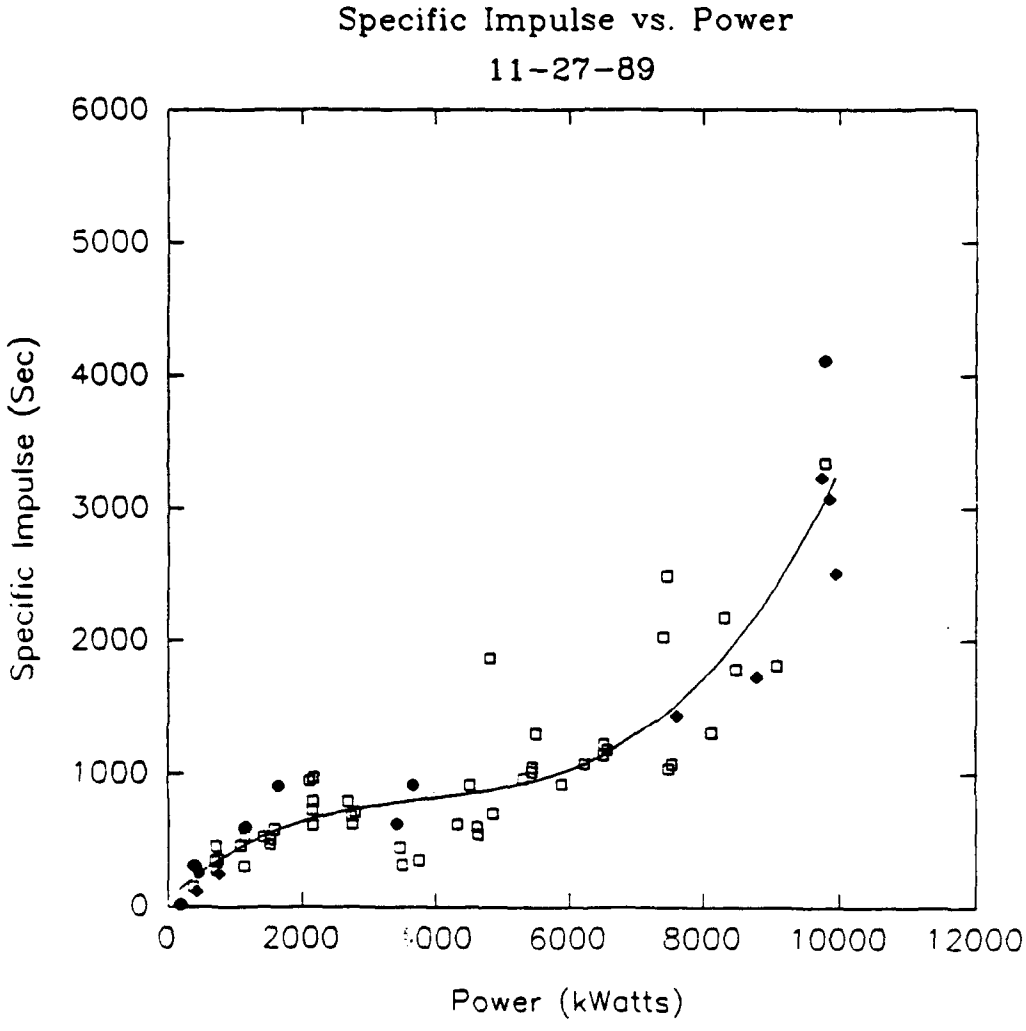
Specific Impulse vs. Power
11-27-89
Specific Impulse (Sec)
6000
5000
4000
3000
2000
1000
0
0
2000
4000
6000
8000
10000
12000
Power (kWatts)

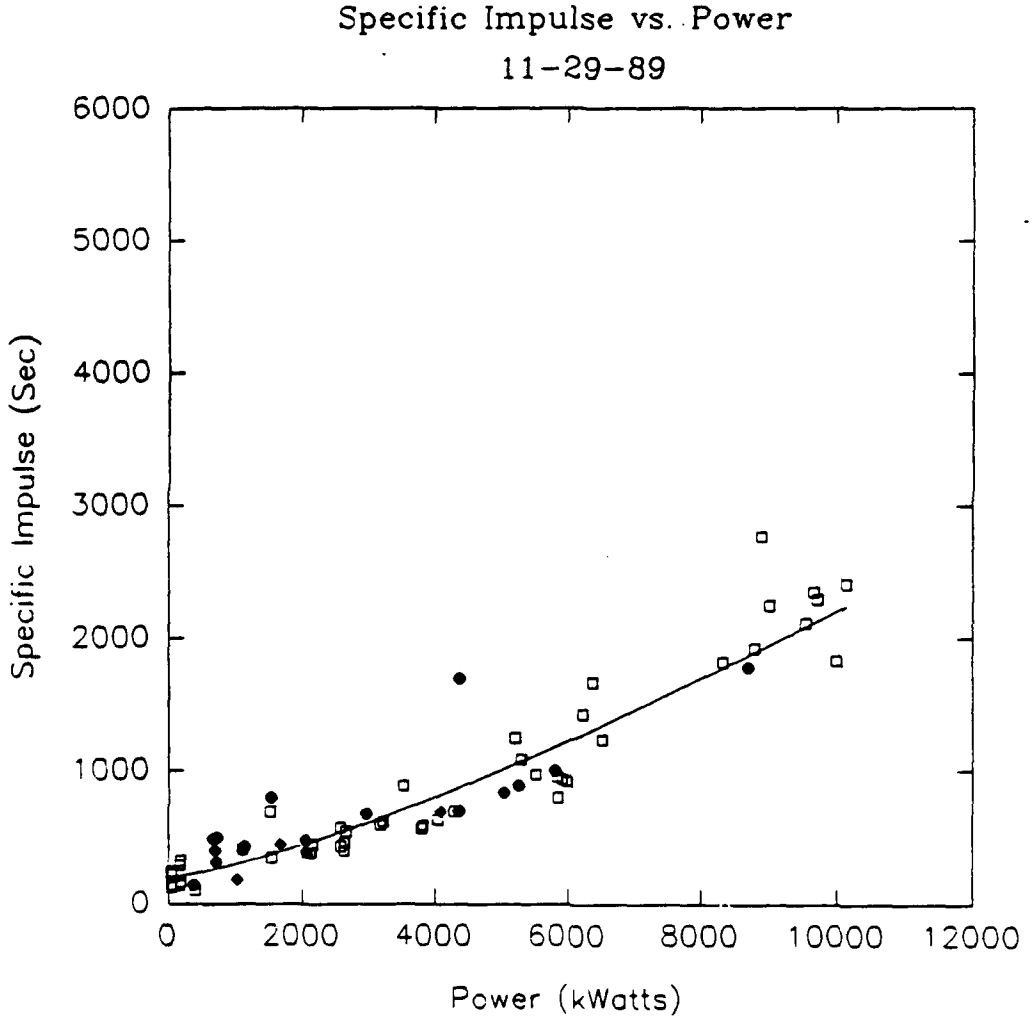
Specific Impulse vs. Power
11-29-89
Specific Impulse (Sec)
6000
5000
4000
3000
2000
1000
0
0
2000
4000
6000
8000
10000
12000
Power (kWatts)

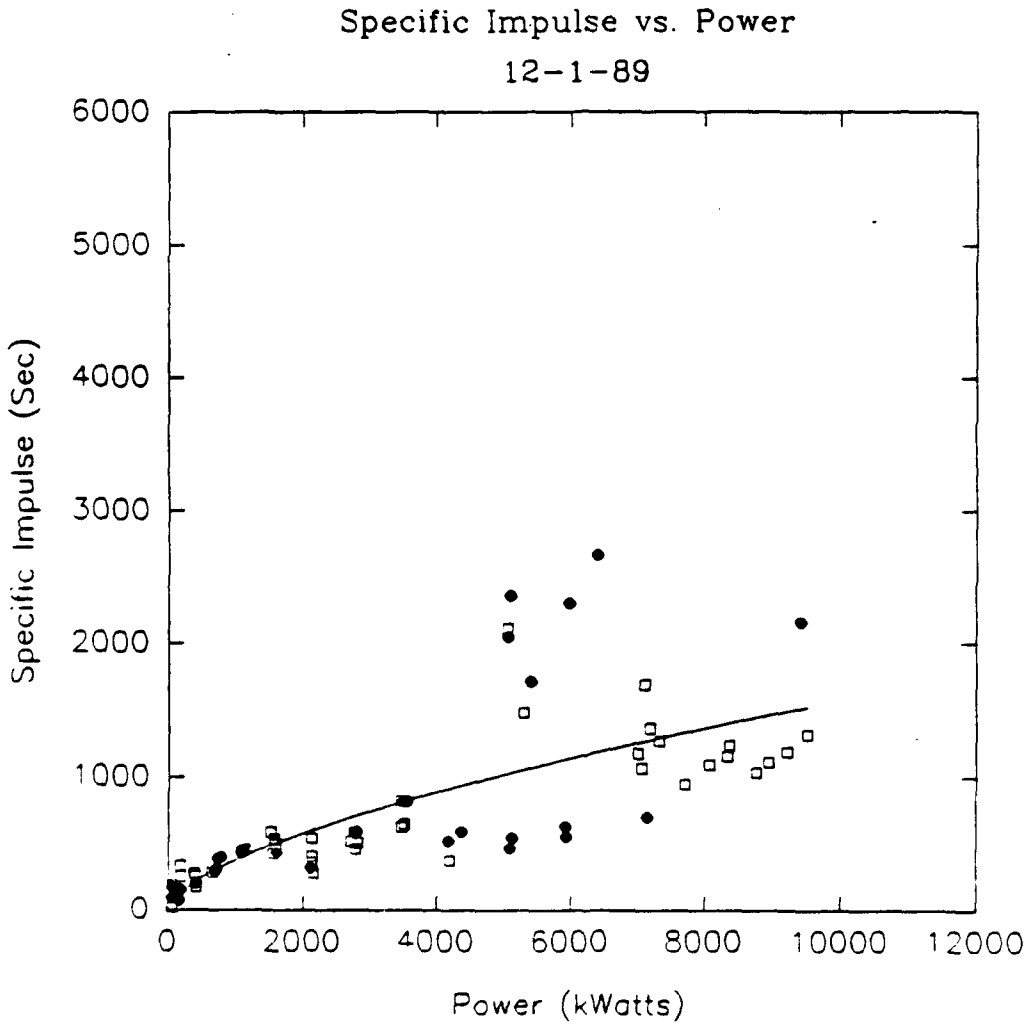
Specific Impulse vs. Power
12-1-89
Specific Impulse (Sec)
6000
5000
4000
3000
2000
1000
0
0
2000
4000
6000
8000
10000
12000
Power (kWatts)

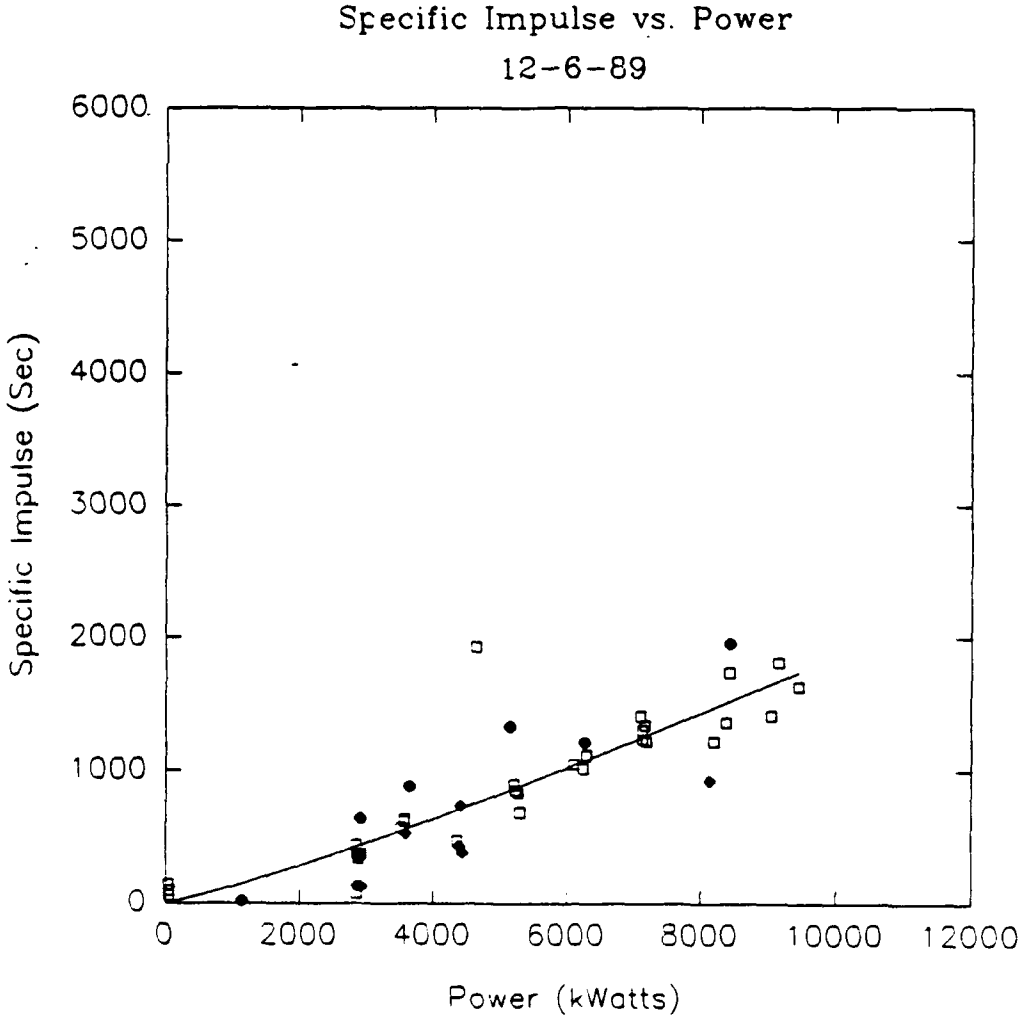
Specific Impulse vs. Power
12-6-89
6000
5000
4000
3000
2000
1000
0
Specific Impulse (Sec)
0
2000
4000
6000
8000
10000
12000
Power (kWatts)

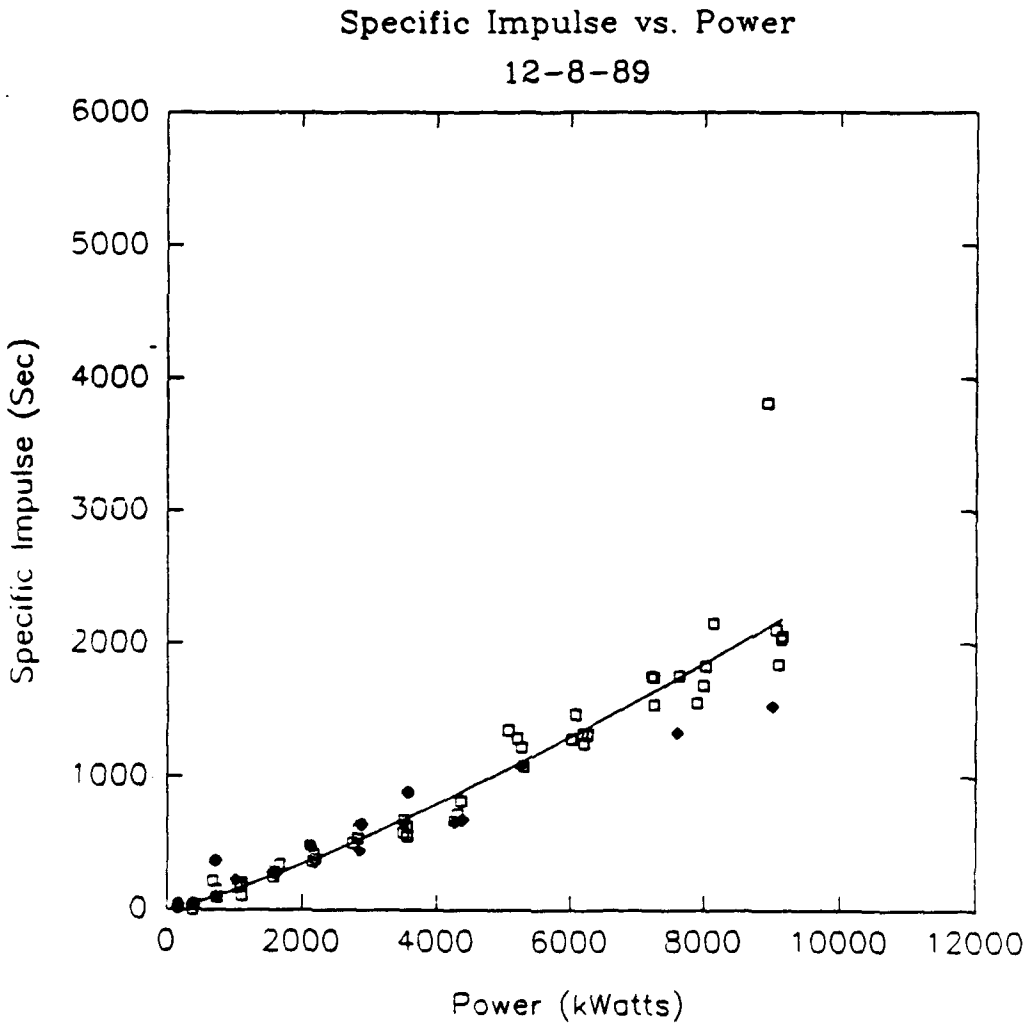
Specific Impulse vs. Power
12-8-89
Specific Impulse (Sec)
6000
5000
4000
3000
2000
1000
0
0
2000
4000
6000
8000
10000
12000
Power (kWatts)

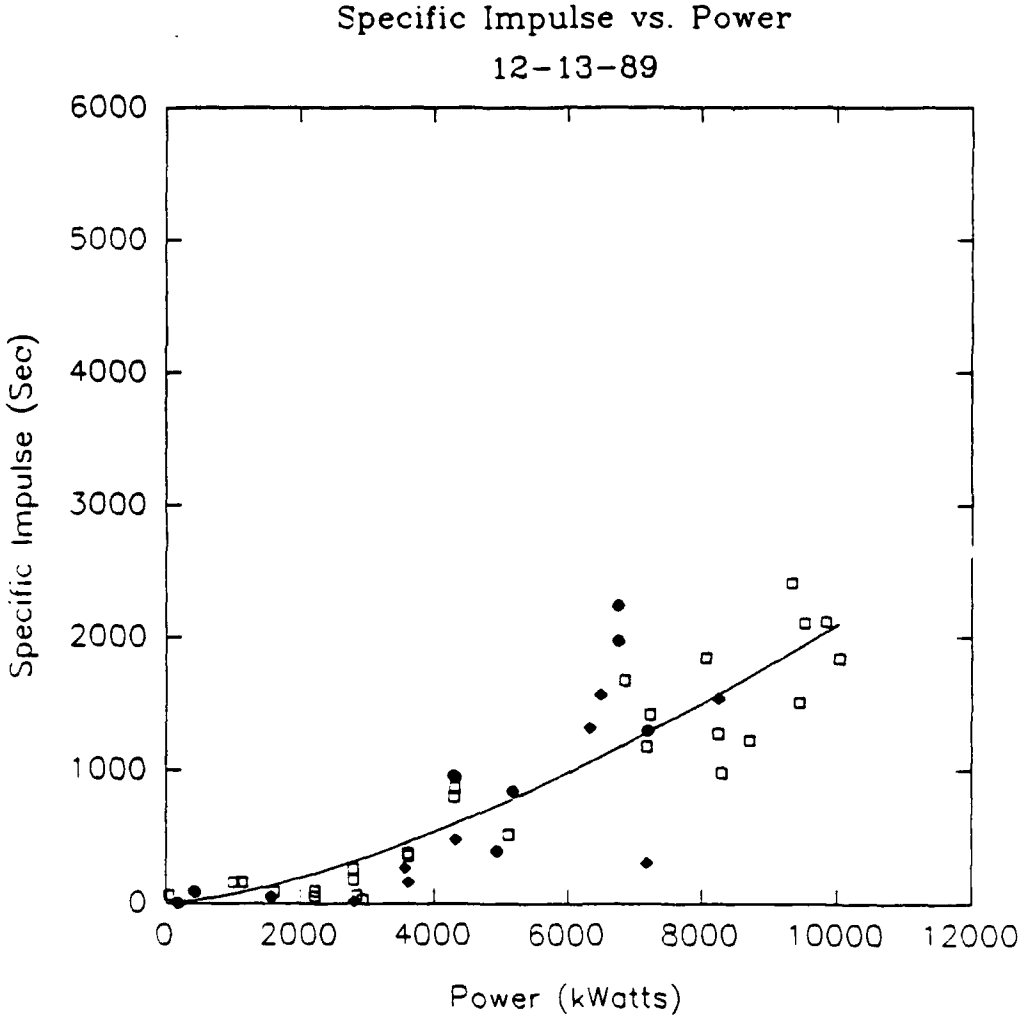
Specific Impulse vs. Power
12-13-89
Specific Impulse (Sec)
6000
5000
4000
3000
2000
1000
0
0
2000
4000
6000
8000
10000
12000
Power (kWatts)

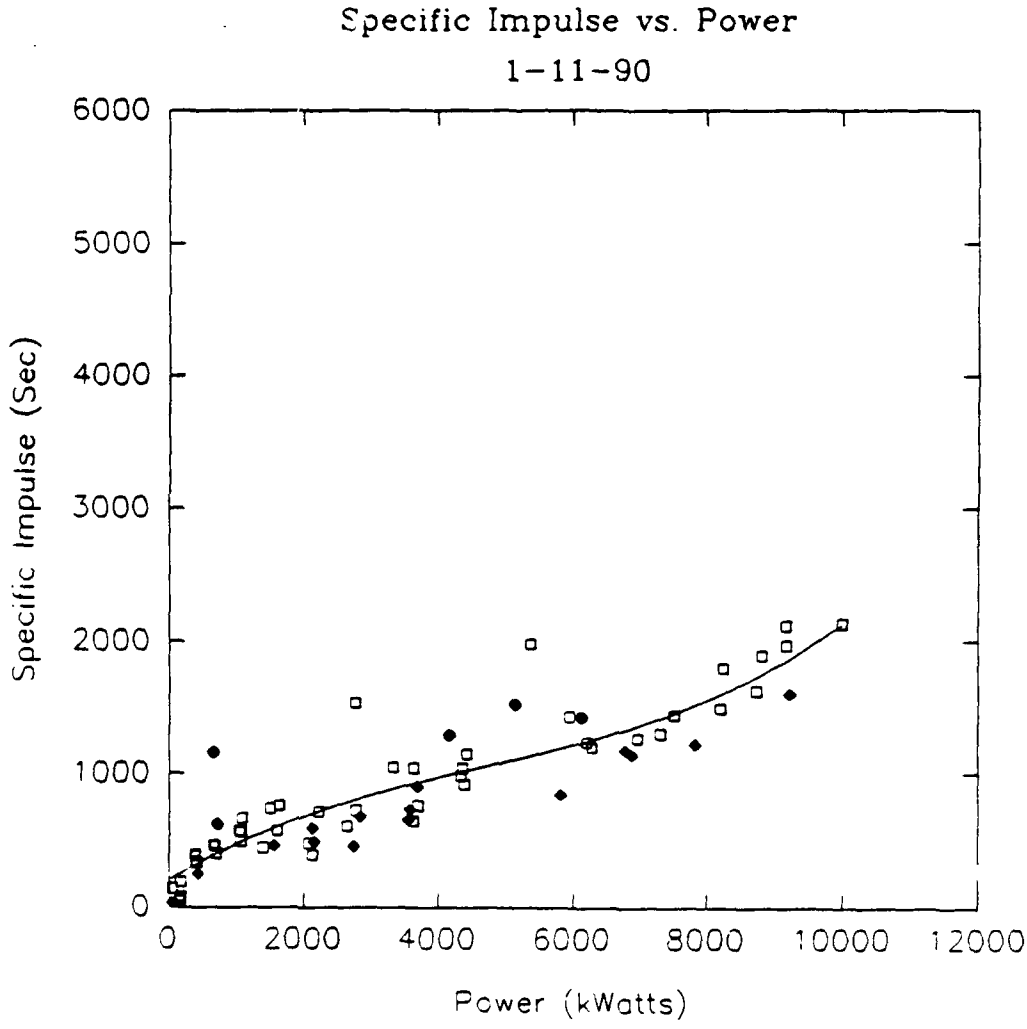
Specific Impulse vs. Power
1-11-90
Specific Impulse (Sec)
6000
5000
4000
3000
2000
1000
0
0
2000
4000
6000
8000
10000
12000
Power (kWatts)

$$n = \frac{T^2}{2\dot{m}IV}$$

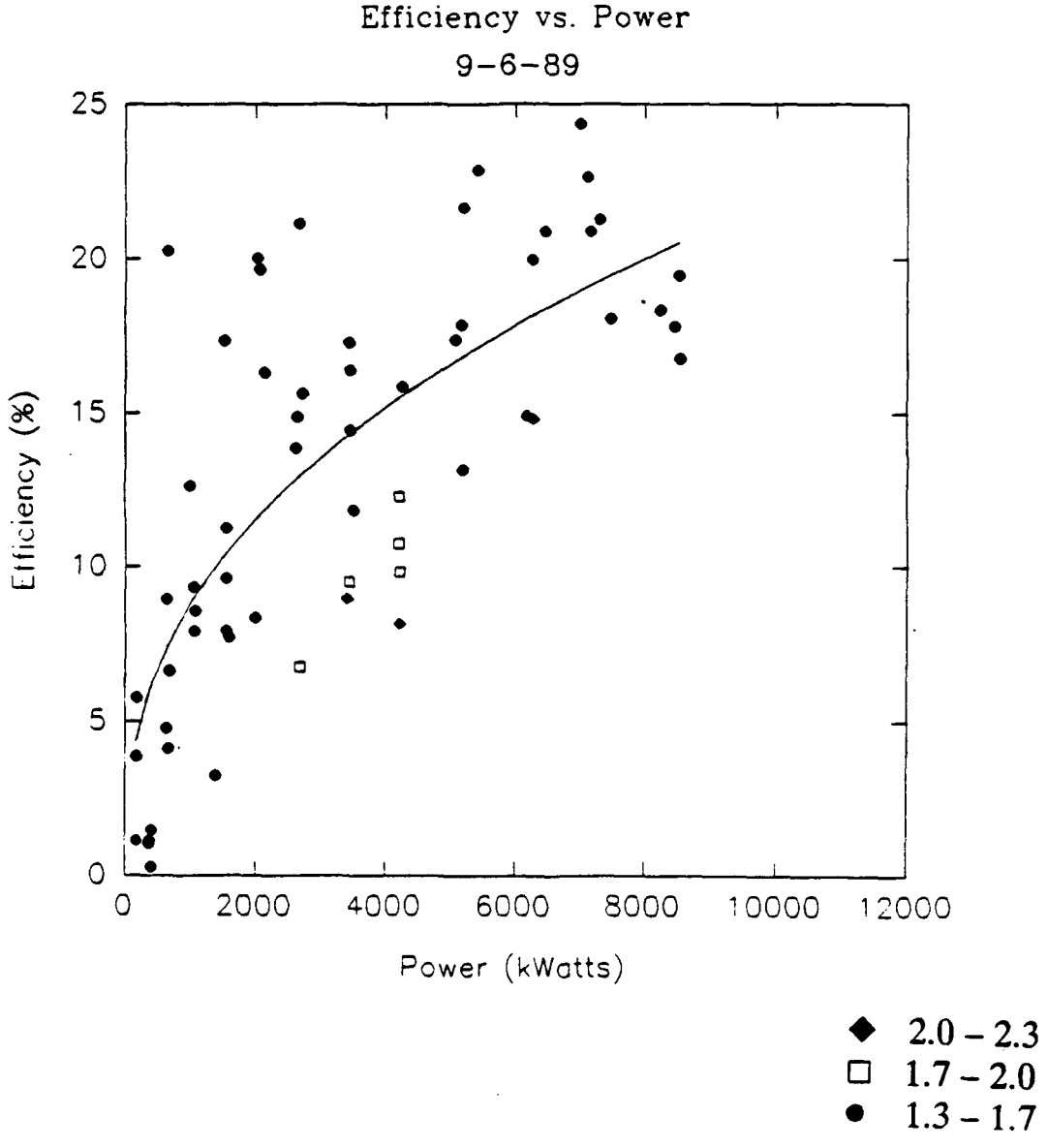

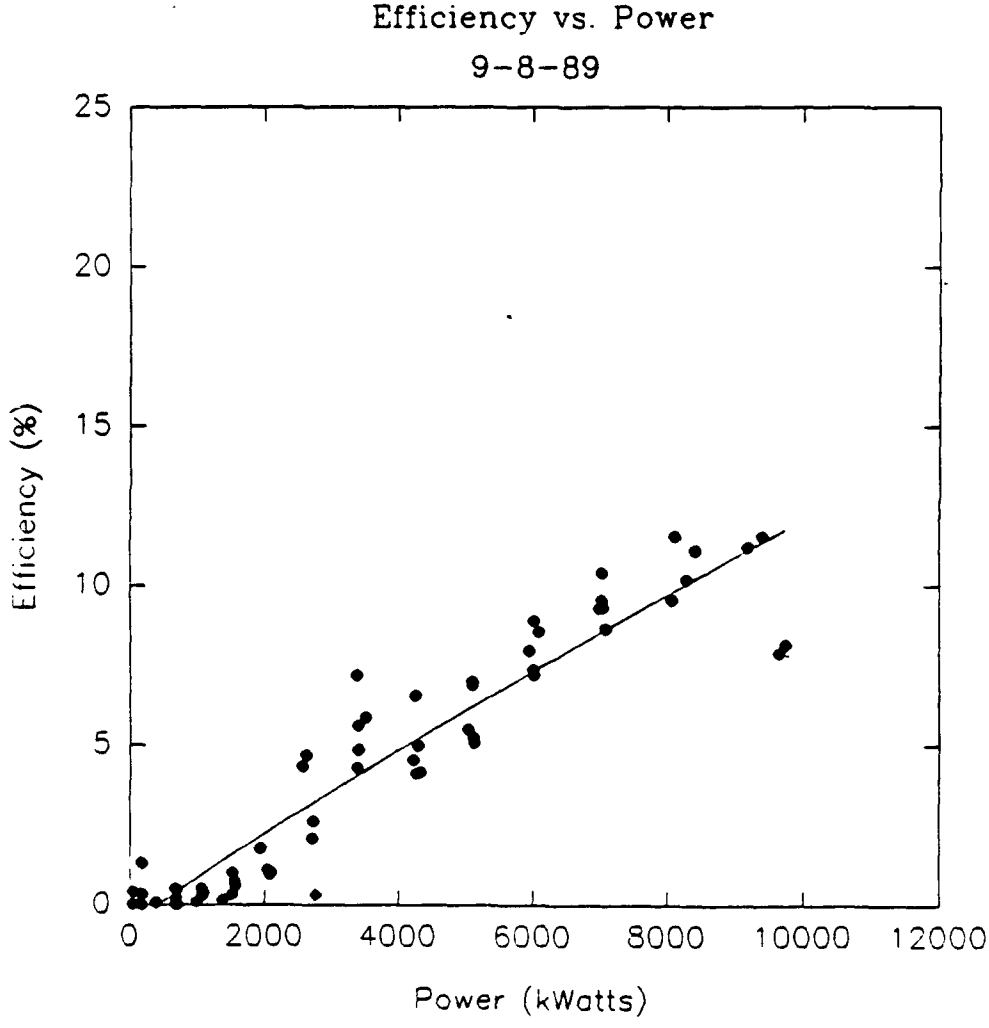
Efficiency vs. Power
9-8-89
Efficiency (%)
25
20
15
10
5
0
0
2000
4000
6000
8000
10000
12000
Power (kWatts)

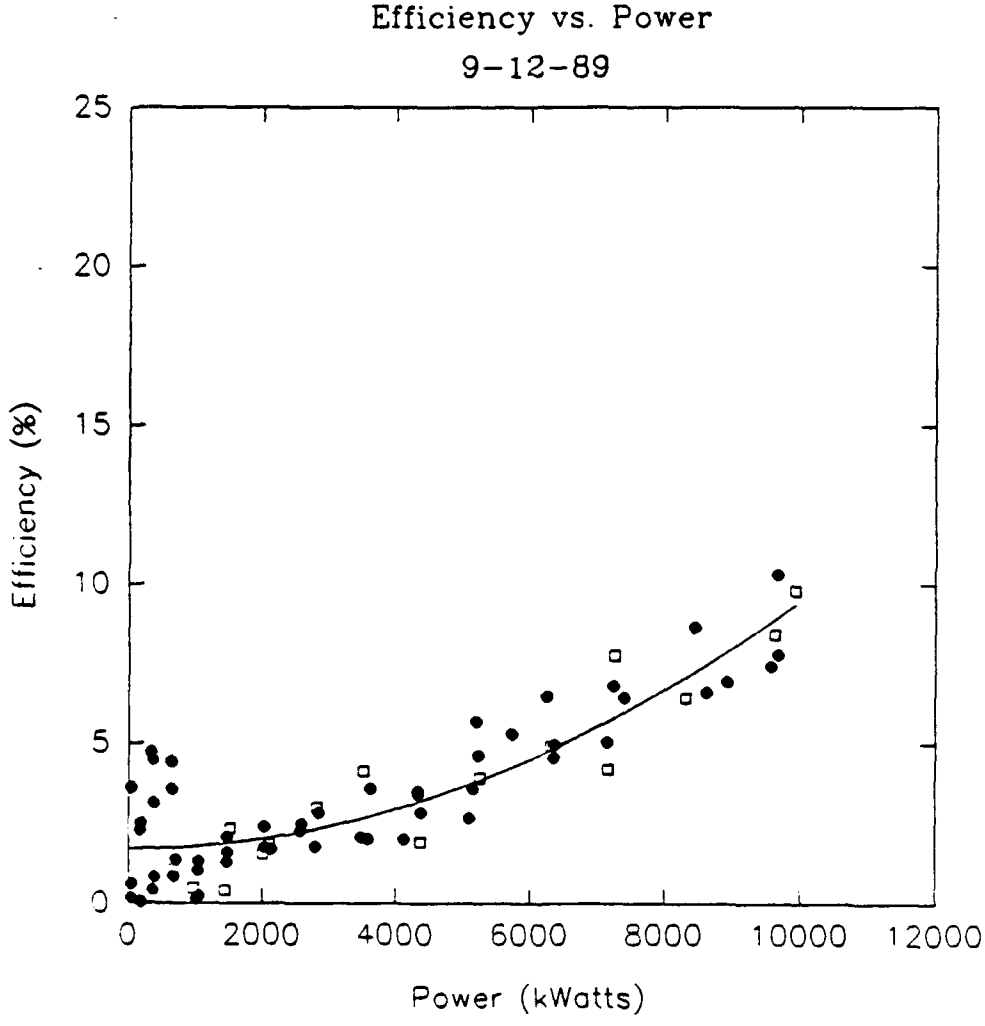
Efficiency vs. Power
9-12-89
25
20
15
10
5
0
Efficiency (%)
0
2000
4000
6000
8000
10000
12000
Power (kWatts)

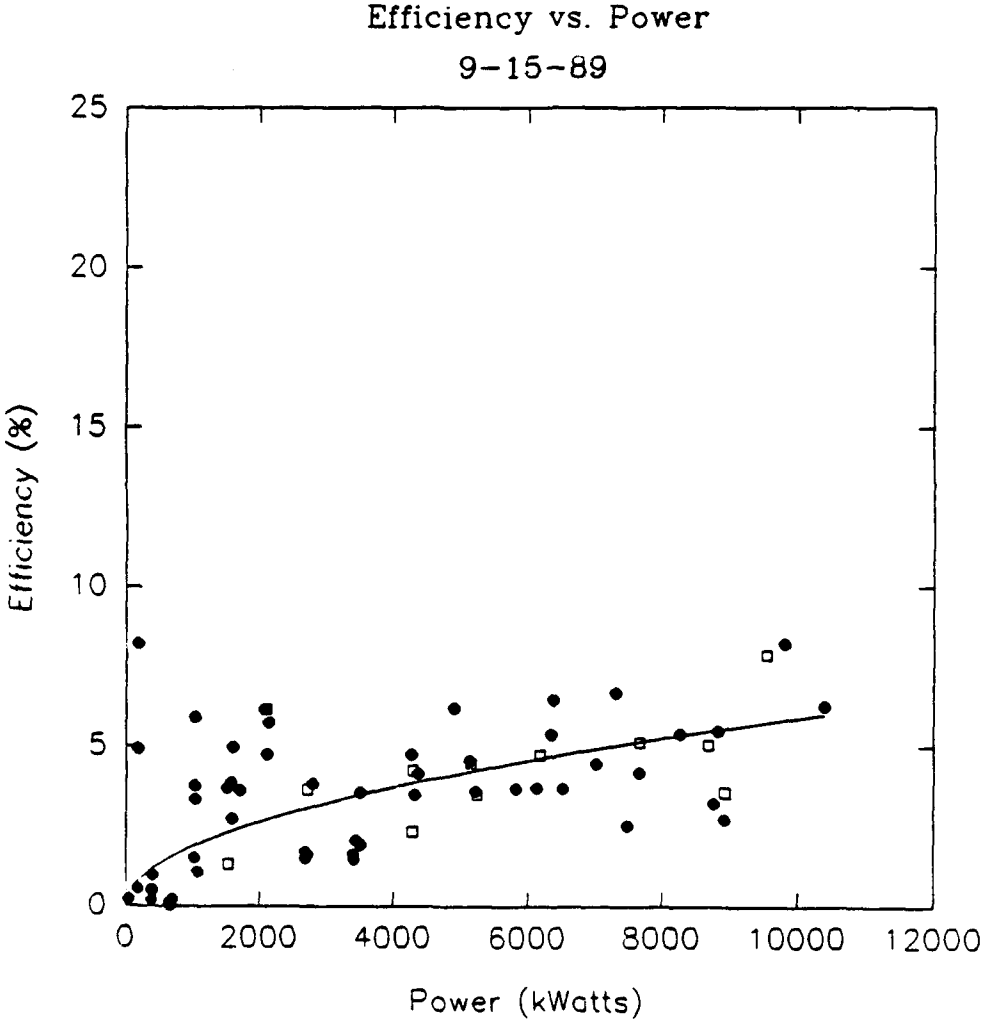
Efficiency vs. Power
9-15-89
25
20
15
10
5
0
Efficiency (%)
0
2000
4000
6000
8000
10000
12000
Power (kWatts)

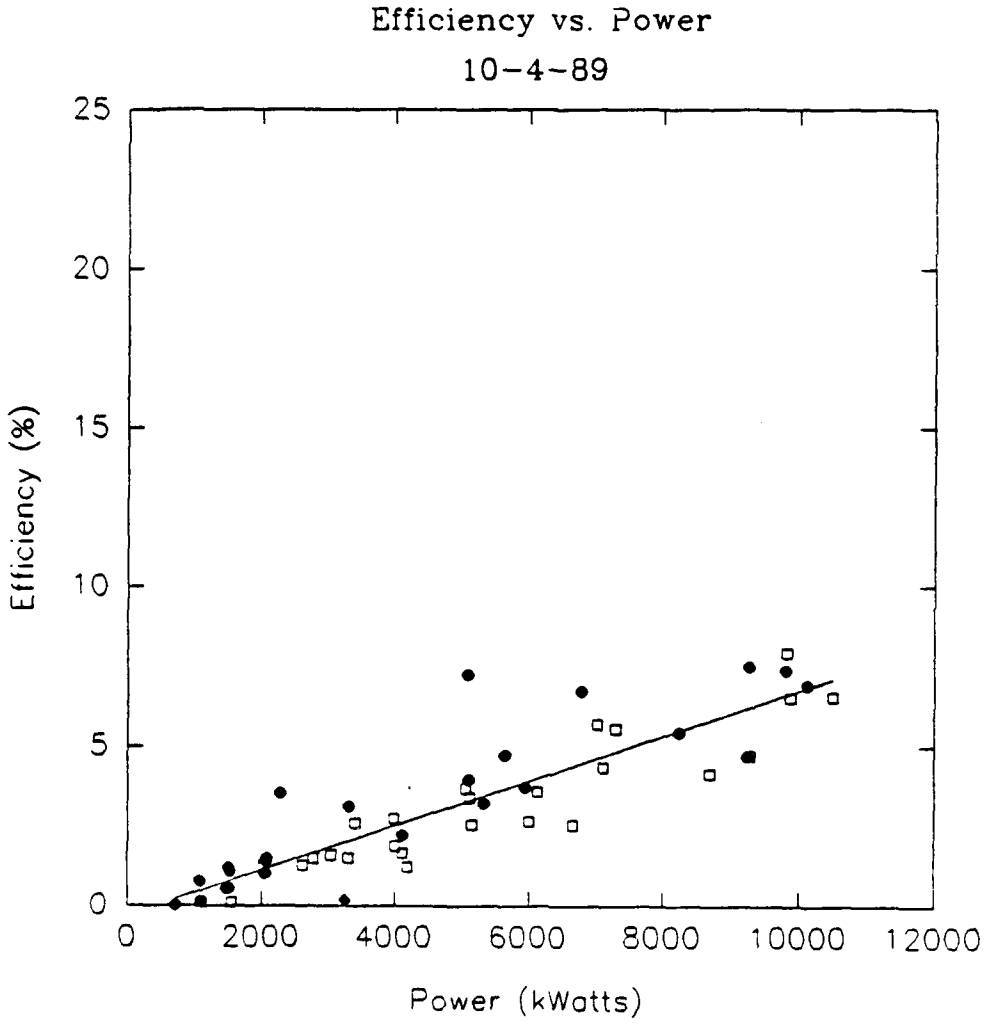
Efficiency vs. Power
10-4-89
Efficiency (%)
25
20
15
10
5
0
0
2000
4000
6000
8000
10000
12000
Power (kWatts)

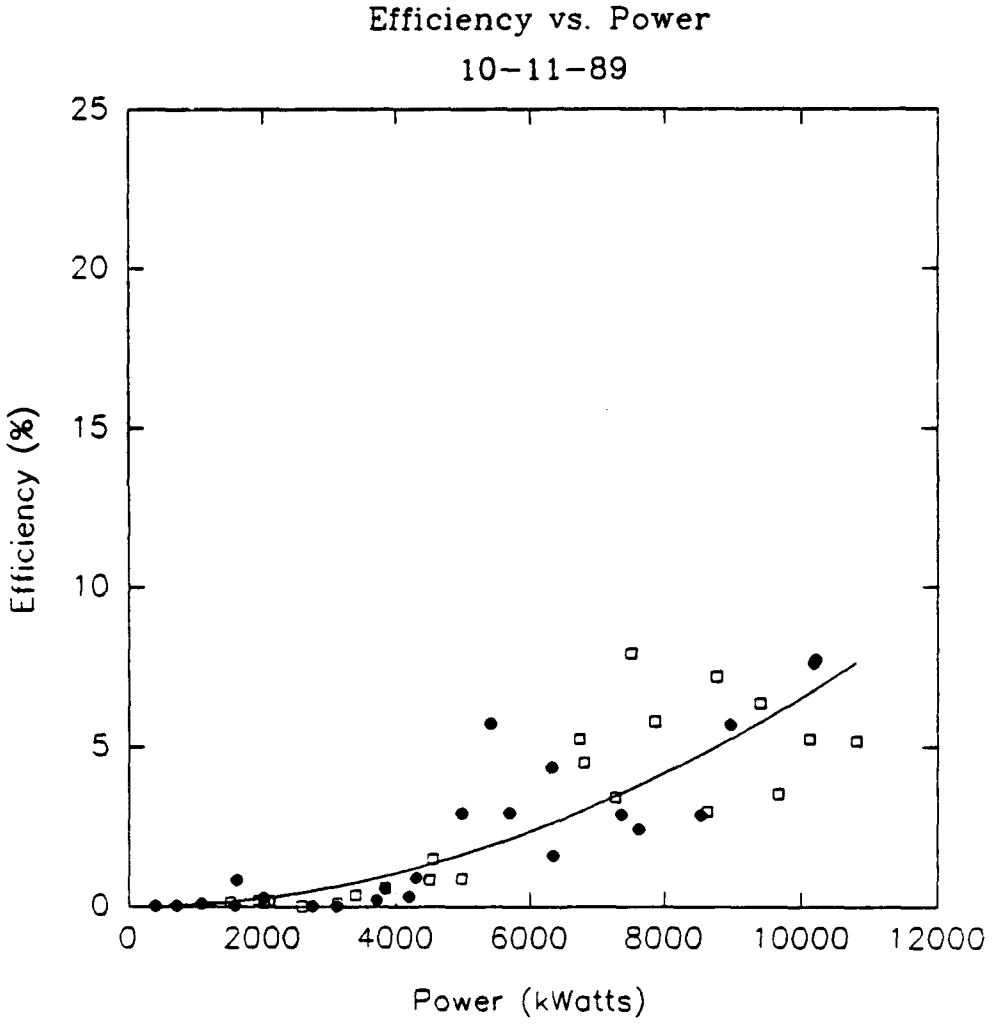
Efficiency vs. Power
10-11-89
25
20
15
10
5
0
Efficiency (%)
0
2000
4000
6000
8000
10000
12000
Power (kWatts)

C: 3.4 A: 13.4

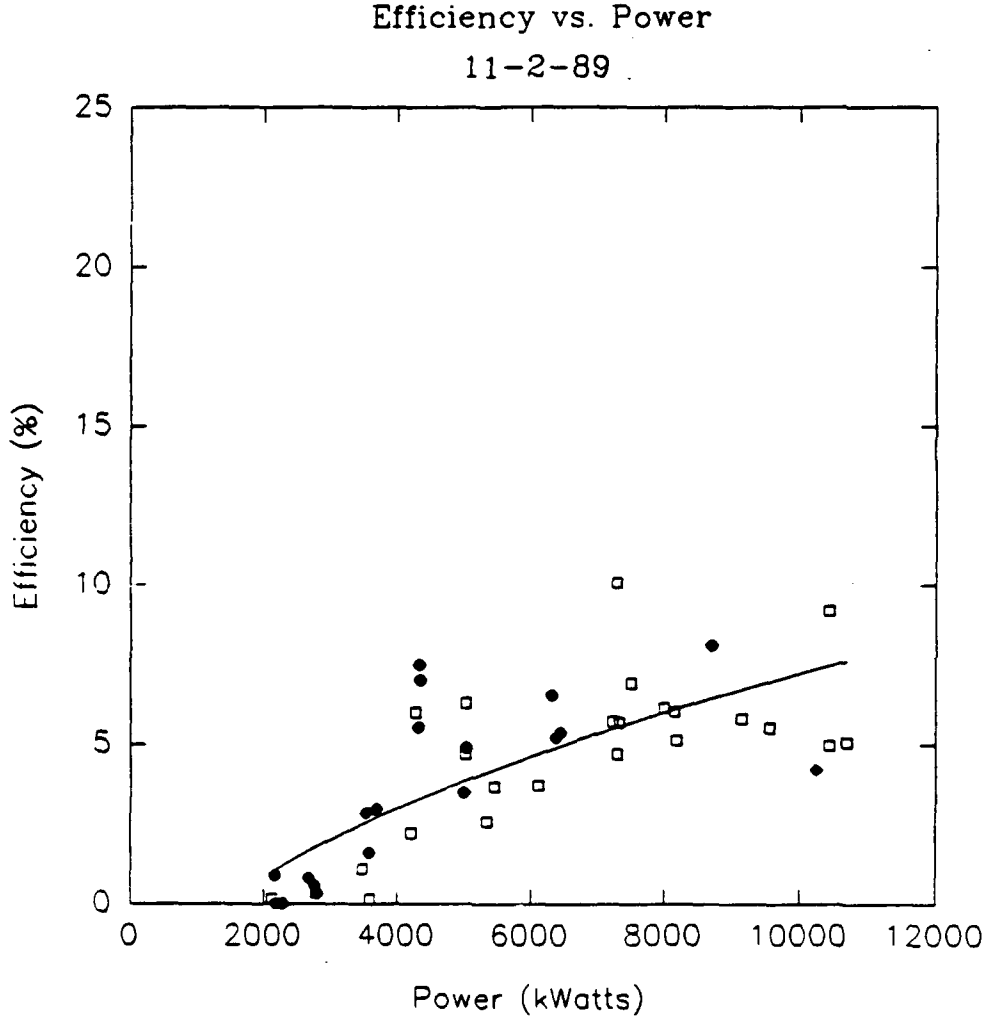
Efficiency vs. Power
11-2-89
Efficiency (%)
25
20
15
10
5
0
0
2000
4000
6000
8000
10000
12000
Power (kWatts)

C: 18.4 A: 18.4

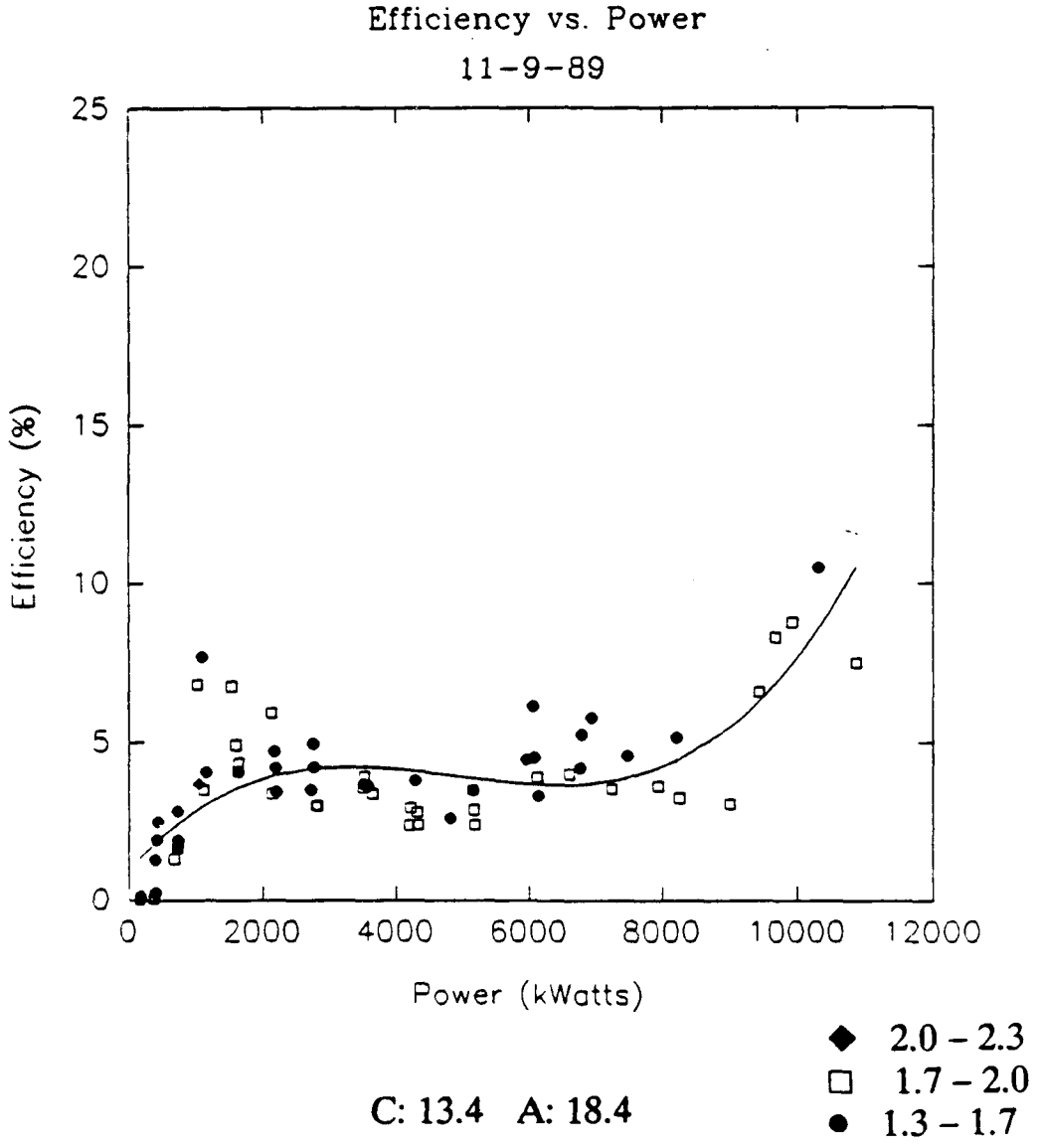
Efficiency vs. Power
11-9-89
25
20
15
10
5
0
Efficiency (%)
0
2000
4000
6000
8000
10000
12000
Power (kWatts)
2.0 – 2.3
1.7 – 2.0
1.3 – 1.7
C: 13.4 A: 18.4

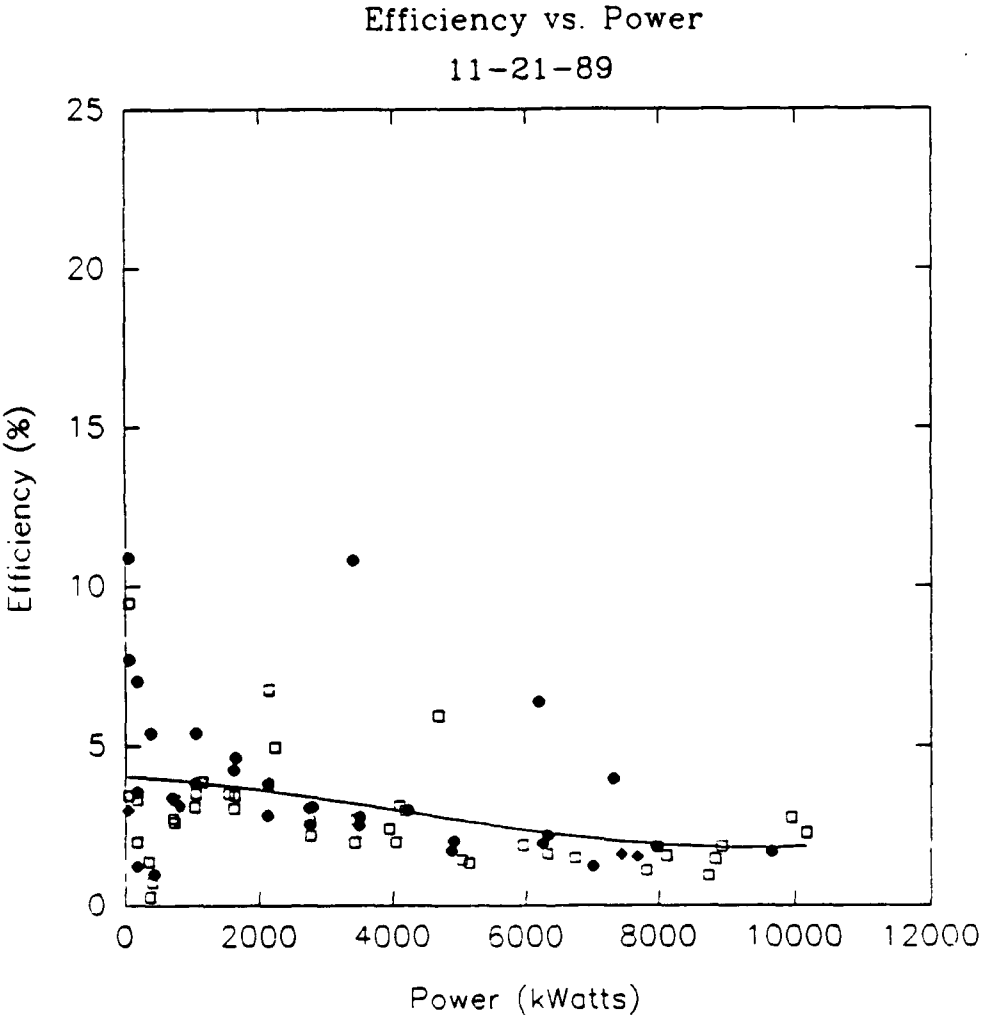
Efficiency vs. Power
11-21-89
Efficiency (%)
25
20
15
10
5
0
0
2000
4000
6000
8000
10000
12000
Power (kWatts)

C: 8.4 A: 18.4

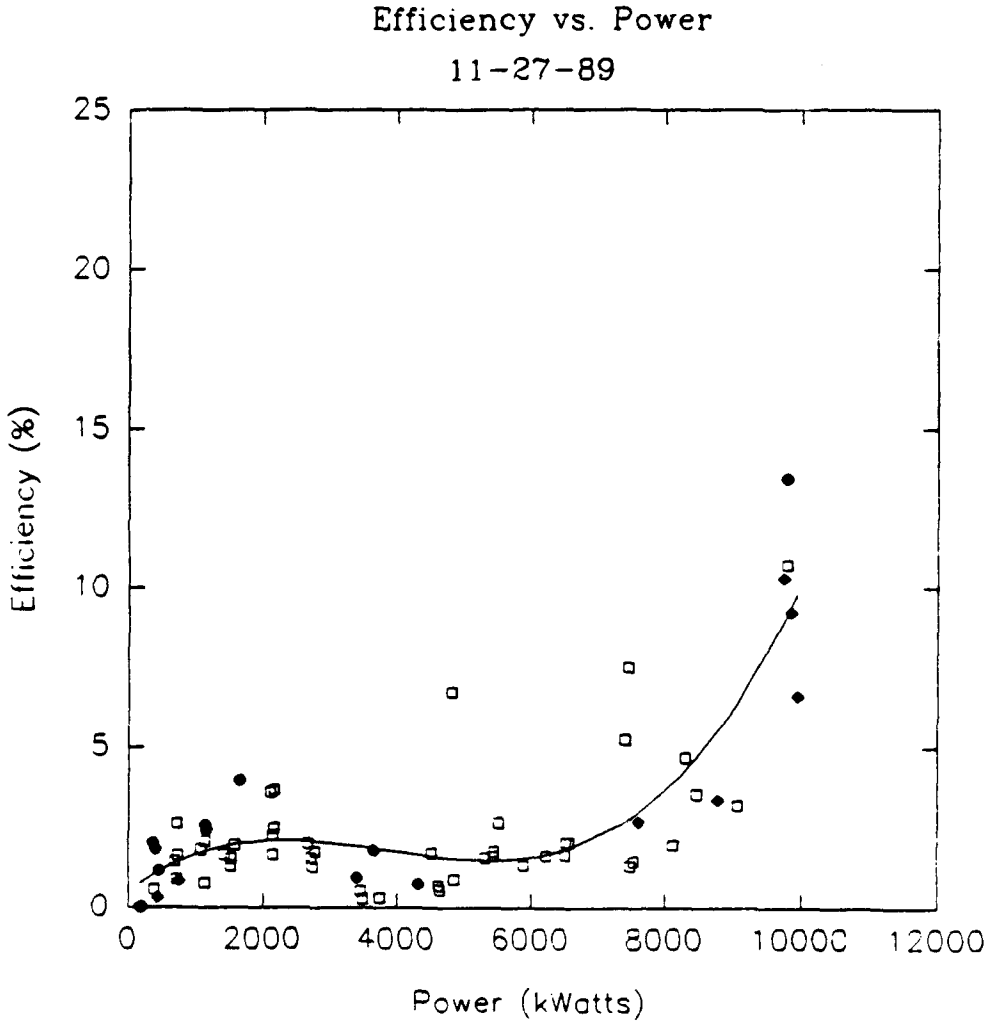
Efficiency vs. Power
11-27-89
Efficiency (%)
25
20
15
10
5
0
0
2000
4000
6000
8000
10000
12000
Power (kWatts)

C: 3.4 A: 18.4

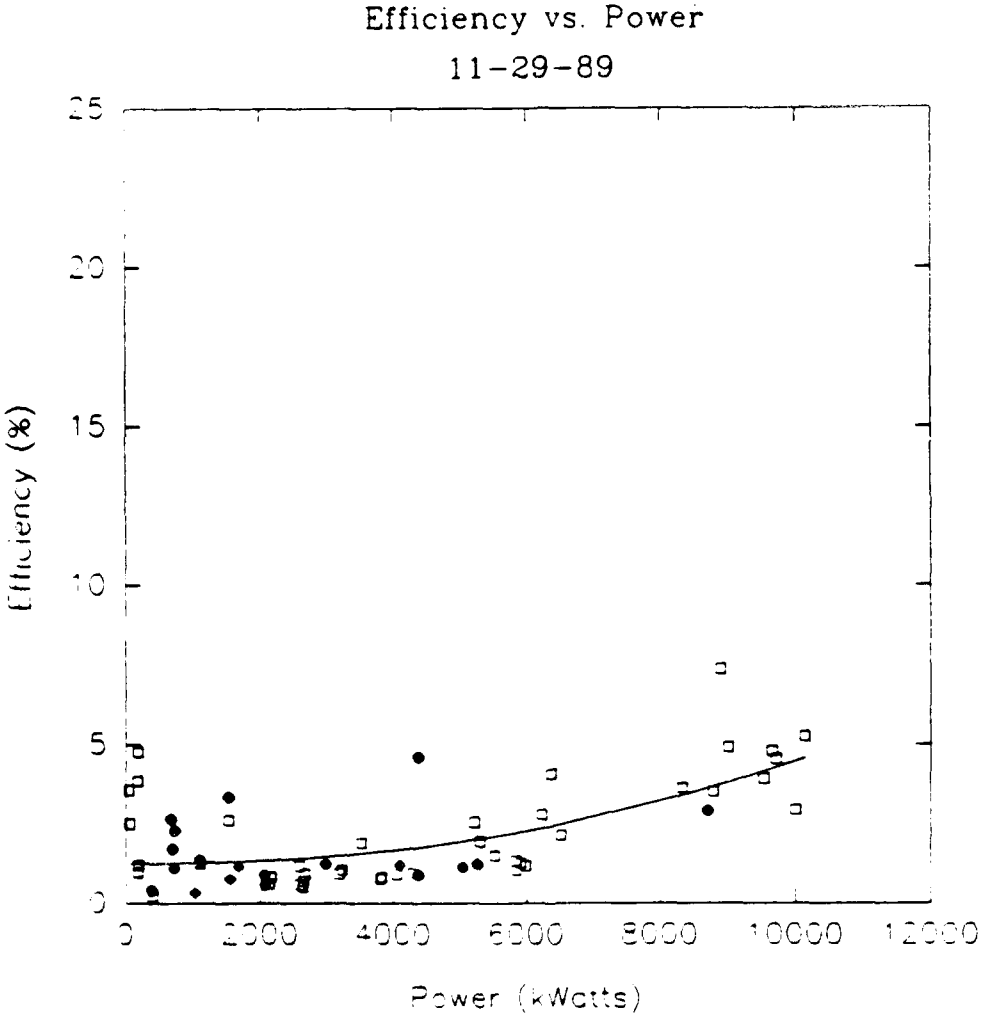
Efficiency vs. Power
11-29-89
Efficiency (%)
25
20
15
10
5
0
0
2000
4000
6000
8000
10000
12000
Power (kWatts)

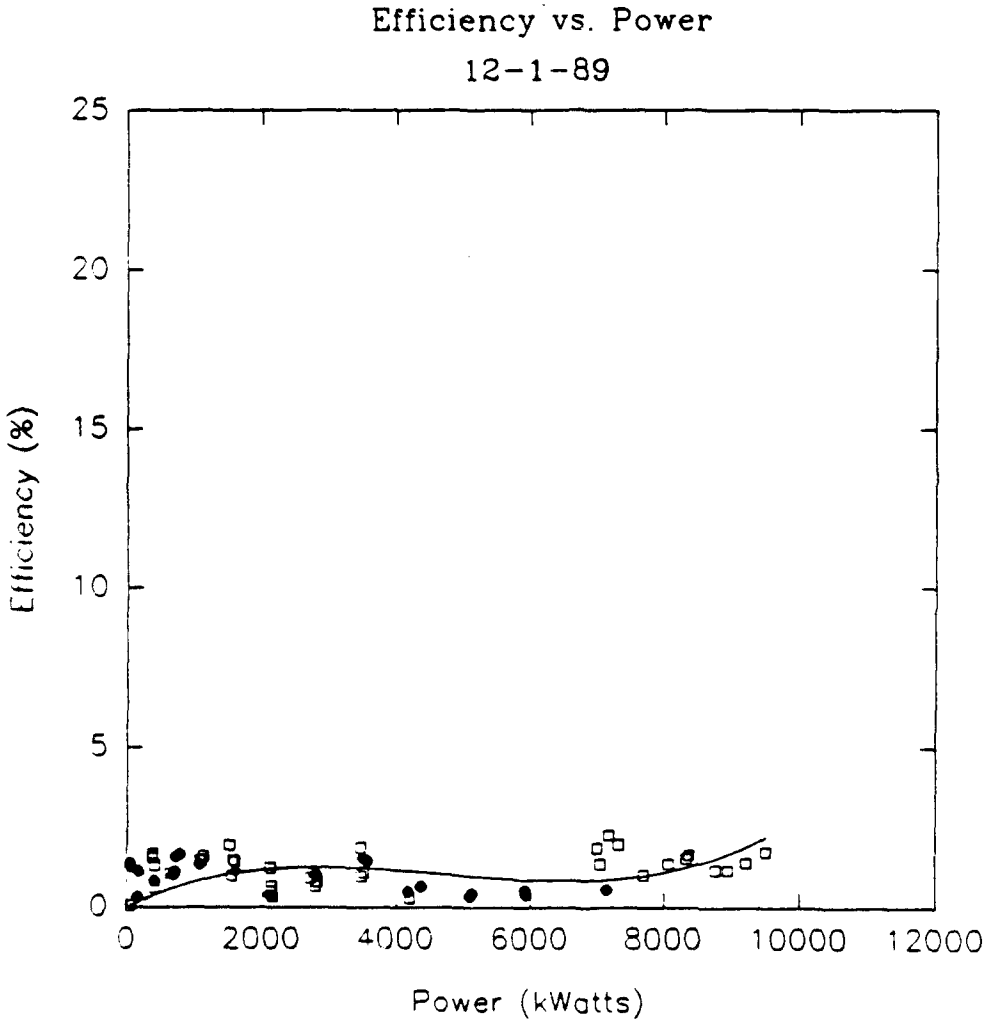
Efficiency vs. Power
12-1-89
25
20
15
10
5
0
Efficiency (%)
0
2000
4000
6000
8000
10000
12000
Power (kWatts)

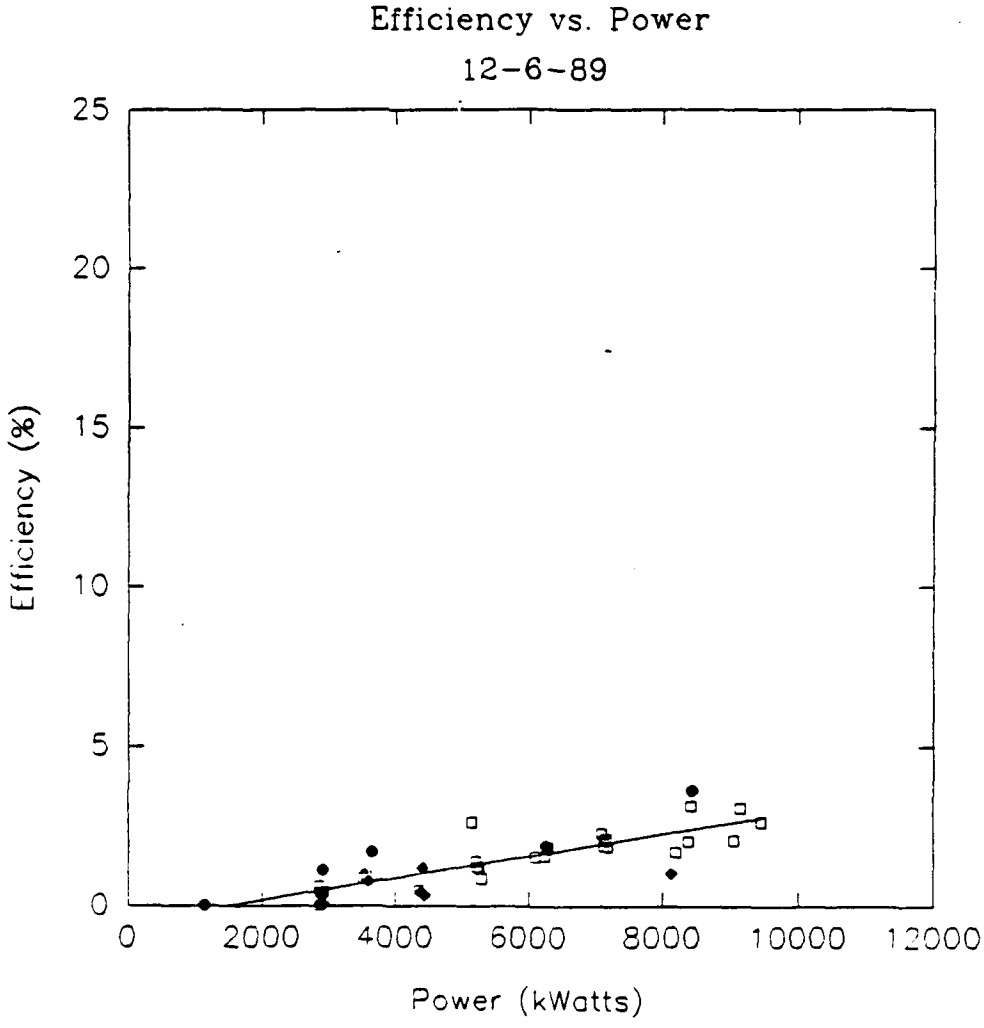
Efficiency vs. Power
12-6-89
25
20
15
10
5
0
Efficiency (%)
0
2000
4000
6000
8000
10000
12000
Power (kWatts)

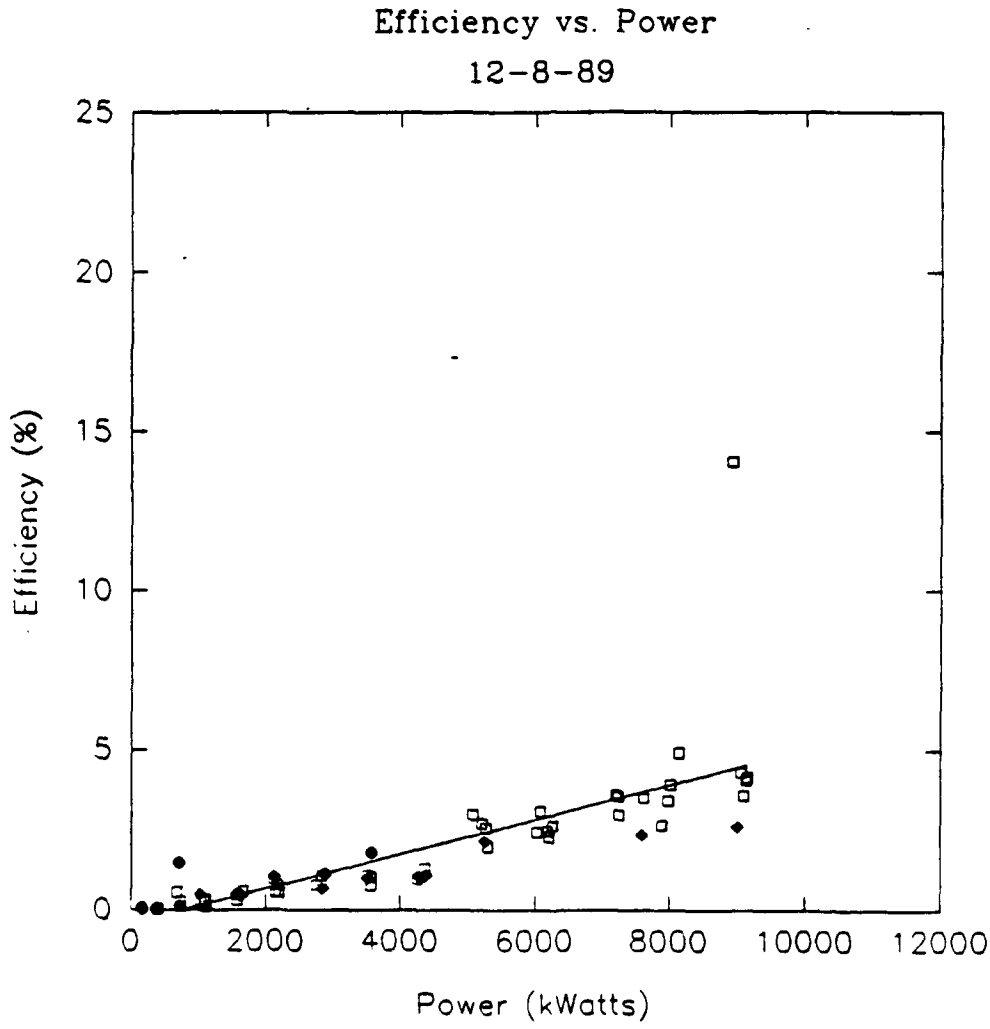
Efficiency vs. Power
12-8-89
25
20
15
10
5
0
Efficiency (%)
0
2000
4000
6000
8000
10000
12000
Power (kWatts)

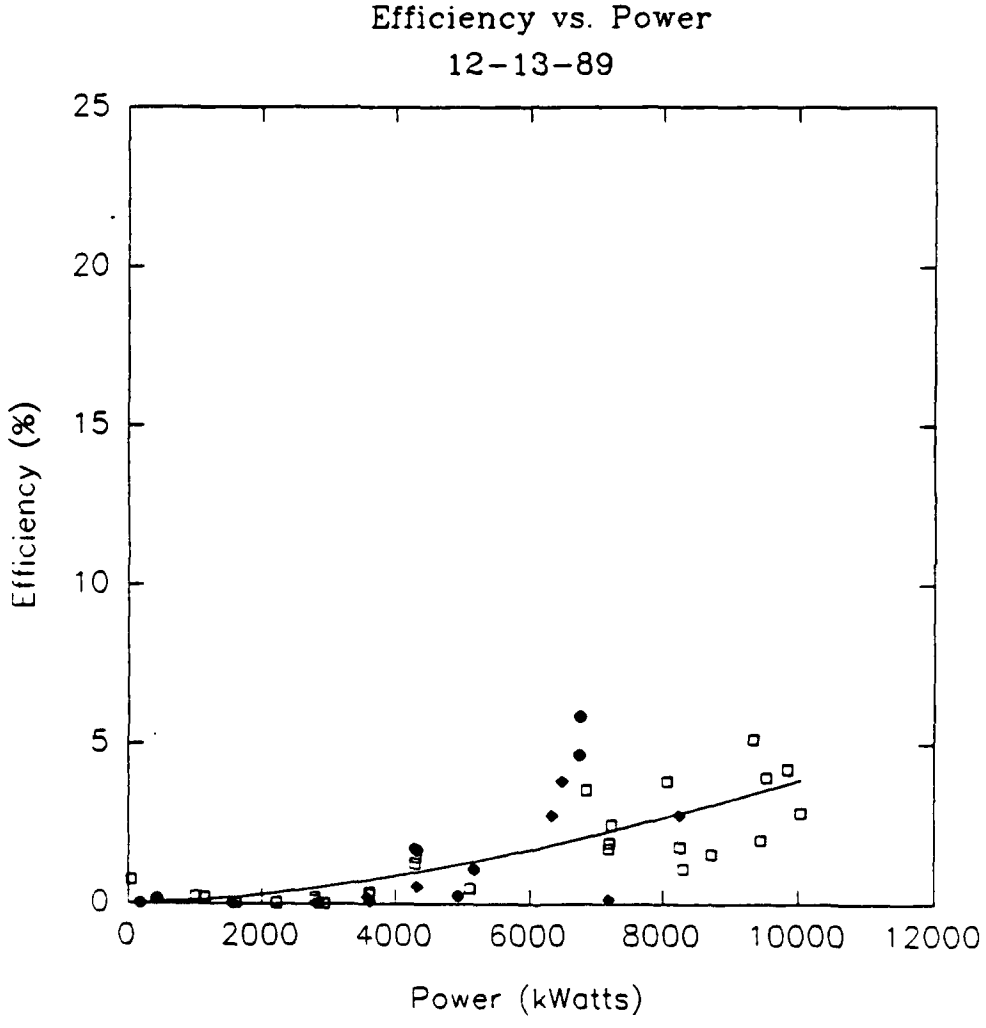
Efficiency vs. Power
12-13-89
Efficiency (%)
25
20
15
10
5
0
0
2000
4000
6000
8000
10000
12000
Power (kWatts)

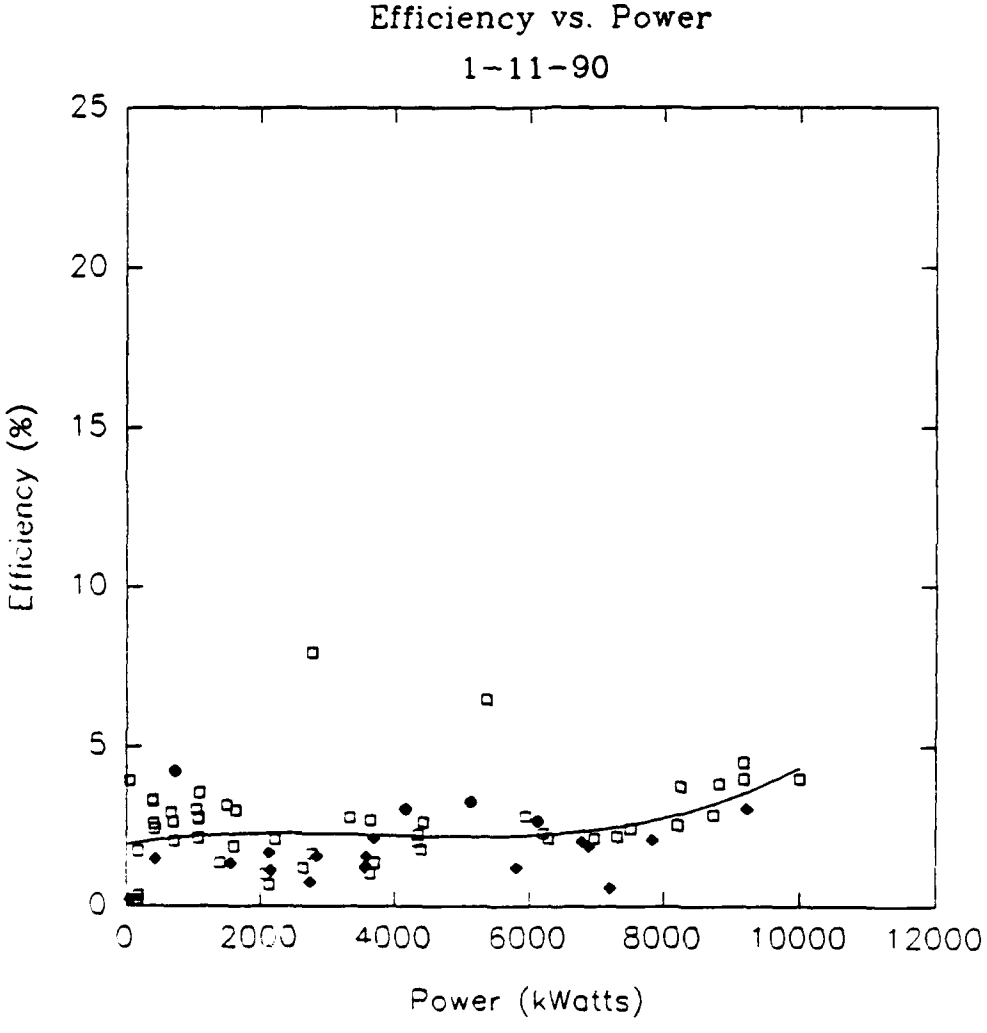
Efficiency vs. Power
1-11-90
25
20
15
10
5
0
Efficiency (%)
0
2000
4000
6000
8000
10000
12000
Power (kWatts)

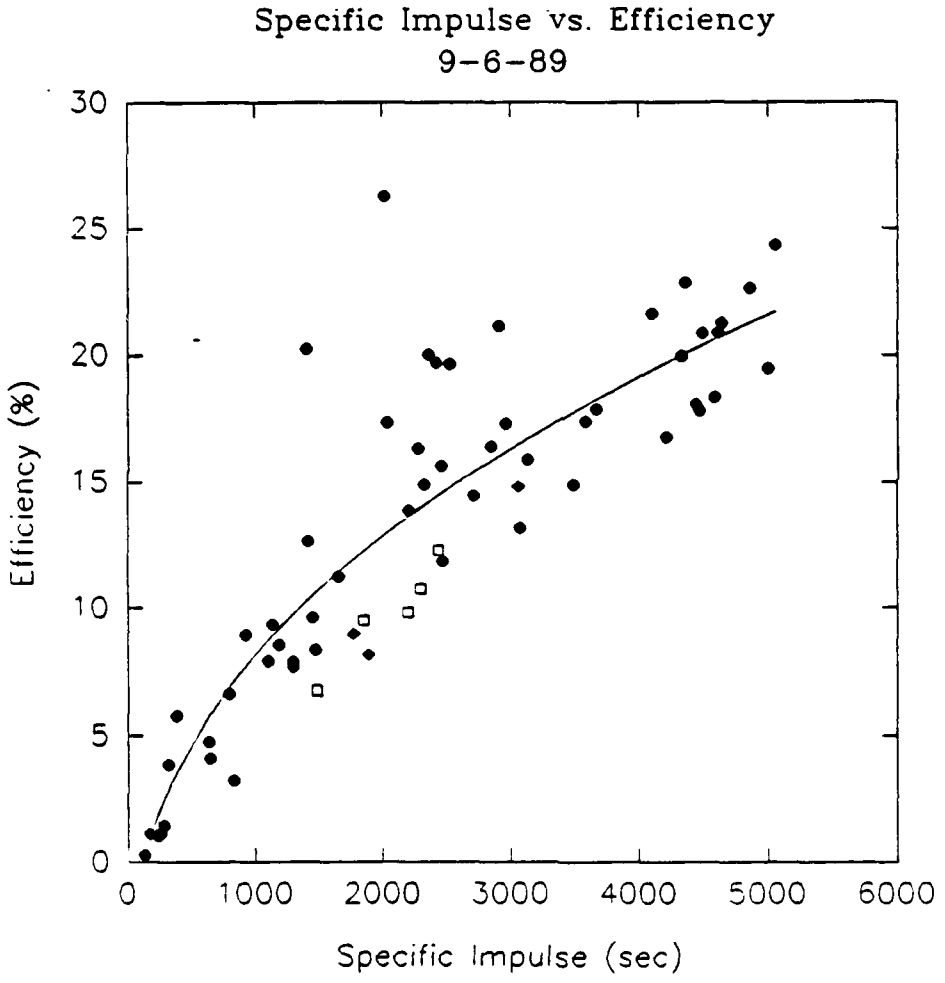
Specific Impulse vs. Efficiency
9-6-89
Efficiency (%)
30
25
20
15
10
5
0
0
1000
2000
3000
4000
5000
6000
Specific Impulse (sec)

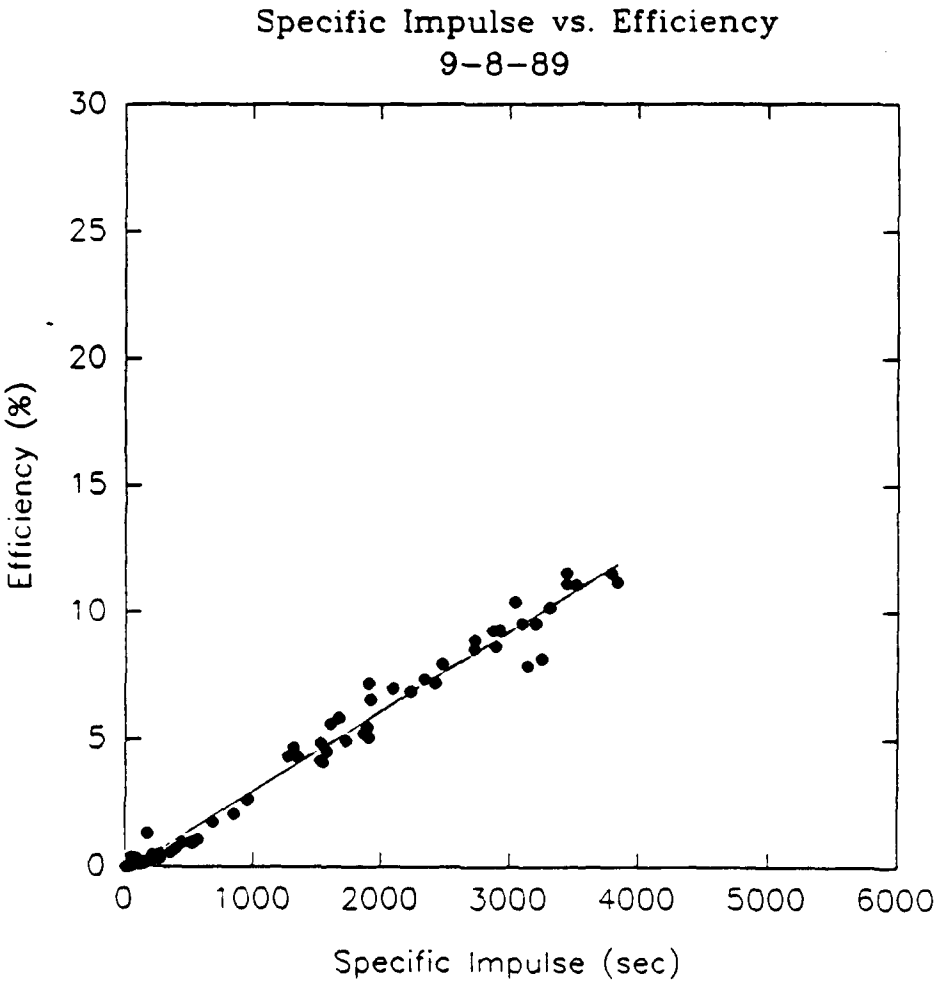
Specific Impulse vs. Efficiency
9-8-89
Efficiency (%)
30
25
20
15
10
5
0
0
1000
2000
3000
4000
5000
6000
Specific Impulse (sec)

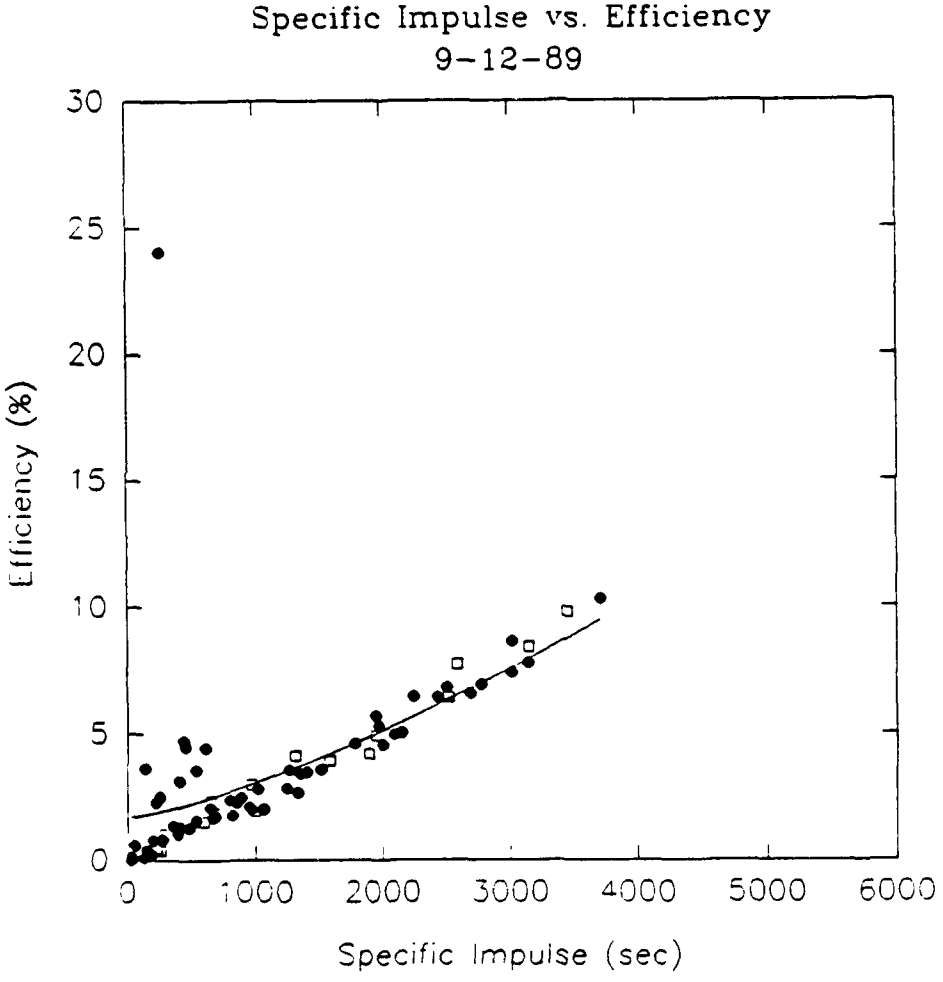
Specific Impulse vs. Efficiency
9-12-89
Efficiency (%)
30
25
20
15
10
5
0
0
1000
2000
3000
4000
5000
6000
Specific Impulse (sec)

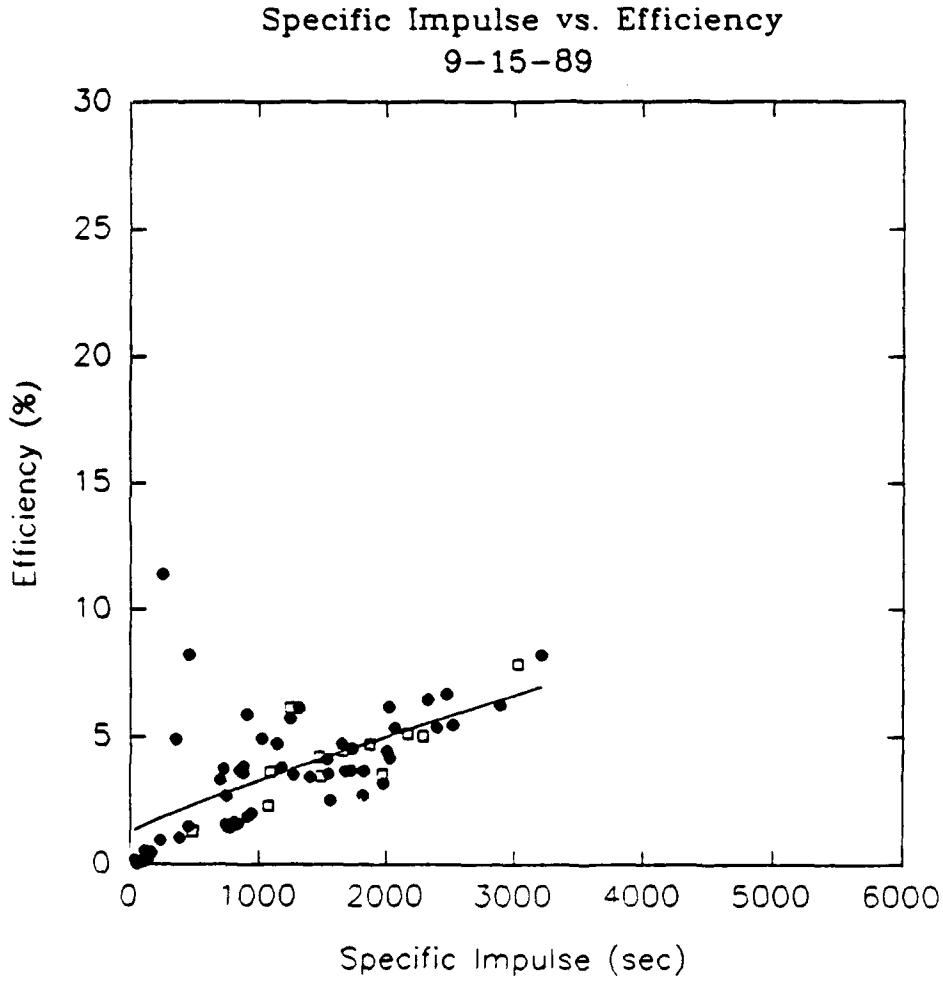
Specific Impulse vs. Efficiency
9-15-89
Efficiency (%)
30
25
20
15
10
5
0
0
1000
2000
3000
4000
5000
6000
Specific Impulse (sec)

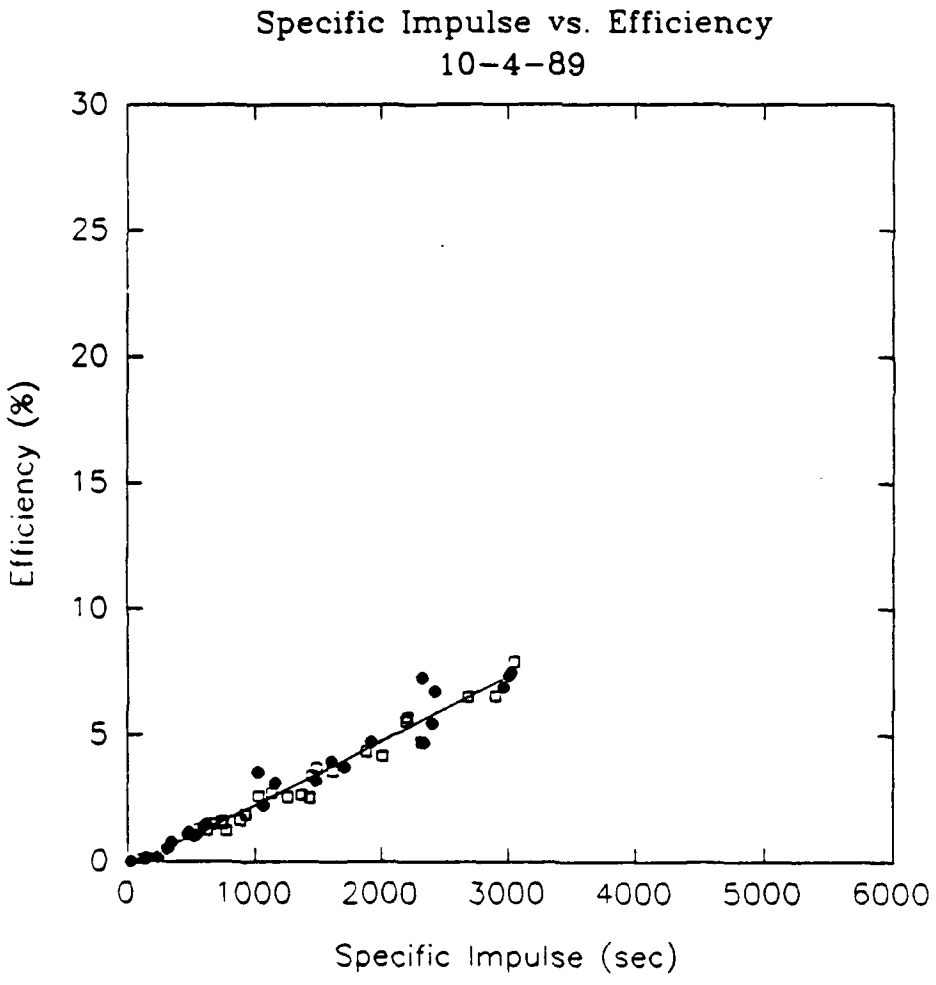
Specific Impulse vs. Efficiency
10-4-89
Efficiency (%)
30
25
20
15
10
5
0
0
1000
2000
3000
4000
5000
6000
Specific Impulse (sec)

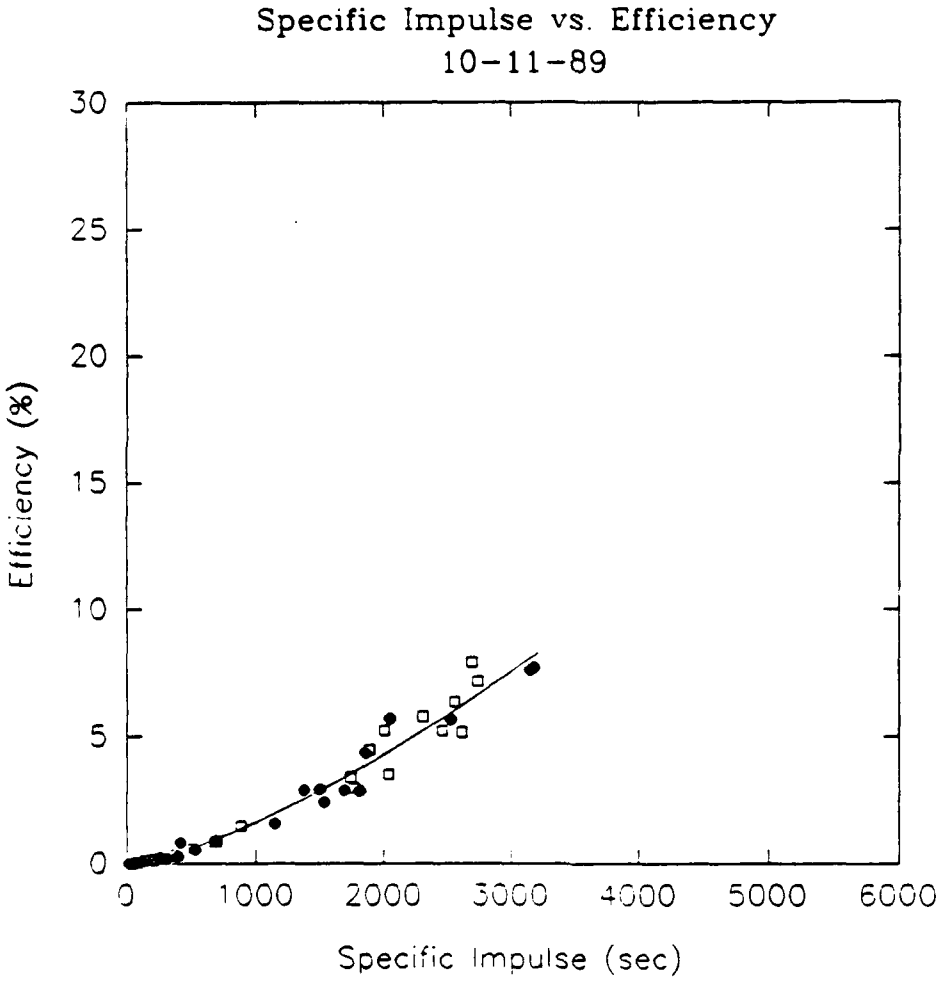
Specific Impulse vs. Efficiency
10-11-89
Efficiency (%)
30
25
20
15
10
5
0
0
1000
2000
3000
4000
5000
6000
Specific Impulse (sec)

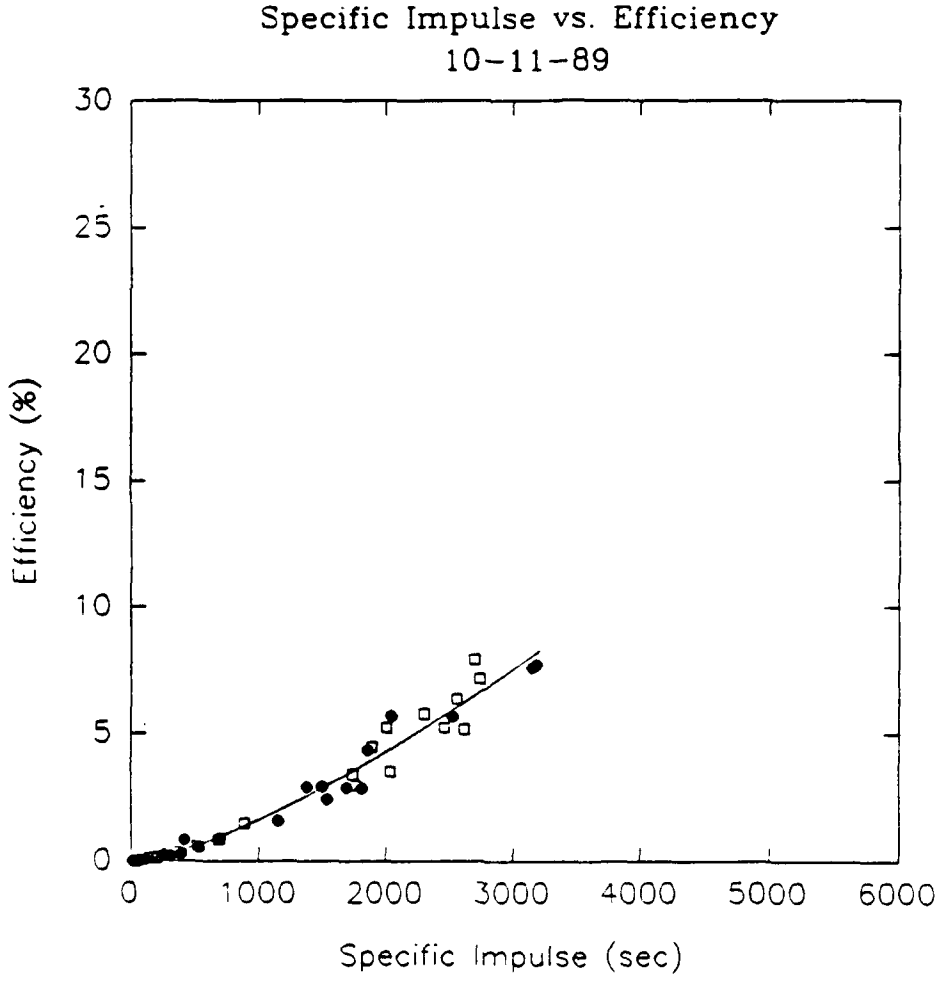
Specific Impulse vs. Efficiency
10-11-89
Efficiency (%)
30
25
20
15
10
5
0
0
1000
2000
3000
4000
5000
6000
Specific Impulse (sec)

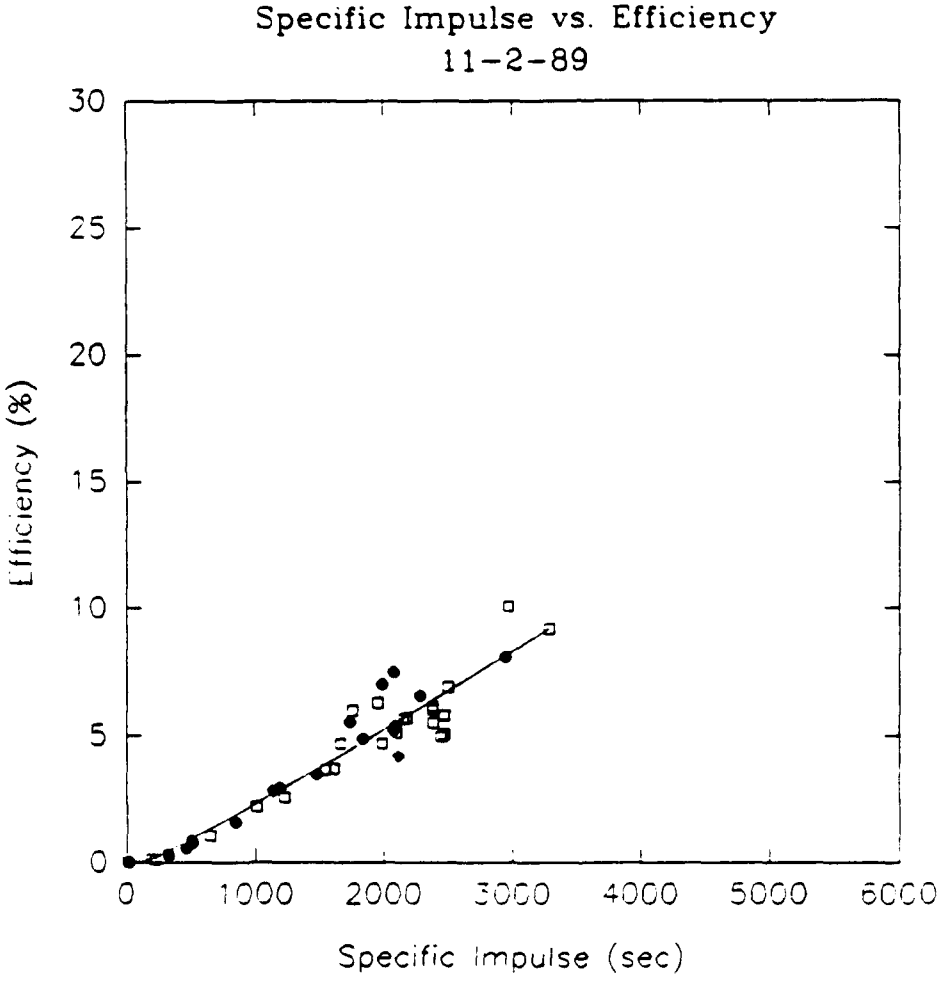
Specific Impulse vs. Efficiency
11-2-89
Efficiency (%)
30
25
20
15
10
5
0
0
1000
2000
3000
4000
5000
6000
Specific Impulse (sec)

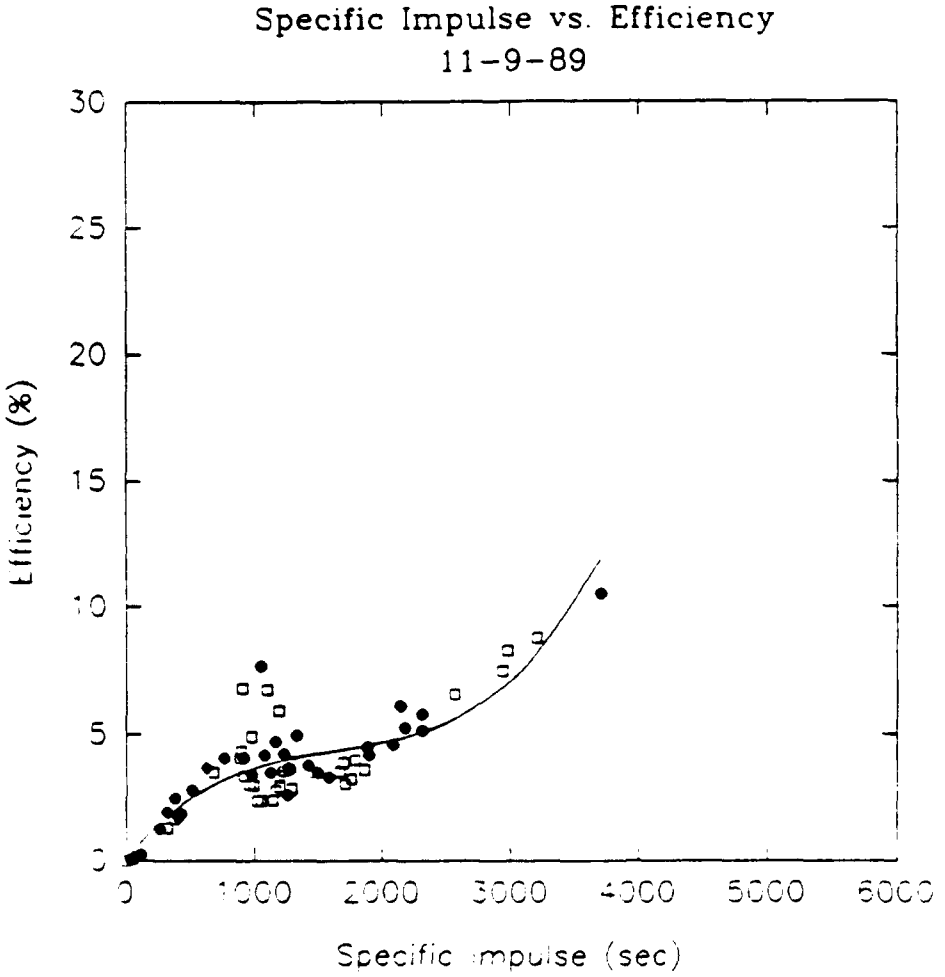
Specific Impulse vs. Efficiency
11-9-89
Efficiency (%)
30
25
20
15
10
5
0
0
1000
2000
3000
4000
5000
6000
Specific Impulse (sec)

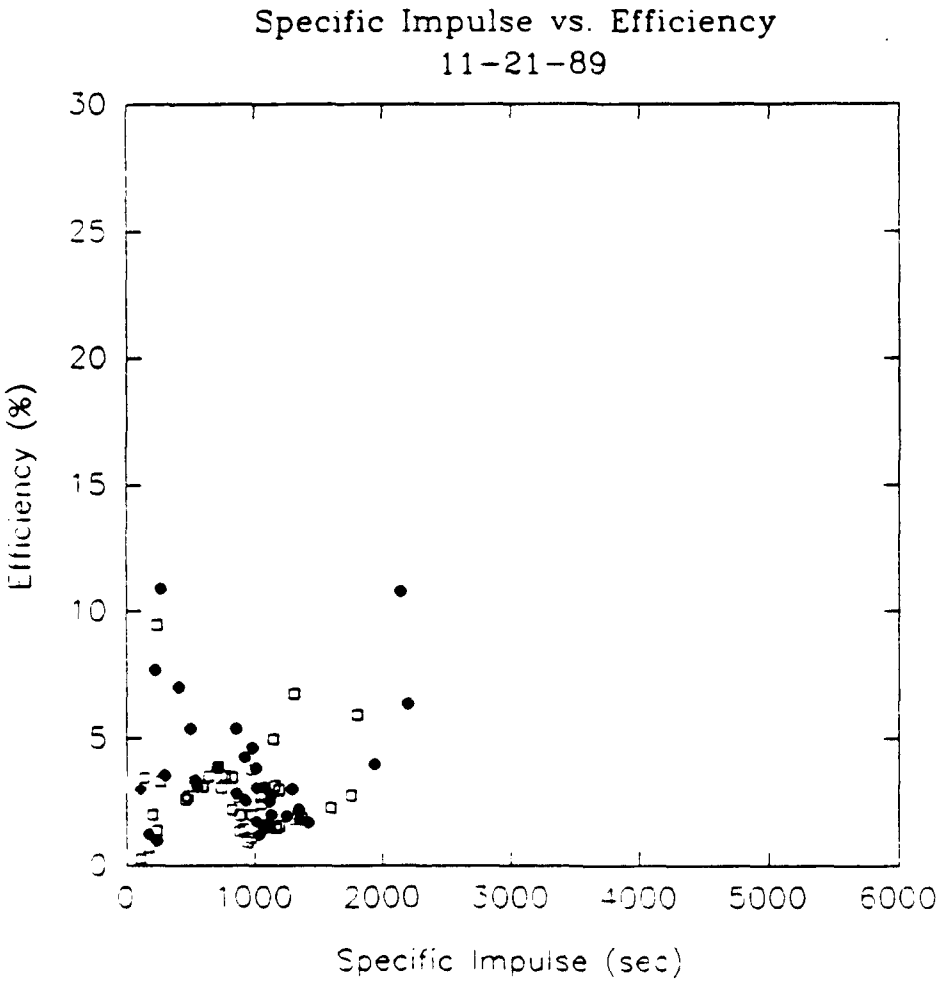
Specific Impulse vs. Efficiency
11-21-89
Efficiency (%)
30
25
20
15
10
5
0
0
1000
2000
3000
4000
5000
6000
Specific Impulse (sec)

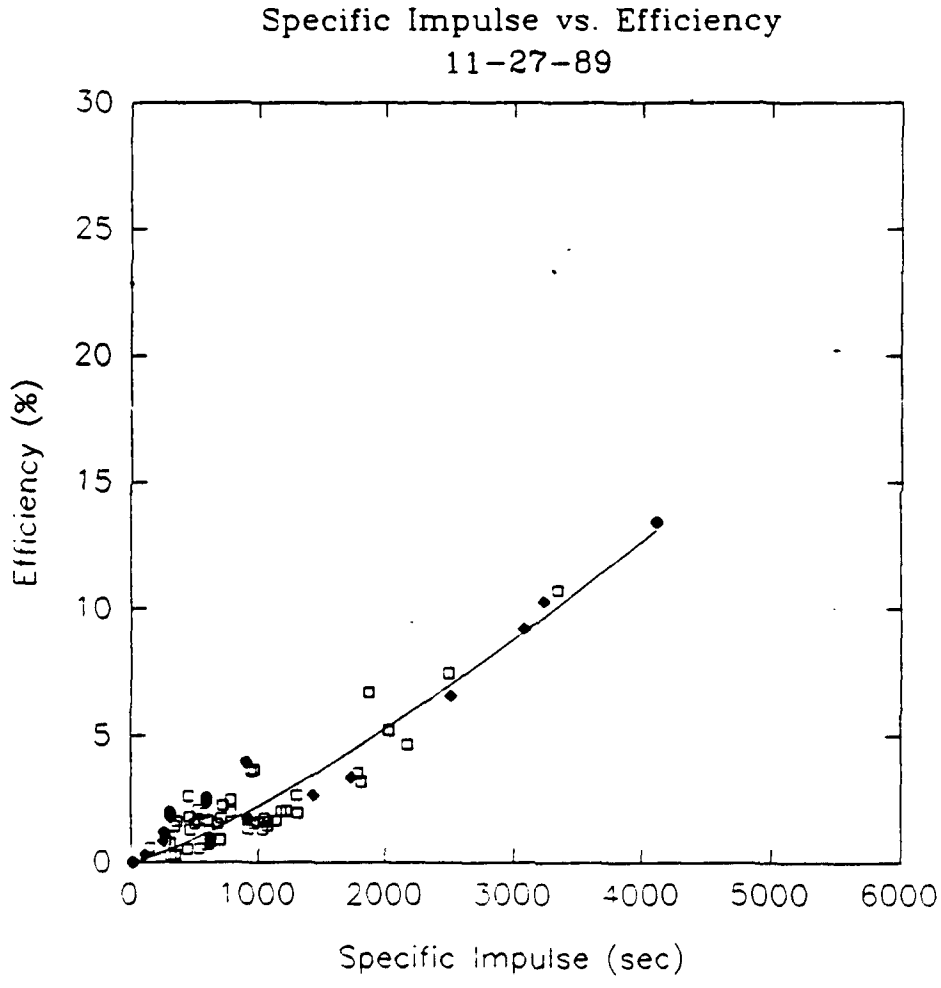
Specific Impulse vs. Efficiency
11-27-89
Efficiency (%)
30
25
20
15
10
5
0
0
1000
2000
3000
4000
5000
6000
Specific Impulse (sec)

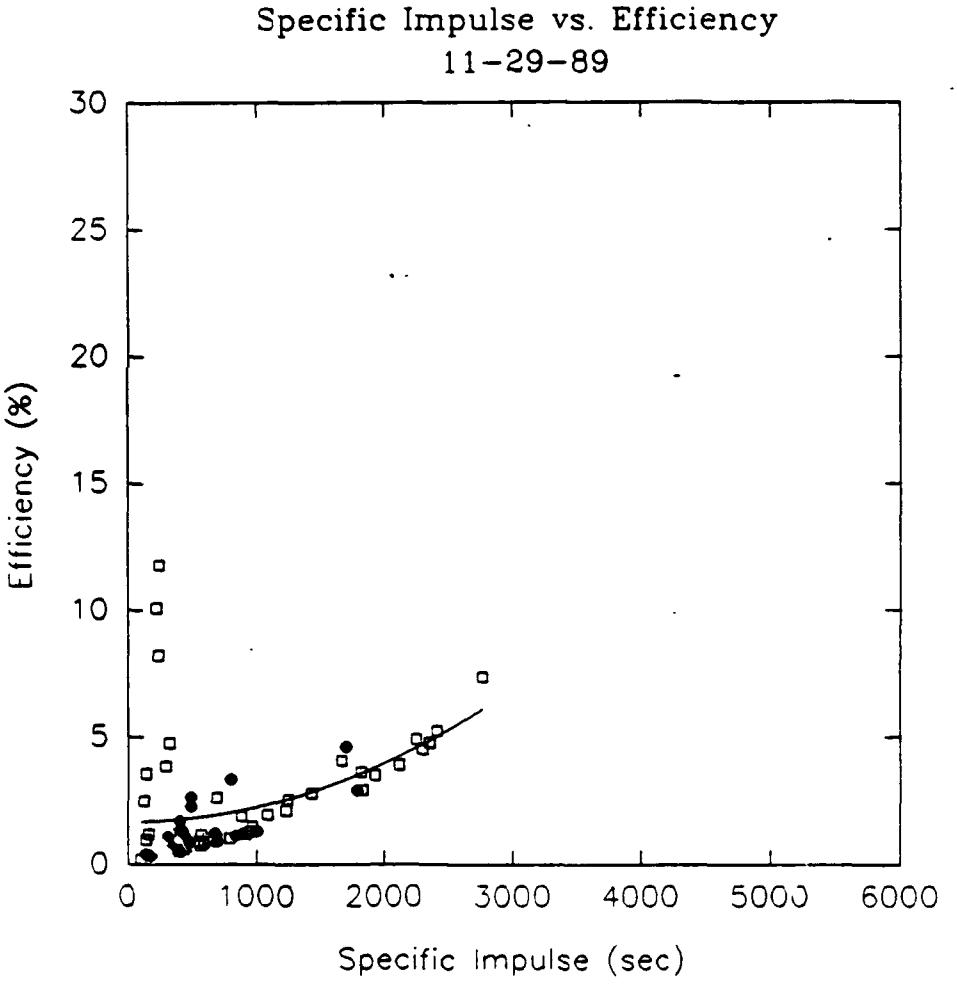
Specific Impulse vs. Efficiency
11-29-89
Efficiency (%)
30
25
20
15
10
5
0
0
1000
2000
3000
4000
5000
6000
Specific Impulse (sec)

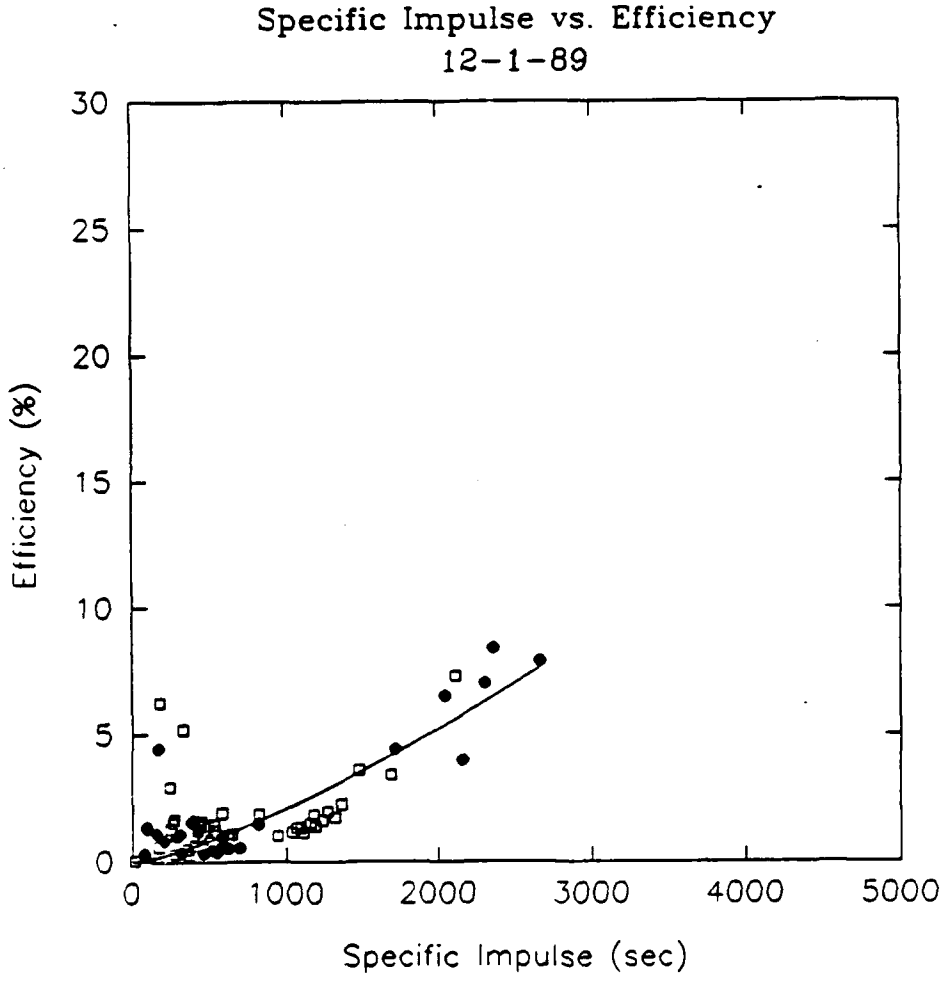
Specific Impulse vs. Efficiency
12-1-89
Efficiency (%)
30
25
20
15
10
5
0
0
1000
2000
3000
4000
5000
Specific Impulse (sec)

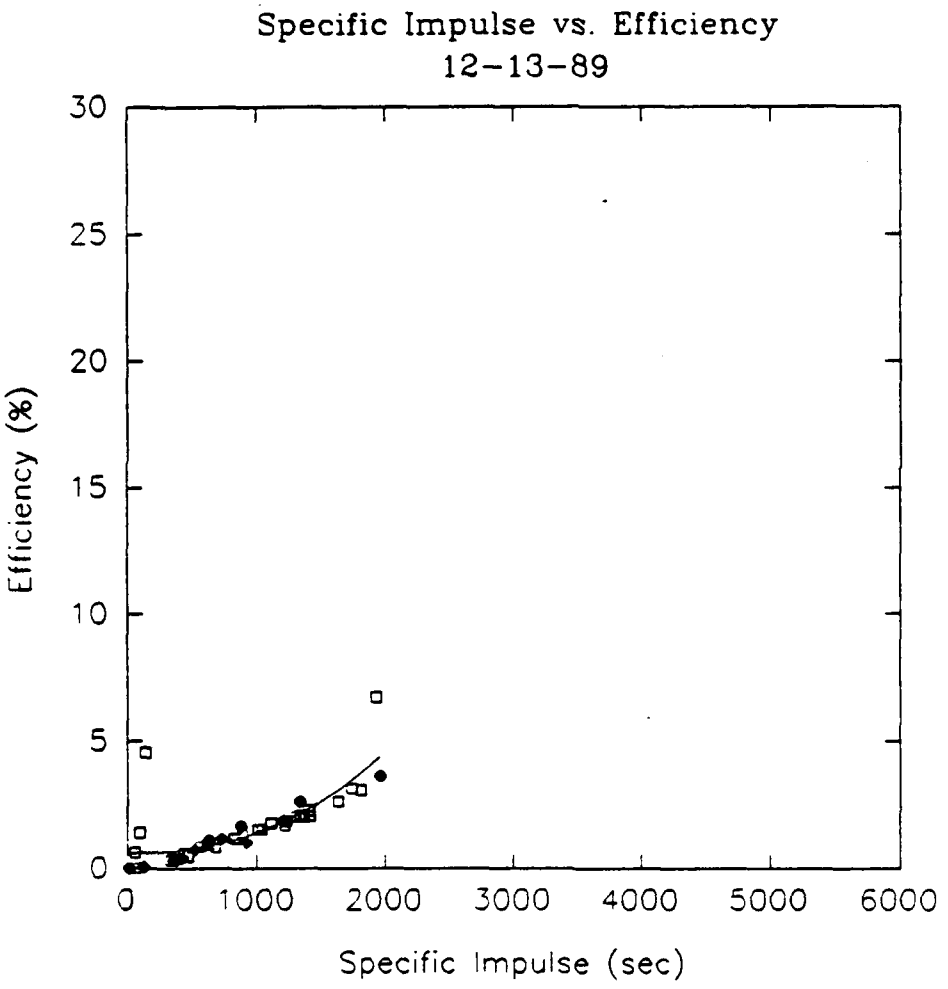
Specific Impulse vs. Efficiency
12-13-89
30
25
20
15
10
5
0
Efficiency (%)
0
1000
2000
3000
4000
5000
6000
Specific Impulse (sec)

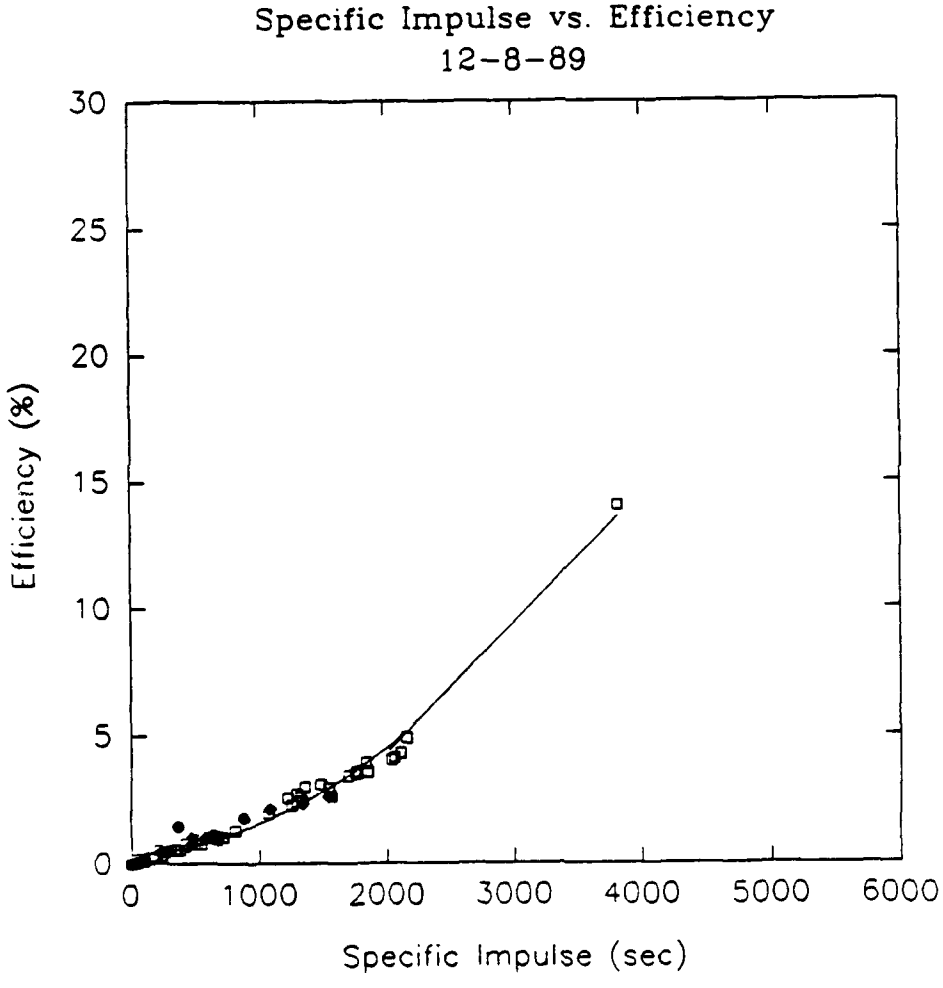
Specific Impulse vs. Efficiency
12-8-89
Efficiency (%)
30
25
20
15
10
5
0
0
1000
2000
3000
4000
5000
6000
Specific Impulse (sec)

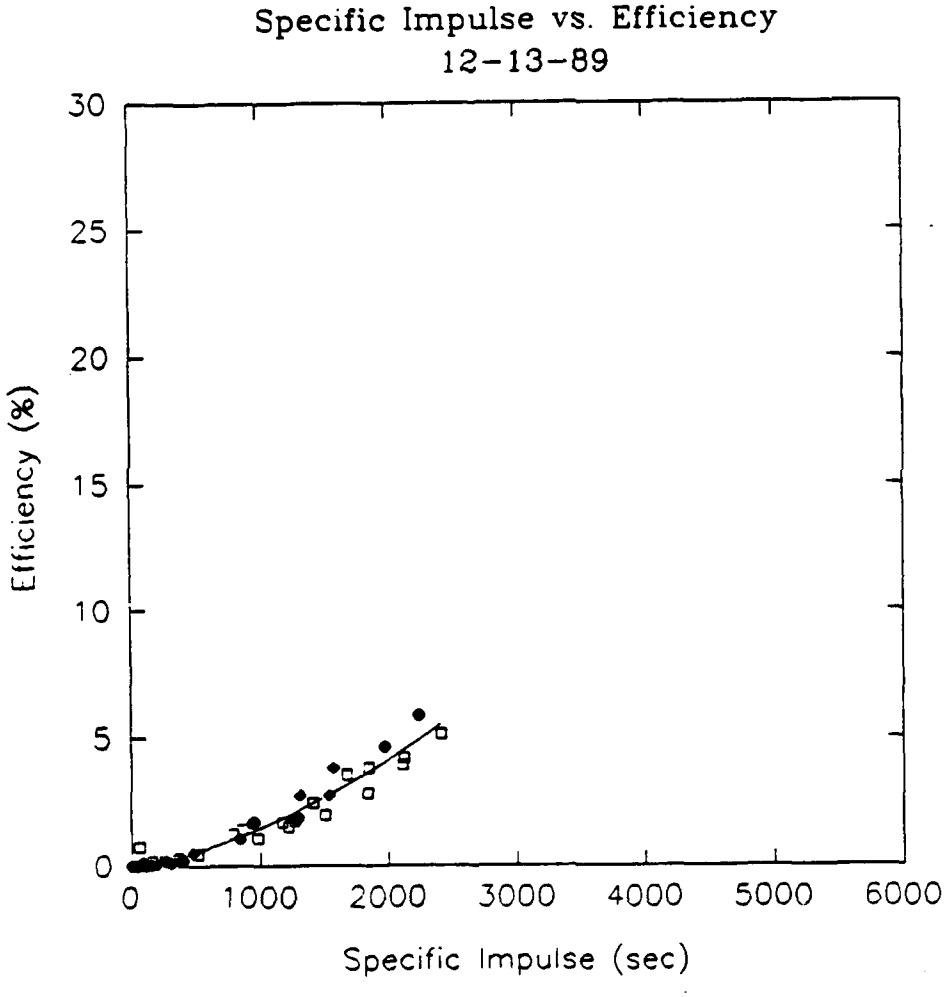
Specific Impulse vs. Efficiency
12-13-89
30
25
20
15
10
5
0
Efficiency (%)
0
1000
2000
3000
4000
5000
6000
Specific Impulse (sec)

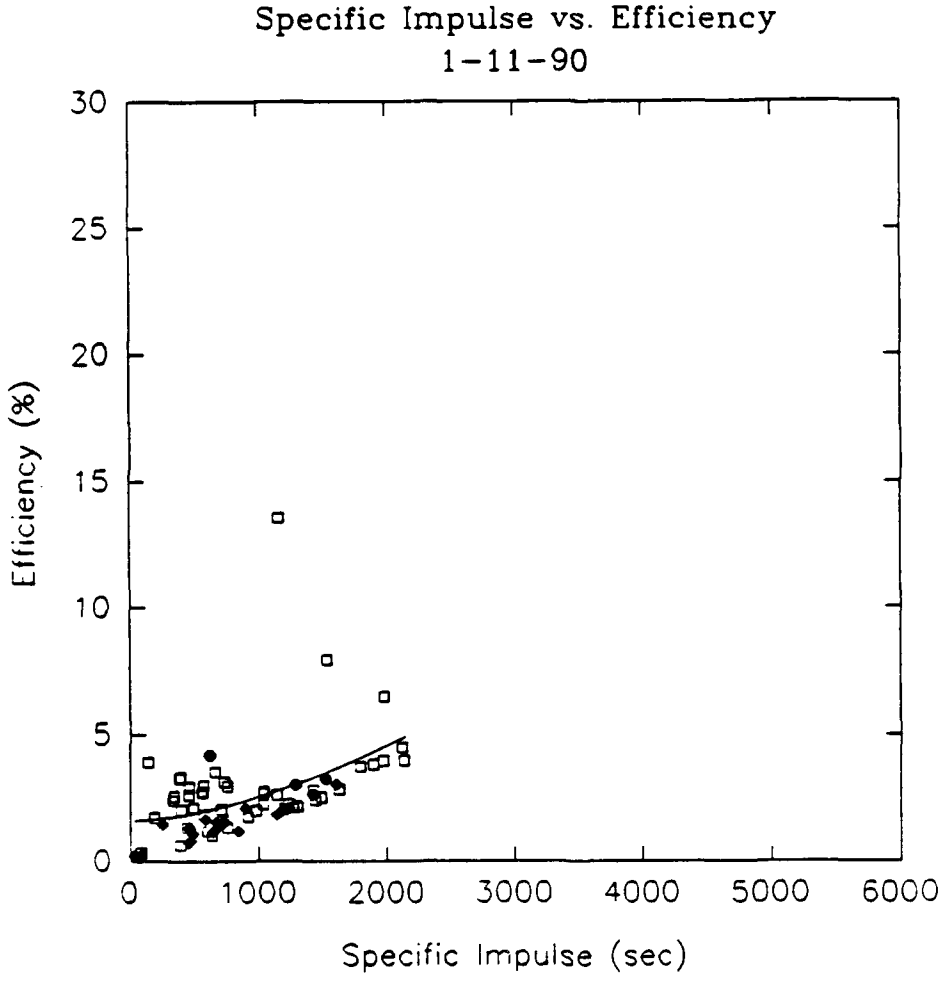
Specific Impulse vs. Efficiency
1-11-90
Efficiency (%)
30
25
20
15
10
5
0
0
1000
2000
3000
4000
5000
6000
Specific Impulse (sec)

Thruster Internal Volume Geometry

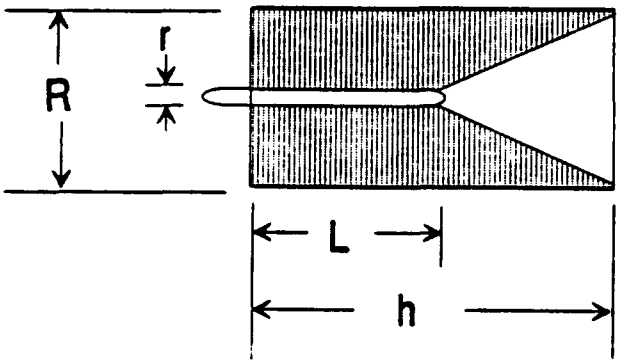

$$V = \frac{\pi}{3} [2R^2 h + L(R^2 - 3r^2)]$$

Note: Shaded region denotes a characteristic volume, not an actual physical component. The actual thruster is a copper cylinder with a tungsten rod.

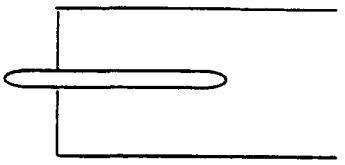

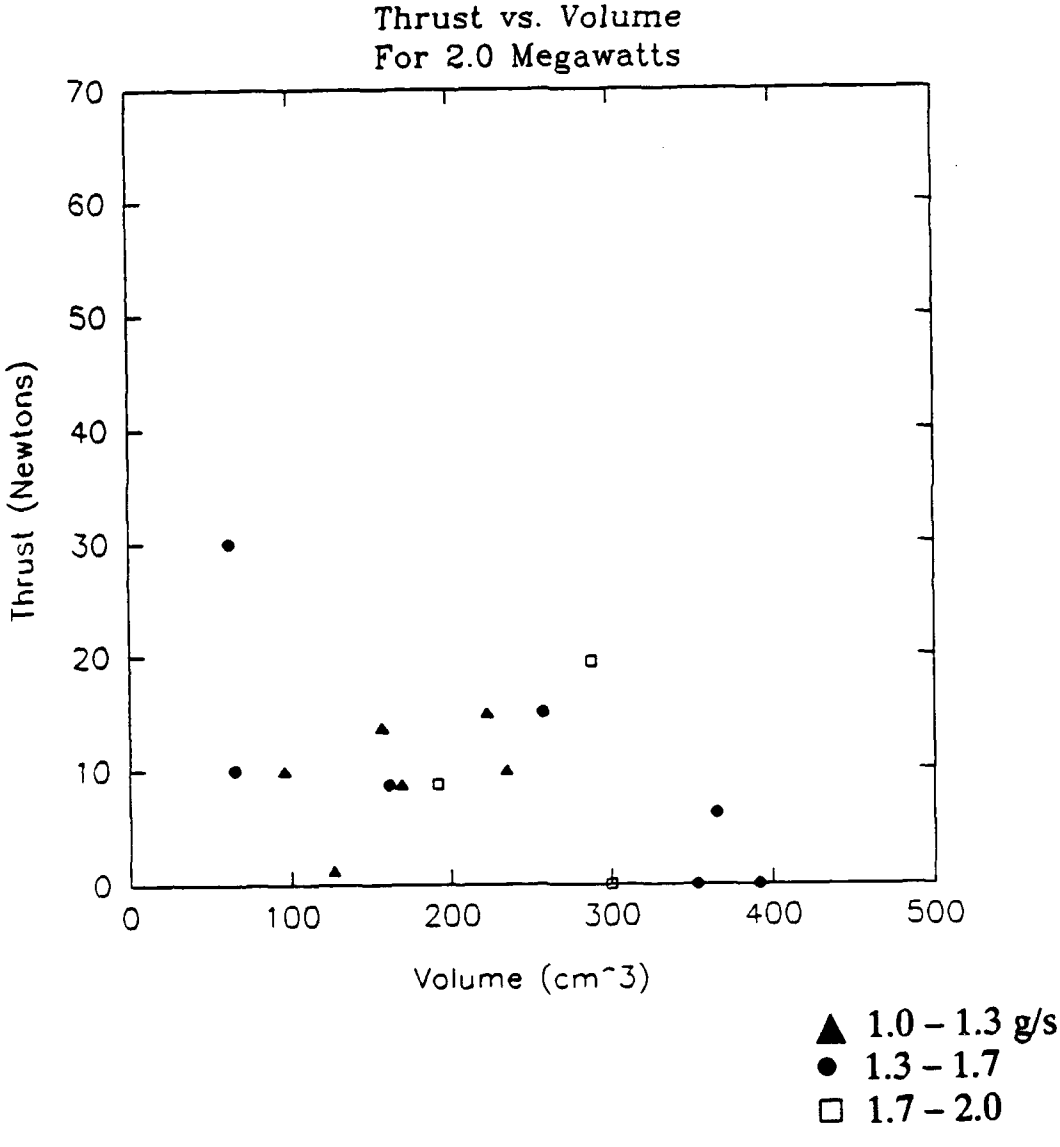
Thrust vs. Volume
For 2.0 Megawatts
Thrust (Newtons)
70
60
50
40
30
20
10
0
0
100
200
300
400
500
Volume (cm^3)
▲ 1.0 – 1.3 g/s
● 1.3 – 1.7
□ 1.7 – 2.0

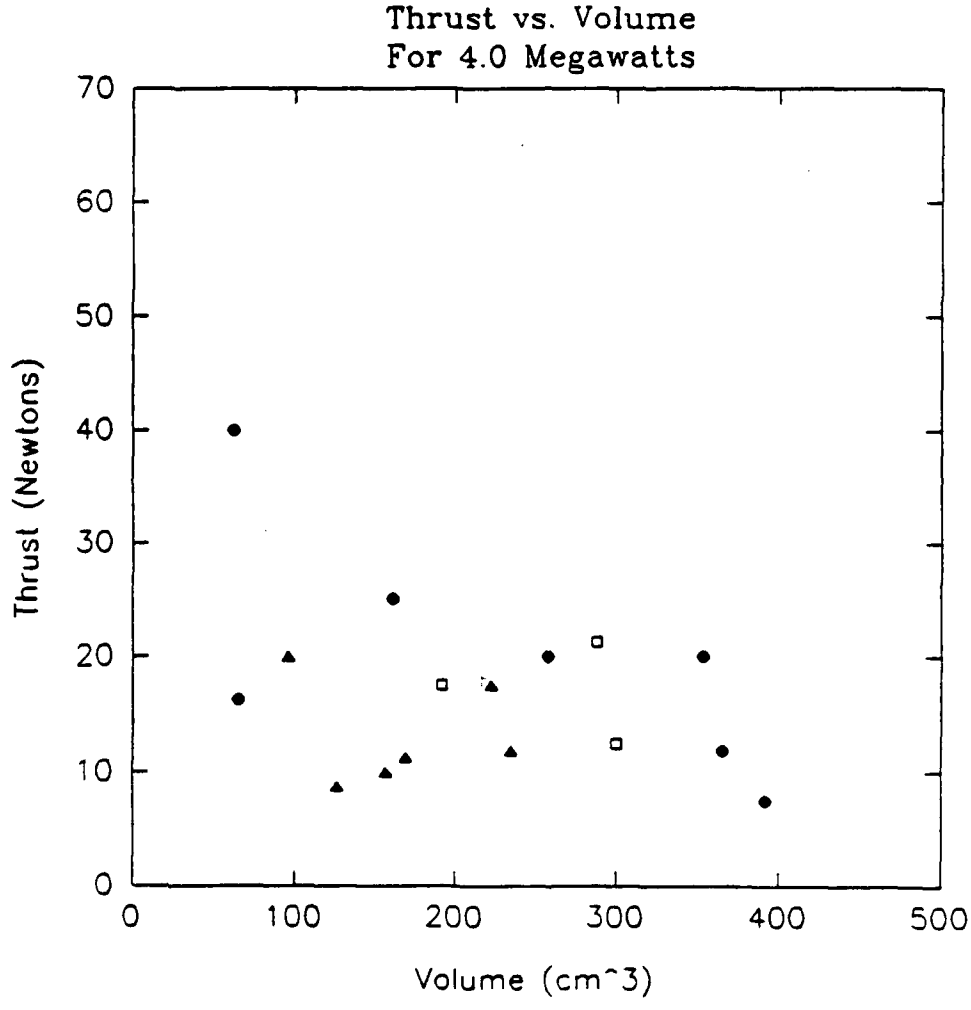
Thrust vs. Volume
For 4.0 Megawatts
Thrust (Newtons)
70
60
50
40
30
20
10
0
0
100
200
300
400
500
Volume (cm^3)

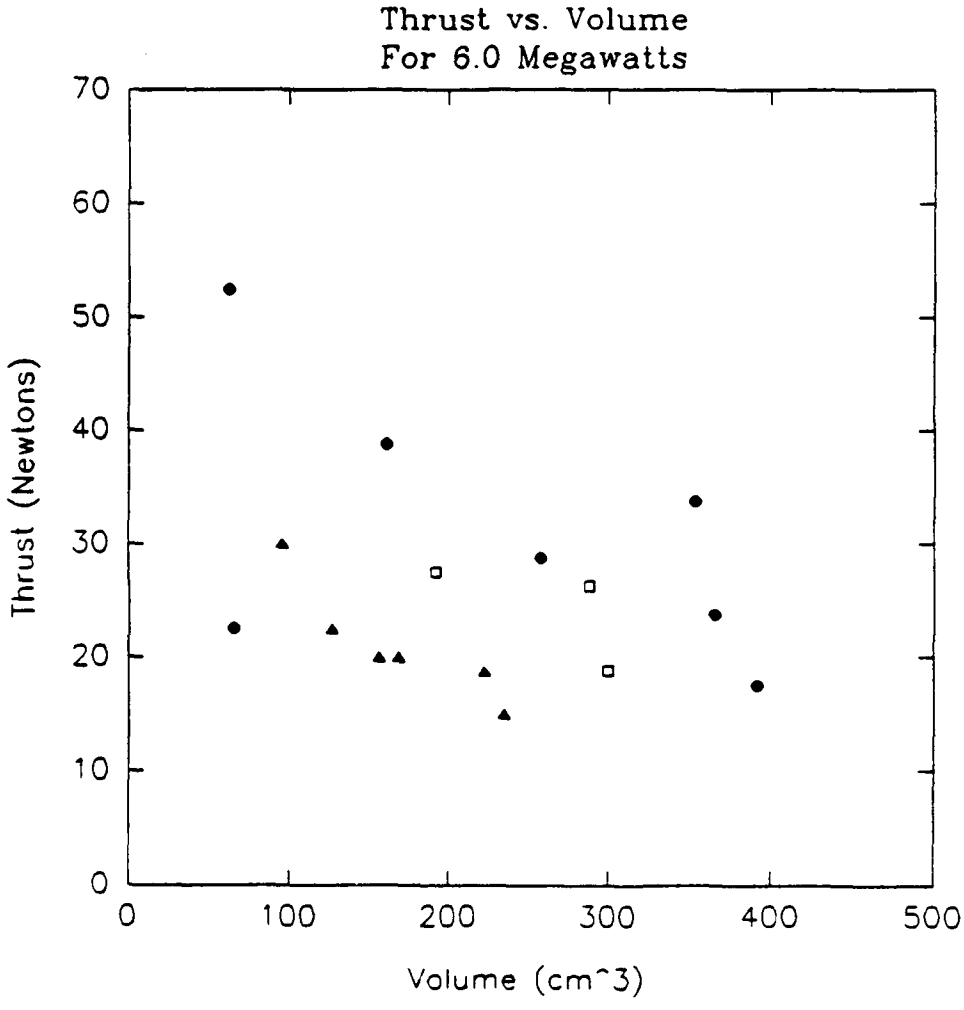
Thrust vs. Volume
For 6.0 Megawatts
Thrust (Newtons)
70
60
50
40
30
20
10
0
0
100
200
300
400
500
Volume (cm^3)

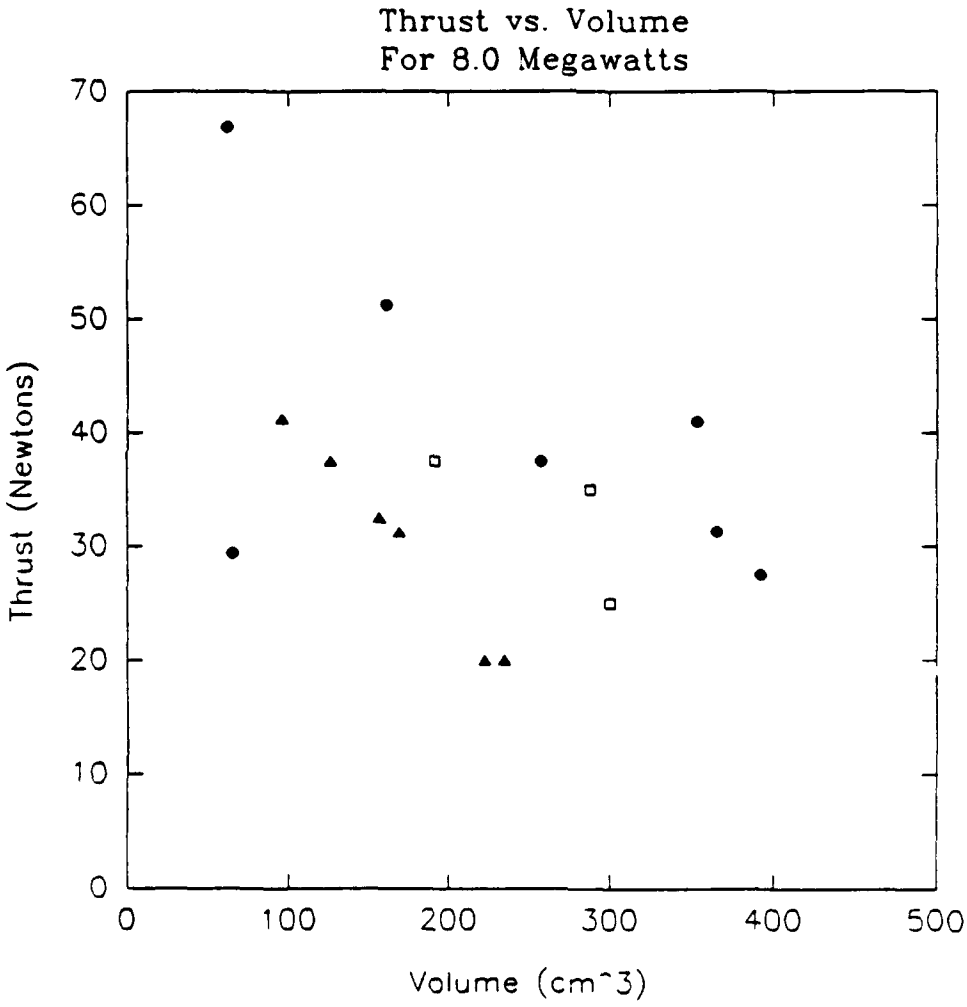
Thrust vs. Volume
For 8.0 Megawatts
Thrust (Newtons)
70
60
50
40
30
20
10
0
0
100
200
300
400
500
Volume (cm^3)

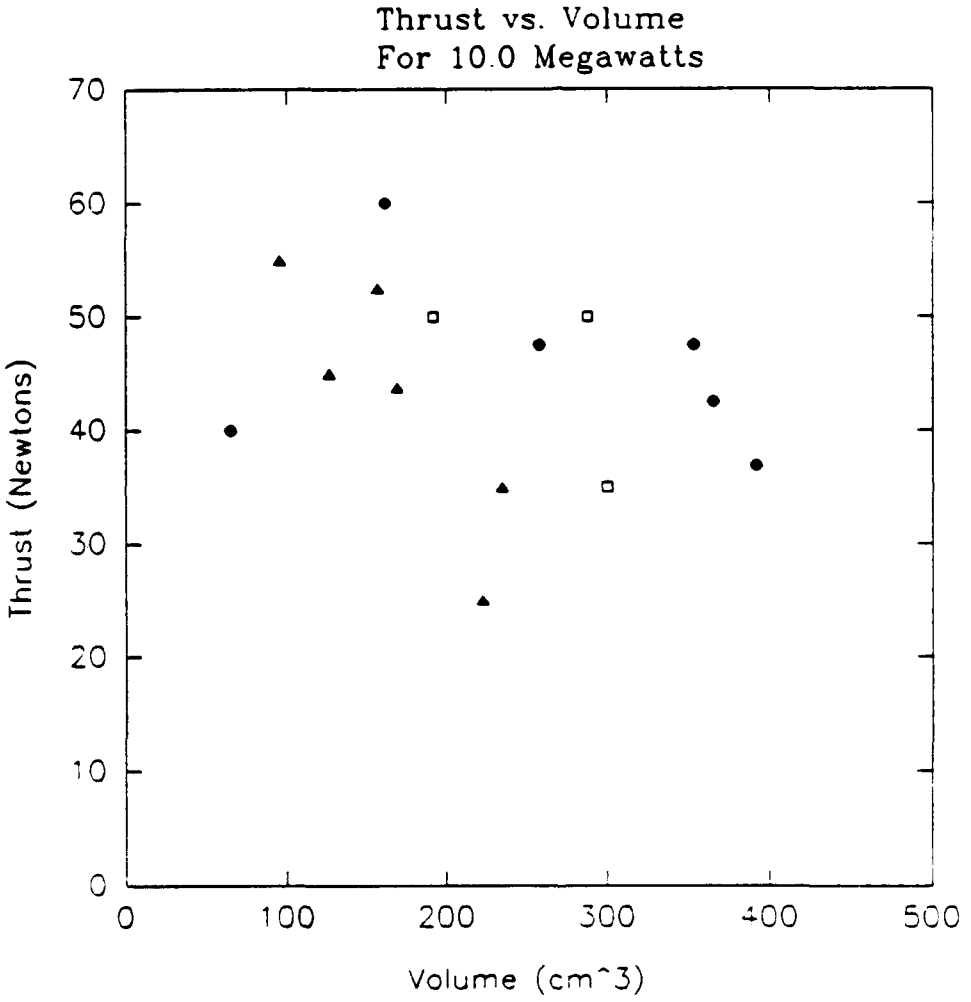
Thrust vs. Volume
For 10.0 Megawatts
Thrust (Newtons)
70
60
50
40
30
20
10
0
0
100
200
300
400
500
Volume (cm^3)